UNIVERSITAT POLITÈCNICA DE VALÈNCIA

UNIVERSITAT POLITÈCNICA DE VALÈNCIA

School of Industrial Engineering

Development of a computational software for Studying the Pharmacological Effects on Heart Failure and Hypertrophic Cardiomyopathy in Human Ventricular Cardiomyocytes

End of Degree Project

Bachelor's Degree in Biomedical Engineering

AUTHOR: Monllor Parres, Raquel

Tutor: Ferrero de Loma-Osorio, José María

ACADEMIC YEAR: 2023/2024

ACKNOWLEDGEMENTS

Atès que este treball ha sigut el fruit de gran part de la meua feina realitzada al llarg del meu darrer any, m'agradaria dedicar-lo a totes aquelles persones que m'han recolzat, encoratjat i validat durant tota la meua etapa acadèmica. Aquest projecte no sols es meu, també es vostre. Gracies.

Primer que tot, a Chema, per tirar-te a la piscina amb mi al llarg de tot el projecte i en totes les idees que anàvem tenint sempre confiant i mantenint un positivisme infinit. No sols eres un gran professional tant a nivell d'investigador com a nivell acadèmic, sempre dispost a bolcar-te en els alumnes i oferir-los el teu temps, sinó també una gran persona, molt propera, amb la que pots parlar de qualsevol tema sempre sentint-te còmode i amb confiança.

Gracies als meus pares i al meu germà, per estar sempre al meu costat en els moments bons i roïns, tant en les etapes d'alegria després d'aprovar exàmens com en les setmanes anteriors als exàmens en les que el meu estat anímic no sempre era el més agradable. Sempre m'heu proporcionat un refugi i un suport incondicional, animant-me i sense deixar de confiar en mi quan jo no ho tenia tot sempre tan clar.

Gracies als meus amics, als que se'ls diu "els de tota la vida", que sempre m'heu proporcionat una llar plena de confiança, un lloc on plorar i riure. Molts heu fet de València un espai on sentir-se com a casa i altres d'Alcoi un lloc ple de records i moments inoblidables.

També m'agradaria agrair als meus amics de la carrera, sens dubte el que més vàlua té de tot el que la carrera m'ha proporcionat ha sigut la vostra amistat. Sols dir que només vull més moments en La Tarongeria, més viatges junts i més jocs de taula, més risses i converses de tota mena tornant a casa amb vosaltres, Carla i Neus i sobretot més moments amb tu, Lucía, la meua confident. Encara que estudiar enginyeria biomèdica no ha sigut bufar i fer ampolles, tornaria a viure cada moment viscut amb vosaltres.

I, per últim, gracies a tu, Ester, la persona que sense voler m'ha ajudat a saber qui soc i qui vull ser.

Vos estime, a tots i a cada un de vosaltres.

ABSTRACT

According to WHO, cardiovascular diseases (CVDs) are the leading cause of death worldwide and includes a variety of conditions such as Heart Failure (HF) and Hypertrophy cardiomyopathy (HCM). Both, HF and HCM, are characterised by boosting arrhythmogenic factors such as the increase of the occurrence of early afterdepolarizations (EADs) or alternans, among others. However, in spite of their clinical relevance, the underlying effects of HF and HCM on cardiac bioelectricity are still unknown and in the meantime the quality of life of people suffering from them is still reduced because the optimal treatments are still unclear.

The objective of this thesis is twofold. On the one hand, the version of the O'Hara-Rudy model (O'Hara et al., 2011) of the human ventricular cardiomyocyte programmed in MATLAB® and developed by Carla Bascuñana in her thesis (Bascuñana Gea, 2023) has been modified to simulate the effects of HF and HCM on ion channels together with the combination of drugs. In this way, the new version of computational model developed in this thesis allows the theoretical study of the underlying effects of both pathologies on electrical activity of human ventricular cardiomyocytes. On the other hand, several modules of programming codes have also been developed in order to analyse both, in which conditions, with or without drug, the arrhythmogenic biomarkers are altered by the effect of HF and HCM depending on their stage and in healthy circumstances which conditions of sex, cell type and heart rate with the highest arrhythmogenicity, with or without the effect of drugs compiled by Clancy and Grandi (Fogli et al., 2021).

The results obtained suggest that midmyocardium and female are respectively the cell type and sex most prone to arrhythmia per se. Regarding the influence of heart rate, data analysis proves that the lower the heart rate is, the greater the ability to handle arrhythmogenic mechanisms. In addition, fortunately, the results show that of the drugs tested, there are some with cardioprotective effects against the proarrhythmic effects of HF and HCM, and against the combined effect with a proarrhythmic drug. In particular, Diltiazem CiPA, Nifedipine 1 and Nitrendipine 2 have proven to be the most cardioprotective agents.

Keywords: cardiomyocyte, bioelectricity, computational modelling, action potential, ion currents, heart failure, hypertrophic cardiomyopathy, arrhythmia, EADs, drug.

RESUMEN

Según la OMS, las enfermedades cardiovasculares son la principal causa de muerte en todo el mundo y abarcan una variedad de condiciones como la insuficiencia cardiaca (IC) y la miocardiopatía hipertrófica (MCH). Tanto la IC como la MCH se caracterizan por potenciar factores arritmogénicos como el incremento de la aparición de postdespolarizaciones tempranas o alternantes, entre otros. Sin embargo, a pesar de su relevancia clínica, los efectos subyacentes de la IC y la MCH sobre la bioelectricidad cardiaca siguen siendo desconocidos y, mientas tanto, las personas que las padecen presentan una calidad de vida reducida debido a que los tratamientos óptimos aún no estan claros.

El principal objetivo de este Trabajo Final de Grado (TFG) es doble. Por un lado, la versión del modelo de O'Hara-Rudy (O'Hara et al., 2011) del cardiomiocito ventricular humano programada en MATLAB® y desarrollada por Carla Bascuñana en su TFG (Bascuñana Gea, 2023), ha sido modificada para simular los efectos de la IC y la MCH sobre los canales iónicos junto con la combinación de fármacos. De esta manera, la nueva versión del modelo computacional desarrollado en este TFG permite estudiar teóricamente los efectos subyacentes de las dos patologías sobre la actividad eléctrica de los cardiomiocitos ventriculares humanos. Por otro lado, también han sido desarrollados varios módulos de código de programación con el fin de analizar ambas, tanto las condiciones, con o sin fármaco, en las cuales los biomarcadores arritmogénicos se alteran por el efecto de la IC y la MCH en función de su estadio, así como, en circunstancias de salud, cuáles son las condiciones de sexo, tipo de célula y frecuencia cardiaca con mayor arritmogenicidad, con o sin el efecto de los fármacos recopilados por Clancy y Grandi (Fogli et al., 2021).

Los resultados obtenidos sugieren que el midmiocardio y femenino son, respectivamente, el tipo de célula y el sexo que más tienden a la arritmia *per se*. En relación con la influencia de la frecuencia cardiaca, el análisis de datos demuestra que, cuanto más baja es la frecuencia cardiaca, mayor es la capacidad para lidiar con los mecanismos arritmogénicos. Además, afortunadamente, los resultados evidencian que, de los fármacos probados, existen algunos con efectos cardioprotectores tanto ante los efectos proarrítmicos de la IC y la MCH, como ante el efecto combinado con un fármaco proarrítmico. En particular, Diltiazem CiPA, Nifedipine 1 y Nitrendipine 2, han demostrado ser los agentes con mayor capacidad cardioprotectora.

Palabras clave: cardiomiocito, bioelectricidad, modelado computacional, potencial de acción, corrientes iónicas, insuficiencia cardiaca, miocardiopatía hipertrófica, arritmia, posdespolarizaciones tempranas, fármaco.

RESUM

Segons la OMS, les malalties cardiovasculars són la principal causa de mort en tot el món i comprenen una varietat de condicions com la insuficiència cardíaca (IC) i la miocardiopatia hipertròfica (MCH). Tant la IC com la MCH es caracteritzen per potenciar factors arritmogènics com l'increment de l'aparició de postdespolaritzacions primerenques o alternants, entre altres. No obstant, malgrat la seua rellevància clínica, els efectes subjacents de la IC i la MCH sobre la bioelectricitat cardíaca segueix sent desconeguda i, mentrestant, les persones que les pateixen presenten una qualitat de vida reduïda degut a que els tractaments òptims encara no estan clars.

El principal objectiu d'aquest Treball Final de Grau (TFG) es doble. Per una banda, la versió del model d'O'Hara-Rudy (O'Hara et al., 2011) del cardiomiòcit ventricular humà programat en MATLAB® i desenvolupat per Carla Bascuñana en el seu TFG (Bascuñana Gea, 2023), ha sigut modificada per a simular els efectes de l'IC i la MCH sobre els canals iònics junt la combinació de fàrmacs. D'aquesta manera, la nova versió del model computacional desenvolupada en este TFG permet estudiar teòricament els efectes subjacents de les dues patologies sobre l'activitat elèctrica dels cardiomiòcits ventriculars humans. Per altra banda, també s'han desenvolupat diversos mòduls de codi de programació amb la finalitat d'analitzar ambdues, tant les condicions, amb i sense fàrmac, en les quals els biomarcadors arritmogènics s'alteren per l'efecte de l'IC i la MCH en funció del seu estadi, així com, en circumstancies de salut, quines son les condicions de sexe, tipus de cèl·lula i freqüència cardíaca amb major arritmogenicitat, amb i sense l'efecte dels fàrmacs recopilats per Clancy i Grandi (Fogli et al., 2021).

Els resultats obtinguts suggereixen que el midmiocardi i femení són, respectivament, el tipus de cèl·lula i el sexe que més tendeixen a la arrítmia *per se*. En relació amb la influència de la freqüència cardíaca, l'anàlisi de dades demostra que, quant més baixa es la freqüència cardíaca, major es la capacitat per bregar amb els mecanismes arritmogènics. A més a més, afortunadament, els resultats evidencien que, dels fàrmacs provats, existeixen alguns amb efecte cardioprotector tant, front els efectes proarrítmics de l'IC y la MCH, com front l'efecte combinat amb un fàrmac proarrítmic. En particular, Diltiazem CiPA, Nifedipine 1 i Nitrendipine 2, han demostrat ser els agents amb una major capacitat cardioprotectora.

Paraules clau: cardiomiòcit, bioelectricitat, modelització computacional, potencial d'acció, corrents iòniques, insuficiència cardíaca, miocardiopatia hipertròfica, arrítmia, postdespolaritzacions primerenques, fàrmacs.

CONTENTS

LIST OF FIGURES

LIST OF TABLES

LIST OF ACRONYMS AND SYMBOLS

WHO	World Health Organization
CVDs	Cardiovascular diseases
HF	Heart Failure
HCM	Hypertrophy Cardiomyopathy
EADs	Early Afterdepolarizations
CCS	Cardiac Conduction System
HH	Hodgkin-Huxley
ESC	European Society of Cardiology
AV	Atrioventricular
SA	Sinoatrial
bpm	beats per minute
HB	His Bundle
RyR2	Ryanodine Receptor 2
SR	Sarcoplasmic Reticulum
SERCA2a	Sarcoplasmic/Endoplasmic Reticulum Ca^{2+} ATPase 2^{a} pump
NCX	Sodium-Calcium Exchanger
ECG	Electrocardiogram
V_m	Membrane Potential
AP	Action Potential
I_{to}	Transient Outward potassium current
APD	Action Potential Duration
QTc	Rate-corrected QT interval
TdP	*Torsades de Pointes*
HFrEF	Reduced Ejection Fraction
HFpEF	Preserved Ejection Fraction
HFmrEF	Heart Failure Mid-range
HT	Hypertension
DM	Diabetes Mellitus

AT	Atrial Fibrillation
CM	Cardiomyopathy
SCD	Sudden Cardiac Death
DADs	Delayed Afterdepolarizations
I_{NaL}	Late Sodium current
I_{Ca}	Calcium current
I_{NCX}	NCX exchanger current
I_{Kr}	Rapid Delayed Rectifier Potassium current
I_{Ks}	Slow Delayed Rectifier Potassium current
I_{K1}	Inward Rectifier Potassium current
I_{CaL}	L-type Calcium current
I_{TI}	Transient Inward current
I_{NS}	Non-Selective cationic current
$I_{Cl,Ca}$	Calcium-activated Chloride current
EC_{50}	Half-maximal Excitatory Concentration
IC_{50}	Half-maximal Inhibitory Concentration
EFTPC	Effective Free Therapeutic Plasma Concentration
I_{stim}	External Stimulation current
C_m	Membrane Capacity
g_S	Conductance of Specific ion
I_S	Specific ion current
I_C	Current across the capacitor
I_p	Current related with pumps, exchangers and cotransporters
γ_S	Unit conductance of Specific ion
f_S	Fraction of open channels
α	Opening rate of voltage-dependent channel gates
β	Closing rate of voltage-dependent channel gates
f_∞	Stationary fraction of open channels
τ_f	Time constant associated with open channels
[L]	Ligand concentration
H	Number of receptors
k_o	Opening rates of ligand-dependent channel gates
k_c	Closing rates of ligand-dependent channel gates
K_m	Semi-activation constant

HPC	High-Performance Computing
GPU	Graphics Processing Unit
ODEs	Ordinary Differential Equations
APD_{90}	Action Potential Duration to reach 90% of repolarization
APD_{30}	Action Potential Duration to reach 30% of repolarization
LAT	Local Activation Time
NLAT	Local Activation Time index
$[Ca^{2+}]_i$ TT	Difference between systolic $[Ca^{2+}]_i$ and diastolic $[Ca^{2+}]_i$
Ca_{TD80}	Calcium transient duration to reach 80% of repolarization
FDA	Food and Drug Administration
MYO	Myoplasm
JSR	Junctional Sarcoplasmic Reticulum
NSR	Network Sarcoplasmic reticulum
SS	Subspace near the T-tubules
CICR	Calcium Induced Calcium Release
I_{Na}	Sodium Ion current
I_{Nab}	Background Sodium current
I_{NaK}	Sodium-Potassium pump current
J_{up}	Calcium Uptake Flux from the SR
J_{Rel}	Calcium Release Flux from the SR
RMP	Resting Membrane Potential
CiPA	Comprehensive in Vitro Proarrhythmia Assay
ACh	Acetylcholine
DNA	Deoxyribonucleic Acid
CIMA	Centro de Investigación online de Medicamentos Autorizados
AEMPS	Agencia Española de Medicamentos y Productos Sanitarios
CYP450	Cytochrome P450
CYP3A4	Enzyme belonging to the cytochrome P450 superfamily
ESC	European Society of Cardiology

I. DISSERTATION REPORT

CHAPTER 1. MOTIVATION, BACKGROUND AND JUSTIFICATION

The heart is the viscera in charge of pumping blood throughout the whole organism, guaranteeing the continuous and appropriate blood flow for all tissues, supplying them in turn, with nutrients and oxygen and collecting cell wastes. Therefore, it is a vital and essential organ so, all pathologies that affect its functionality have a great impact on quality of life of the patients that suffer from them.

According to World Health Organization (WHO), cardiovascular diseases cause the death of 17.9 million people each year. In particular, Heart Failure (HF) is a multi-faceted and life-threatening syndrome which has a significant morbidity and mortality, implies high costs and the affected people have a poor functional capacity and quality of life. HF is characterised by a reduced capacity of the heart to pump and fill in with blood, or even by an insufficient cardiac output due to an abnormality in the heart structure or function. On the other hand, Hypertrophic Cardiomyopathy (HCM) is a genetic cardiac muscle disorder characterized by an increased left ventricular wall thickness causing several complications such as arrhythmias, diastolic dysfunction, myocardial ischemia and left ventricular outflow obstruction, among others. According to European Society of Cardiology (ESC), both, HF and HCM, have a significant prevalence, 1-3% in general adult population and 1 in 500 adults, respectively. Therefore, reducing the social and economic impact of these pathologies has become a major public health priority worldwide.

It has been known for decades that it is possible to computationally model the electrical activity of the heart, which is closely related to cardiac action potentials, a signal of the waveform of membrane potential of myocardial cells. The electrical activity of each cell is due to efflux and influx of ionic currents through ion channels, which are glycoproteins located in the cell membrane whose structure defines a pore where the ion fluxes are allowed. When some conditions alter ion channels, such as a drug or a pathology like HF or HCM, action potential is also affected having then consequences on the cardiac electrical activity. This results in consequences on cardiac rhythm and overall cardiac function, leading to arrhythmias or other cardiovascular disorders. For this reason, the study of proarrhythmogenic factors is essential both for the increasing study of these pathologies and for the development of effective treatments for them.

The cardiac modelling research group that belongs to the Research and Innovation in Bioengineering Research (Ci2B in Spanish) of the Polytechnic University of Valencia (UPV), which supervised this thesis, has published several articles using computational models trying to simulate heart electrical phenomena. Nevertheless, few focus on the study of the effects of HF and HCM on myocardium and the study of treatments to palliate their symptoms.

Taking all these reasons into account, the present thesis has as its main objective to study the proarrhythmic factors underlying HF and HCM and to search for an efficient and viable pharmacological treatment to alleviate these conditions using computational simulation.

Using computational modelling, the electrical effects of several pathologies can be studied due to that this these models make it possible to simulate the action potential with great realism and in

conditions that are difficult to reproduce experimentally, allowing its study without the limitations of experimentation, although suffering from those inherent in mathematical modelling.

The most immediate antecedent of the present project is the thesis carried out by the student of Degree in Biomedical Engineering, Carla Bascuñana Gea (Bascuñana Gea, 2023), during the academic year 2022-2023, supervised by the same research group as the present work. In this aforementioned thesis, the computational simulation of the combination of drugs was addressed in order to study the effect they present together on cardiac electrical activity. The main difference between both works is that in the present thesis not only is the pharmacological treatment for proarrhythmic mechanism underlying HF and HCM tackled, but also the combination of drugs modelled by Carla Bascuñana is used in order to analyse the impact of different conditions such as sex, cell type and, as a new feature, the heart rate.

The main underlying motivation to fulfil the main objectives of this thesis is improving the quality of life of people with any of the cardiovascular diseases studied, taking into account the differences between several conditions such as sex, cell type and heart rate. In addition, another encouragement is that developing computational modelling of the mechanisms of action of drugs can reduce the large amount of costs both economically and in terms of animal lives that the first phases of experimental studies generate. Therefore, this thesis includes the fulfilment of 3 Sustainable Development Goals (SDG), goal 3 “Good health and well-being”, goal 5 “Gender equality” and goal 10 “Reduced inequalities” (see Appendix 8.2).

In short, with the aim of improving the quality of life of people with such cardiovascular diseases and improving the security related with the current pharmacological therapies, in the present thesis it has been considered the study of the underlying arrhythmogenic mechanism of HF and HCM and the addition of 95 drugs obtained from Fogli Iseppe et al. (2021), to analyse their arrhythmogenic and anti-arrhythmogenic effect. The mathematical model used is O’Hara-Rudy ventricular cardiomyocyte model (O’Hara et al., 2011). From my point of view this is the perfect project to finish my academic period as biomedical engineering student applying the MATLAB® programming skills and the knowledge learnt in the field of bioelectricity and mathematical modelling throughout the degree.

Thus, this thesis will provide knowledge that will favourably contribute to this area of research. According to the tasks that will be developed throughout the thesis such as computational modelling, user interface development and analysis of data and drawing conclusions, several transversal competences are accomplished, being the most evident one the “ability to develop, programme and apply mathematical methods in the analysis, modelling and simulation of the functioning of living beings and of systems and processes used in biology and medicine” which constitutes the **Specific Competence 14 of the Degree in Biomedical Engineering** of the UPV.

All the above-mentioned reasons justify the relevance of the present thesis.

CHAPTER 2. INTRODUCTION

2.1. CIRCULATORY SYSTEM, HEART, CARDIAC CAVITIES AND CONDUCTION SYSTEM

2.1.1. Circulatory System

The circulatory system is responsible for transporting and exchanging nutrients, cellular waste products, hormones, and other vital substances throughout the organism. The main components of this system are the blood, which is the fluid that functions as a transport medium; blood vessels, arteries, and veins, which are the tubes where the blood circulates and is distributed to the different organism's tissues; the heart, the main organ of the circulatory system, in which it serves as a pump to circulate the oxygenated and deoxygenated blood throughout the body; and the lymphatic system, which is part of the immune system and an accessory pathway where large molecules circulate to avoid their accumulation in the interstitial space (Iaizzo, 2015).

2.1.2. Cardiac anatomy and physiology

In humans, the heart is a cardiac viscera located in the central thoracic region, concretely in the middle and inferior mediastinum between the two lungs. It is slightly displaced to the left of centre and rests on the diaphragm.

It is constituted by four hollow chambers, two atriums at the top and two ventricles at the lower part, thus having an inverted cone shape. The two atriums and ventricles are separated by the atrium and ventricle septum, respectively. However, four valves open and close passively according to the direction of the pressure gradient across them, permitting a unidirectional blood flow, as it can seen in Figure 2.1 (A) (Iaizzo, 2015). Of these four, there are two atrioventricular valves (AV) that separate atria from ventricles: the mitral valve in the left heart and the tricuspid valve in the right one; the aortic valve that connects the left ventricle with the aorta; and finally, the pulmonary valve that connects the pulmonary artery with the right atrium.

Moreover, the four chambers are made up of several tissue layers (see Figure 2.1 (B)). From the outside in, the epicardium is the outermost layer, composed of mesothelial cells, connective and adipose tissue. Then, the myocardium is the middle layer and the primary component of the cardiac wall, it is a muscle layer comprised of cardiomyocytes. Finally, the endocardium is the innermost layer formed by endothelial cells. It covers the myocardium and heart valves and continues with the large vessels' endothelium and a layer of subendocardial connective tissue (Dudás, 2023). Apart from that, another layer called the pericardium, a double-walled sac made up of elastic and collagenous matrices, surrounds the heart and extends up the roots of the great vessels and pulmonary veins (Hutchison, 2009).

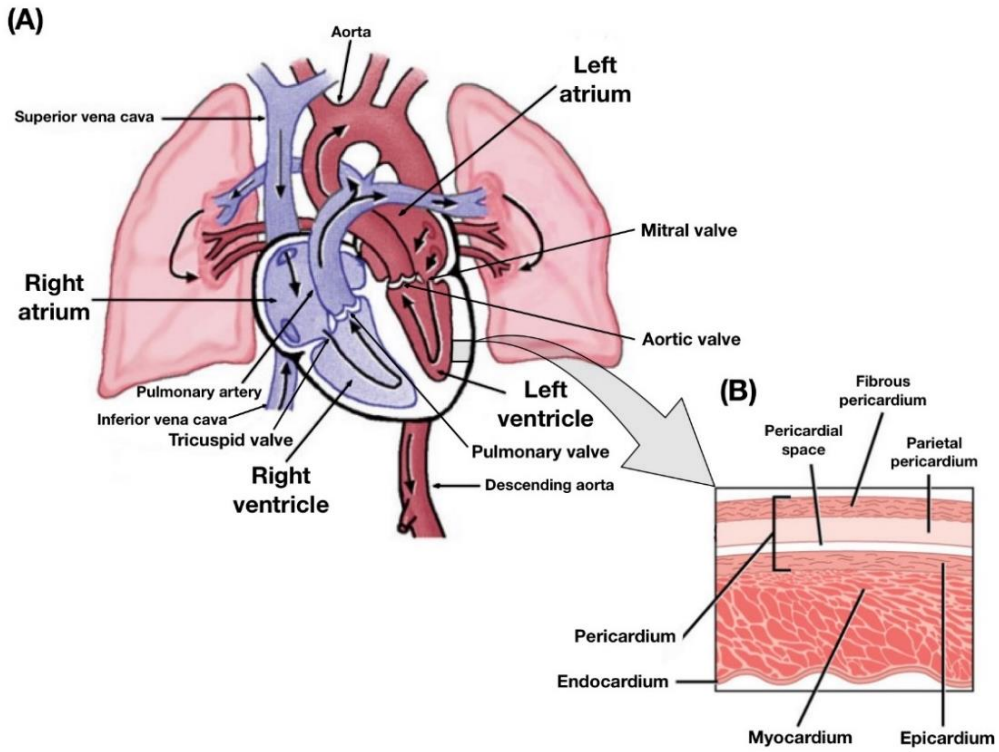

Figure 2.1. Anatomical representation of the heart. (A) shows the four hollow cardiac chambers, the cardiac valves, the main blood vessels, and the blood flow pathway. (B) shows the layers that make up the cardiac wall. Source: modified from Iaizzo (2015) and Molnar & Gair (2022).

2.1.3. Cardiac cycle: the heart as a pump

As mentioned above, the heart is the main component of the circulatory system, since it is in charge of pumping blood to the rest of the organism's tissues. This ability as a pump is due to the cardiac cycle. The cardiac cycle is a sequence of cardiac movements that alternate contraction (systolic phase) and relaxation (diastolic phase) of the atria and ventricles. On the one hand, during the diastole, the heart chambers are relaxed and are filled with blood that is received from the veins. On the other hand, during the systole, the heart chambers contract and pump the blood towards the rest of the organism through the arteries.

In particular, in each beat, when the ventricular systole is produced, the aortic valve opens, and the heart ejects oxygenated blood from the left ventricle to the aorta, which ramifies and, when the blood reaches capillary bed, it supplies the systemic organs' cells with oxygen and nutrients that have been obtained from breath and digestion, respectively. Once the cell metabolism has been produced, the deoxygenated blood with cell wastes is collected, and the veins are responsible for carrying the blood back to the heart, specifically from the superior and inferior vena cava to the right atrium during the diastole. In this way, the systemic circulation closes (see Figure 2.2).

However, once in the right atrium, the blood circulates through the pulmonary circulation. Due to the pressure gradient, the tricuspid valve opens, and the deoxygenated blood passes into the right ventricle during the ventricular diastole. As soon as the right ventricle contracts, the pulmonary valve opens and the deoxygenated blood flows through the pulmonary arteria. After crossing the pulmonary capillary beds, the blood oxygenates and returns to the left atrium through the pulmonary veins. Finally, the cardiac cycle is closed when the mitral valve opens, and the oxygenated blood is spilled on the left ventricle (Anttila & Farrell, 2022; Cohen & Taylor, 2009).

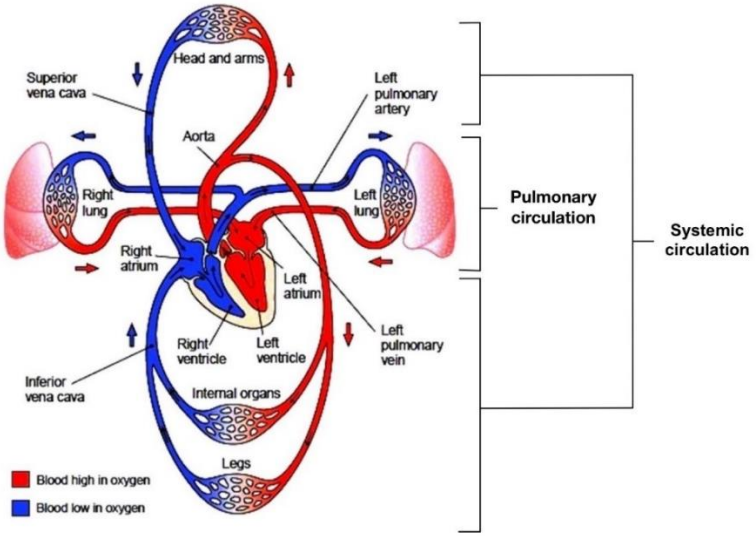

Figure 2.2. Systemic and Pulmonary circulation. Source: modified from Cohen & Hull (2020).

When the organism demands more energy, the heart reacts increasing its beat frequency.

2.1.4. Cardiac Conduction System (CCS)

The aforementioned cardiac cycle takes place thanks to the electric conduction system of the heart (also called the cardiac conduction system, CCS). The CCS produces electrical impulses that excite cardiomyocytes, and then this excitation is followed by their mechanical contraction. In this way, the main objective of the CCS is to ensure the coordinated contraction of the heart chambers, allowing the heart to act as a pump, generating each heartbeat with a determined cardiac frequency.

The CCS is comprised of several specialized cells that are either able to generate electrical activity by themselves (named pacemaker cells) or carry this activity throughout the heart chambers in coordinated way.

Specifically, in a healthy heart, the electrical impulses first originate in the sinoatrial node (SA node, also called sinus node), located in the right atrium. The pacemakers cells of the SA node manifest spontaneous depolarizations and their function is to produce a continuous electrical impulse. Thus, SA node establishes when the heart should contract, and since it has the fastest rate, 70 beats per minute (bpm), it sets the heart rate. Then, the depolarization spreads throughout the atrium thanks to internodal tracts until the excitatory signal reaches the atrioventricular node (AV node). The AV node lies at the lower back section of the interatrial septum in the so-called floor of the right atrium and is the unique electrical communication tract between the atriums and ventricles. As its propagation is slow, it delays the impulse transmission in order to allow optimal ventricular filling during atrial systole. Later, impulses are conducted to the His Bundle (HB, also called common bundle or bundle of His), a set of myocardial cells specialized in electrical conduction. HB bifurcates into the right and left bundle branches, whereby the normal wave of cardiac depolarization propagates through the right and left ventricles, respectively. Finally, the electrical signal spreads through the Purkinje fibers, located in the inner ventricular walls. The electrically excitable cells that compose the Purkinje fibers are responsible for conducting the electrical impulses to ventricular cardiomyocytes, thus provoking the ventricular contraction during diastole (Laske et al., 2015).

However, the binding between calcium and troponin C at myofilaments is actually what initiates muscle contraction. As has been explained above, cardiomyocyte depolarization triggers the opening of the L-type calcium channels; thus, the calcium ions enter the intracellular space and link the

sarcoplasmic calcium release channel thanks to ryanodine receptor 2 (RyR2), inducing a massive release of calcium from the sarcoplasmic reticulum (SR) to the cytosol. This mechanism is called "calcium induced calcium release". When the released calcium binds troponin C, the muscle contraction is produced. Afterwards, the relaxation is produced, pumping back the cystolic calcium. About 70% of this calcium is returned into the SR via the SR calcium ATPasa pump (SERCA2a) and the other 30% is released to extracellular space mainly by the sodium-calcium exchanger (NCX) (Feldman & Mohacsi, 2019). All this process where cardiomyocyte contraction and relaxation take place is called excitation-contraction coupling.

Relationship between CCS, AP from each CCS' region and ECG

At the same time that the excitatory wave spreads throughout the cardiac muscle, cardiomyocytes' cell membrane depolarizes, increasing the value of its membrane potential, and repolarizes, decreasing it and returning to the resting state.

All these electrical events associated with the myocardium contraction and relaxation produce electrical dipoles. The summation of individual dipoles generates general electrical vectors with a determined magnitude and direction. Body surface electrodes can record these electrical waves, providing a method for visual representation of cardiac electrical activity as a function of time, the electrocardiogram (ECG).

Figure 2.3 shows how the depolarization and repolarization waves of the different heart structures give rise to the principal ECG components: the P-wave, the QRS-complex, and the T-wave. The P-wave represents the moment in which the atrial depolarization is produced, and the blood is spilled through the ventricles. The QRS-complex includes the whole electrical activity of the ventricle depolarization and subsequent atrial repolarization. The interval comprised between P-wave and R-wave, called PR-segment, is the period where the atrial plateau happens while the ventricles are still at rest. The T-wave represents the electrical activity produced during the ventricular relaxation once the blood has been ejected from the ventricles. The period between S and T wave is called ST-segment and represents the ventricular plateau while the atria are repolarized. Finally, the U-wave is related to the slow repolarisation of Purkinje fibers, but this is not always detected (Anttila & Farrell, 2022).

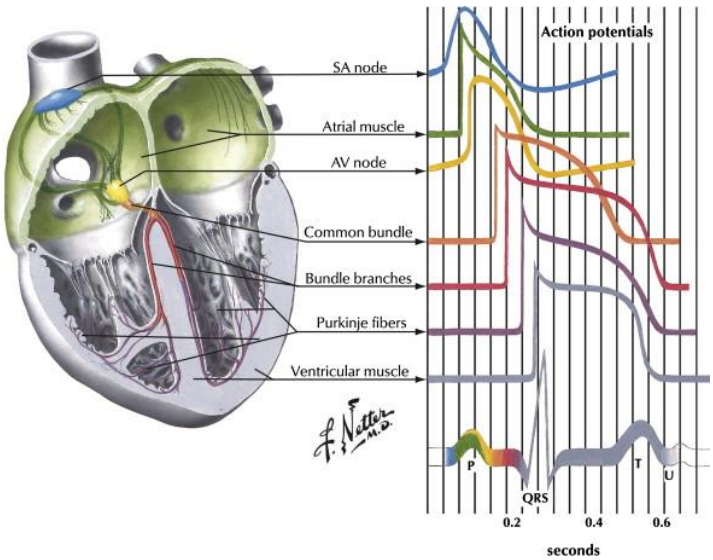

Figure 2.3. Relationship between action potential from CCS' components and the surface electrocardiogram (ECG). Source: taken from Saranzan (2014).

2.2. CARDIAC ELECTROPHYSIOLOGY

2.2.1. Cardiomyocyte membrane

As stated above, the heart is a muscular pump whose cardiac muscle cells are called cardiomyocytes. Cardiomyocytes can develop a rhythmic electrical activity that provokes the contraction of the whole cardiac muscle. The excitability of the cardiomyocyte membrane is the principal mechanism of their depolarization and contraction, which describes the ability of the cell to depolarize to initiate an action potential. All this cardiac electrical activity depends on sodium, potassium, calcium, and chloride ion fluxes through the cell membrane (Sigg et al., 2010). The cell membrane is composed of a phospholipid bilayer whose function is to separate the intracellular fluid from the outside, each one of which presents different ionic concentrations. As the membrane is insulating and both environments are conductors, the electrical equivalent for these three components is a capacitive branch of 1μF/cm^2 (Hall, 2011).

Although the cell membrane is not permeable, it has numerous proteins embedded, forming microscopical structures and allowing the passive or active transport of ions across the membrane. The ionic movements are propelled by two forces: diffusion and electric field. On the one hand, as a consequence of the differences in the ionic concentrations between intra- and extracellular compartments, the tendency is for the ions to move from the area of greater to lower concentration due to diffusion forces. In this case, the direction of the ionic movement never changes because the ionic concentrations do not alter enough to modify it. On the other hand, the electric field establishes ionic movement depending on the ion's charge. A positive charge tends to move from the area of greater to lower potential, while a negative one follows the inverse path. As the electric field depends on membrane potential (V_m), the direction of ionic movement will change according to the latter (Sigg et al., 2010).

The diffusion and electric field gradients for each one of the main ions are shown in Figure 2.4.

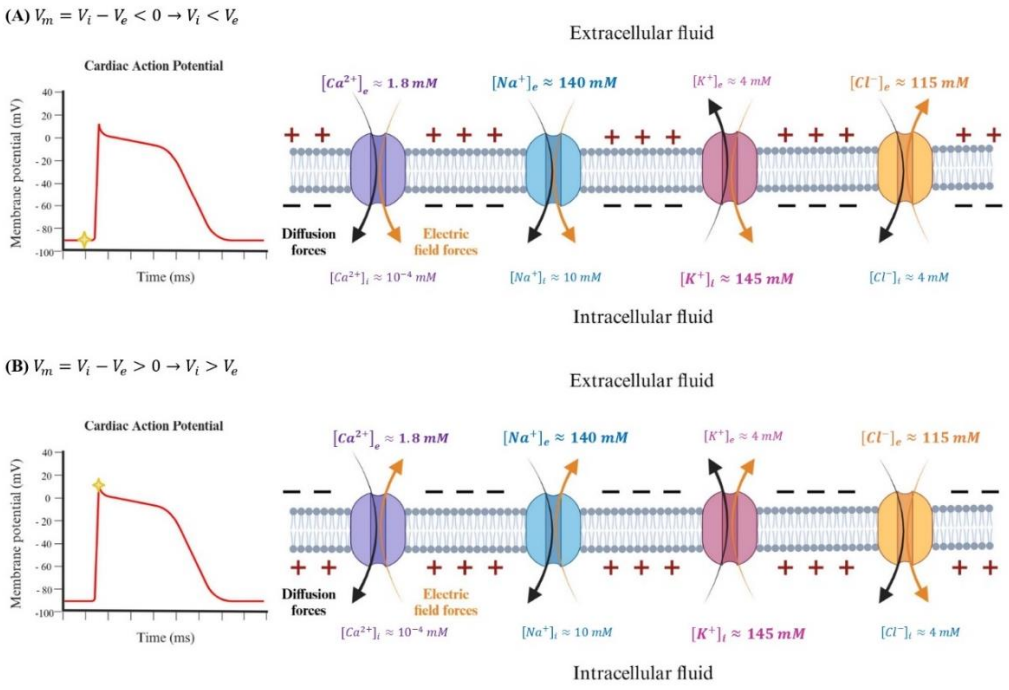

Figure 2.4. Ion currents due to diffusion and electric field gradients. (A) The membrane potential is negative because the intracellular potential is lower than the extracellular. (B) The membrane potential is positive because the intracellular potential is greater than the extracellular. Source: own elaboration based on Ferrero (2022). Created with BioRender.com.

2.2.2. Mechanisms of transport.

As previously mentioned, some specific transport mechanisms are needed, classified as passive and active. Passive mechanisms are the ones that do not require external energy, for instance, ion channels, exchangers, and cotransporters. Apart from the ion movement down the electrochemical gradient, intracellular ionic concentrations are balanced by active transport via pumps, which need energy to move ions across the cell membrane against the concentration gradient (Sigg et al., 2010).

Ion channels

Ion channels are protein complexes that consist of pore-forming subunits that span through the cell membranes. The pores are selective for specific ions, and thanks to their hydrophilia, they allow ions to avoid the membrane's hydrophobic core that would otherwise slow or block their entry into the cell. The ion flux across the cell membrane can be measured with an electric current.

Most ion channels have different conformational states promoting gate mechanisms that, in turn, allow ion channels to vary between two states, conducting (open channel) and non-conduction (closed or inactivated channel). These different states can be modulated by several factors, such as changes in membrane potential, ligand binding, protein-protein interaction, intracellular second messengers and metabolites, among others (Petkov, 2009).

However, the ion channel state, open, closed, or inactivated, is a stochastic matter, but fortunately, the probability of each state can be calculated. Each probability may depend on different factors according to the type of channel. For instance, in the case of voltage-gated channels, the probability of the opening or closing of a channel depends on the state of activation and inactivation gates. These gates are presented in different quantities in each type of ion channel and their state depends on the membrane potential; the probability of opening activation gates increases with increasing membrane potential, whereas the probability of opening inactivation gates decreases, as shown in Figure 2.5 (Ferrero, 2022).

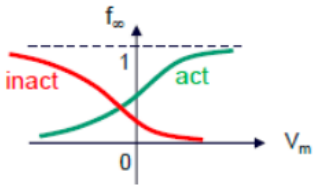

Figure 2.5. Opening and closing probability curves of the voltage-dependent activation and inactivation gates. Source: taken from Ferrero (2022).

Only in the case where the ion channel is open will there be ionic current by both diffusion and electric field, as mentioned in section 2.2.1.

Exchangers

The main objective of ion exchange is to exchange ions between intracellular and extracellular spaces. Na^+–Ca^{2+} and Na^+–H^+ exchangers are the most significant. On the one hand, Na^+–Ca^{2+} exchanger extracts one intracellular Ca^{2+} ion for every three extracellular Na^+ ions it takes into the cell. It uses the favourable sodium gradient to extract calcium without requiring extra energy. On the other hand, the Na^+–H^+ exchanger extracts a proton from the cell to the extracellular space, taking advantage of the energy that is supplied for each extracellular Na^+ ion it carries into the cell thanks to diffusion gradients. It contributes to the pH regulation (Jennings, 2018).

Cotransporters

Cotransporters are transport mechanisms in which the energy produced for an ion when it gets out the intracellular space passively is used to extract another ion at the same time. This is the case of Cl^- - K^+ cotransporter that is the basic extraction mechanism of chlorine ion. When a K^+ ion leaves the intracellular space by diffusion gradients, it provides enough energy to also extract a Cl^- despite the unfavourable chlorine gradient (Johnsen et al., 2023).

Pumps

Unlike passive mechanisms, active mechanisms such as pumps need an extra energy input because of the movement of the ions is opposite to the diffusion gradient or electric field gradient. Two types of pumps stand out: exchanger pumps and single-ion pumps. Na^+ - K^+ pump is an exchanger pump, in which for every two K^+ ions that enter the cell, three Na^+ ions leave it. Ca^{2+} pump, for its part, is a single-ion pump in charge of extracting calcium from the intra to the extracellular space (Stapleton et al., 2014).

2.2.3. The action potential

Cardiac myocytes are electrically excitable, thus being able to conduct electrical impulses, which allows cardiac pumping. Contraction of each cardiomyocyte is initiated when it receives a big enough electric excitation; such excitation promotes a voltage change in the cell membrane called the cardiac action potential (AP). As cardiac myocytes are electrically connected, the AP is transmitted to all heart muscle cells in each heartbeat, and the fast and controlled spread of the AP fosters that the cardiac muscle contracts to produce the diastole (Vornanen et al., 2023).

When the electrical and chemical forces are exactly equal, and so the net sum of all the ionic currents that pass through the membrane is zero (there is no net movement of ions across the cell membrane), there is a transmembrane potential that is called the resting membrane potential (V_{rest} or RMP). The value of V_{rest} is a weighted average of the equilibrium potentials of the different ions. In the case of cardiomyocytes, as in the rest state, almost all ion channels are closed except for K_1 family channels, the cardiomyocytes resting membrane potential is almost equal to potassium equilibrium potential. For this reason, in most cardiac cells, the V_{rest} is about -85 to -90 mV (Iaizzo, 2010; Sigg et al., 2010).

As shown in Figure 2.6, the AP can be explained in phases ordered in time sequence. Before an AP begins, the ions maintain the resting membrane potential thanks to their equilibrium potentials. The AP is initiated with the depolarization phase (phase 0), in which the membrane potential increases to positive values due to the entrance of Na^+ inside the cell by the activation of fast Na^+ channels. Then, phase 1 begins with the inactivation of Na^+ channels and the potassium output by the opening of transient outward K^+ channels (I_{to}). This phase corresponds to an initial repolarization with a notch shape on the AP waveform. Afterwards, there is a plateau (phase 2) in which the change in the value of V_m is much slower because competition occurs between the entrance of calcium current through Ca^{2+} channels and the exit of K^+ through open K^+ channels. When inactivation gates of Ca^{2+} channels close, the calcium channels are inactivated, so the membrane potential decreases due to potassium output, resulting in the repolarization phase (phase 3). During this third phase, the V_m returns to negative polarity. While the repolarization phase is taking place, the membrane potential decreases enough to close potassium channel activation gates. The remaining potassium ions exit through the ungated K_1 channels until the resting membrane potential is reached again (phase 4).

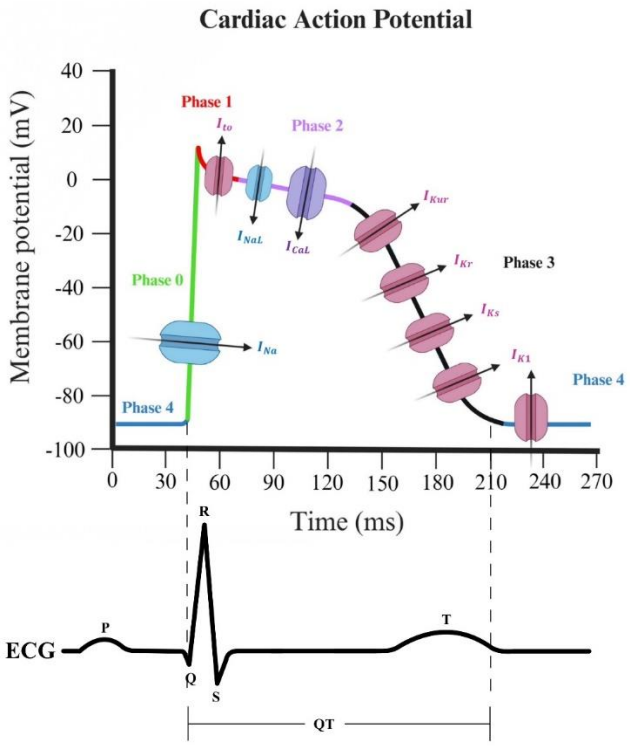

Figure 2.6. Diagram of the phases that make up the cardiac action potential, their associated currents and correlation with the ECG. Source: own elaboration based on Beledo et al. (2013) and Rosen & Pham (2004). Created with BioRender.com.

Moreover, considering that the electrical waveforms of an ECG are the result of local action potentials recorded from the various regions of the heart (see Figure 2.3 and Figure 2.6), the duration of QT interval in an ECG reflects the AP duration (APD) of millions of individual ventricular cells in situ. For this reason, the measurement of single-cell APD can estimate the QT interval duration. Using single ventricular cardiomyocytes APD to estimate changes in the QT intervals, clinical data indicates there has been an increasing appreciation that women have faster resting heart rates and longer rate-corrected QT intervals (QTc) than men. This means that women are at greater risk of arrhythmia and there is a female predisposition towards the life-threatening arrhythmia called *torsades de pointes* (TdP) (Rosen & Pham, 2004).

2.3. PATHOLOGIES

As the main aim of this thesis has been modelling the effect of some drugs in unhealthy hearts, it is necessary to explain the diseases that have been modelled: heart failure (HF) and hypertrophic cardiomyopathy (HCM).

2.3.1. Heart Failure (HF)

During the years there have been many definitions of HF, but nowadays the most agreed one is that HF is a clinical syndrome caused by a heart structural or functional alteration, and it is characterized by signs like peripheral oedema, elevated jugular venous pressure and pulmonary rales and symptoms such as dyspnea, fatigue and ankle swelling. As it is important to demonstrate the underlying cause of the cardiac abnormality, its most used evaluation is done by use of two-dimensional echocardiography coupled with Doppler flow studies.

There are two different types of HF according to the measurement of the cardiac function calculating EF: HF with Reduced Ejection Fraction (HFrEF) and HF with Preserved Ejection Fraction (HFpEF). Several studies have estimated that about half of HF patients suffer from HFrEF, which are patients with a systolic dysfunction defined by having an EF value $\leq 40\%$, coexisting with symptoms and signs typical of HF. On the other hand, HFpEF is much more difficult to define. This type of HF includes a percentage of patients greater than 50%, which is not as low as EF values considered in HFrEF, but they still are not normal EF values. The prevalence of HFpEF is increasing, and it is estimated to vary between 40% and 70% depending on the EF values used as a threshold. However, patients with an EF value between 41% and 49%, are not included in these two subtypes, for this reason, some guidelines define a third subtype of HF patients called Heart Failure Mid-range (HFmrEF) or borderline HFpEF.

Moreover, the prevalence of HF appears to increase with age, and it is known that HF is heavily underdiagnosed, in spite of having a progressively increasing incidence across age groups and being greater in men than in women. These findings, together with the fact that the mean age of the population of more developed countries is increasing, are strongly contributing to the so-called HF epidemic, which makes necessary new diagnoses and therapies to mitigate the consequences of HF.

Talking about risk factors, HF is associated with both cardiovascular as well as non-cardiovascular comorbidities. However, risk factors may vary in prevalence depending on the HF type. Generally, patients with hypertension (HT), diabetes (DM), atherosclerotic disease, obesity, atrial fibrillation (AF) and with three of the following five metabolic syndromes: abdominal adiposity, hypertriglyceridemia, low high-density lipoprotein, HT and fasting hyperglycemia, are at high risk of developing HF. With regard to the most frequent non-cardiac comorbidities, there are chronic kidney disease, anemia, chronic obstructive pulmonary disease, sleep-disordered breathing and depression.

Furthermore, unfortunately, many studies demonstrated that HF has an elevated morbidity and mortality as well as a poor quality of life and a high social cost. Despite using guidelines recommended drugs, the death rate in HF and the number of hospitalizations are still unacceptably elevated. As a consequence, there is a need to study how to prevent HF. One option is trying to reduce the risk factors due to the fact that many of them are modificable. On the one hand, studies have evidenced that treating HT is the most effective strategy for preventing HF. On the other hand, DM and HF are commonly comorbid diseases and the problem is that the prevalence of DM is increasing. Insulin resistance and hyperflycemia induce myocardical dysfunction causing the so-called diabetic cardiomyopathy. Therefore, controlling DM may be a way to prevent HF. Another possibility is to use biomarkers as a screening tool in order to improve the early diagnosis. Moreover, some studies have shown that living a healthy lifestyle might prevent HF to this extent. All in all, the best initiatives to prevent HF are practicing healthy habits and having a correct blood pressure.

Undoubtedly, HF patients have a poor prognosis in spite of actual treatments. In fact, some studies have determined that the mortality is higher than the one found in other common malignant diseases. As the age of HF patients and the proportion of HFpEF are increasing, there is a great interest in seeking the mortality differences between HF subtypes. Although both of them have a similar and substantial mortality, the difference is that there is an actual treatment for HFrEF patients but not for HFpEF ones, so the found survival improvement is more evident in HFrEF patients (Feldman & Mohacsi, 2019).

The real issue lies in the inter- and intracellular mechanisms of HF that are underneath cardiac dysfunction. What underlies muscle contraction has been explained in section 2.1.4; however, in a failing heart, cardiomyocyte contraction function is characterized by being reduced as a consequence

of inadequate excitation-contraction coupling. These defects show up in changes in the calcium transient because its amplitude reduces, its duration increases, its decay prolongs and the cytosolic calcium concentration in diastole increases. In addition, the SR calcium content is commonly reduced as a result of reduced SERCA2a activity and the fact that RyR2 channel becomes leaky in the failing cardiomyocytes. Thereby, there is a reduction of calcium release from the SR in systole, leading to a reduced myofilament contraction. Moreover, as the NCX exchanger is less effective in ejecting calcium from intra- to extracellular space, the diastolic calcium abundance increases, resulting in impaired cardiomyocyte relaxation. This phenomenon may trigger delayed after-depolarisations precipitating arrhythmias. Health scientists are evaluating multiple potential treatment approaches to handle disturbed excitation-contraction given in HF (Feldman & Mohacsi, 2019).

Furthermore, HF habitually goes with cardiomyopathy (CM), which is a disease characterized by a morphologically abnormal myocardium. CM includes the second pathology that is going to be described in this thesis, hypertrophic cardiomyopathy (HCM) (Feldman & Mohacsi, 2019).

2.3.2. Hypertrophic Cardiomyopathy (HCM)

HCM is a common genetic cardiovascular disease of the myocardium in which a section of cardiac muscle is thickened (hypertrophied) without any cause, and in the absence of valve disease or other clinically significant loading conditions. HCM is characterized by presenting larger cardiomyocytes, resulting in thickening and disrupting both the cellular alignment and electrical functions of the heart. All these complications lead to an impaired filling and outflow, thus limiting the heart output.

There are four HCM subgroups according to the developed morphological patterns of hypertrophy: reversed curvature, neutral, sigmoid and apical HCM, and epidemiological parameters change between them (Naidu, 2019). It is estimated that its prevalence is in a range of 0.02 to 0.23% in adults, being more common in males. Nevertheless, even though women prevalence is between 30-40% of HCM cohorts, they appear to have more symptoms and a worse prognosis than men (Feldman & Mohacsi, 2019).

However, although HCM is a complex disease, the most common symptoms are dyspnea, arrhythmias and palpitations, chest pain, syncope, dizziness and fatigue, and it may result in stroke or SCD (caused by tachycardia or ventricular fibrillation) and progression to HF. It should be emphasised that approximately 50% of HCM cases present some degree of HF.

Talking about mortality, HCM-related deaths are due to not only the three above-mentioned feared outcomes, SCD, stroke-related and HF-related deaths, but also the ones related to complications produced in transplant and interventional procedures. Definitely, the high risk of dying suddenly falls on those patients who develop progressive HF with dyspnea and functional limitations or who develop paroxysmal or chronic AF. Specifically, AF is a very common arrhythmia in patients with HCM accompanied with systolic dysfunction and advanced HF and it is linked to elevated age, impaired left atrial EF or greater left atrial volume (Naidu, 2019).

Studies have shown that HCM cardiomyocytes have abnormally prolonged action potentials. The inter- and intracellular phenomena underlying this abnormality are an increment in the late sodium current and a prolongation of calcium transients with diastolic calcium overload and myocyte tension development. In turn, all these alterations lead to prolonged APD and early afterdepolarizations (EADs) and enhance arrhythmogenicity (Naidu, 2019).

2.4. BIOELECTRICITY OF CARDIAC ARRHYTHMIAS

A regular heart rate is characterized by an orderly activation and recovery of myocardium electrical excitation. It is necessary in order for the heart diastole and systole to provide enough force for pumping oxygenated blood to peripheral tissues and propelling deoxygenated blood away from them. However, there are several phenomena that lead to abnormalities in the generation of electrical impulses like the ones initiated at wrong sites or disruptions in normal electrical heart pathways. A coexistence of these two types of alterations can provoke an irregular heart rate, so-called arrhythmia or dysrhythmia (Tse, 2016).

The normal heart rate is also known as sinus rhythm because it begins at the sinus node. It is 60-100 bpm; for this reason, when the heart rate exceeds 100 bpm, it is defined as tachycardia, and when it is below 60 bpm, it is called bradycardia. Although the two above-mentioned situations can be physiological, they can also be pathological when we talk about arrhythmias. Dysrhythmias are classified as supraventricular and ventricular. The most common cardiac arrhythmias are atrial fibrillation for the first case and ventricular tachycardia (such as *Torsades de pointes* (TdP)) and ventricular fibrillation for the second one (Ferrero, 2022).

Regarding abnormal electrical impulses, also called triggered activity, can be promoted by several factors, such as ventricular ectopicity, which is due to a heterogeneity in the repolarization. In such a case, triggered activity is caused by the premature activation of cardiac tissue, which in turn results from afterdepolarizations. Afterdepolarizations are depolarizations unleashed by other preceding AP. As Figure 2.7 shows, this phenomenon is classified into two types: early afterdepolarizations (EADs), which in turn are divided into two subtypes, the ones that occur early (phase 2) or late (phase 3); and delayed afterdepolarizations (DADs), which are the ones that occur during the last phase (phase 4) of the AP (Tse, 2016).

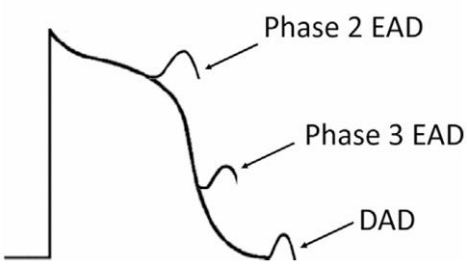

Figure 2.7. Afterdepolarization phenomena: phase 2 EAD, phase 3 EAD and DAD. Source: figure taken from Tse (2016).

DADs and EADs are similar phenomena, both take place when there is an intracellular calcium overload and a release of calcium from the SR, as explained in the following section 2.4.1. However, the difference lies in the AP's phase when that release occurs, before and during the repolarization phase in the case of EADs and in the resting phase in the case of DADs. Despite the differences, both seem to be implicated as the mechanisms underneath arrhythmogenesis in AF cases (Tse, 2016).

2.4.1. Abnormal impulse. Afterdepolarizations: EADs and DADs

As it has been stated, EADs can develop during the second and third phase of human cardiac action potential. EADs are commonly associated with prolonged APDs, even though not exclusively, because they also have been related to shortened APD.

Firstly, phase 2 EADs are more associated with prolonged APD that can be caused by an increase in the late sodium current (I_{NaL}), the calcium current (I_{Ca}) or I_{NCX}, or a decrease in potassium currents (I_{Kr}, I_{Ks}, I_{K1}) responsible for repolarization. On the one hand, L-type Ca^{2+} channels can be reactivated

by depolarizing shifts in the membrane potential, thereby the increased I_{CaL} further depolarising the membrane, initiating a positive feedback loop that triggers an AP. On the other hand, when the membrane potential has negative values regarding the threshold of I_{CaL} activation, SR can release calcium ions. The resulting increase of intracellular Ca^{2+} load can lead to an activation of I_{NCX}, resulting in membrane depolarization.

Secondly, phase 3 EADs have been more associated with shortening in APDs. In this case, although normal calcium release from SR is permitted, if the intracellular calcium concentration stays elevated when the membrane potential is negative in relation to the equilibrium potential for the NCX exchanger, I_{NCX} can activate, leading to membrane depolarization.

Moreover, with regard to DADs, characterized by developing after the repolarization finishes, are observed when there is an intracellular calcium overload as well as EADs. In this case, the unique proposed mechanism underlying the origin of DADs is that high intracellular calcium levels promote spontaneous calcium liberation from the SR, thus activating a transient inward current (I_{TI}) composed by three activated currents: non-selective cationic current (I_{NS}), I_{NCX} and the calcium-activated chloride current ($I_{Cl,Ca}$). This I_{TI} is the one responsible for membrane depolarization.

In every case, if the alterations in membrane potential caused by EADs or DADs are large enough, I_{Na} will be activated causing triggered activity. All these phenomena are thought to be underneath the arrhythmias noticed in HF and QT syndrome (Tse, 2016).

2.4.2. Abnormal impulse conduction. Re-entries.

The cardiac electrical impulse propagates thanks to the wavefront advance. The wavefront is the area of depolarized cardiomyocytes while cardiac impulse expands, excitating the neighbouring cells. However, after the PA, there is a period of time during which the excited cell becomes refractory and is unable to re-excite or respond to an electrical stimulus, this interval is called refractory period (Pandit & Jalife, 2013). Taking that into consideration, re-entry occurs when there is a change in the PA propagation pathways, promoting that a region that has recovered from refractoriness is reactivated. There are two types of re-entries: circus-type, which are the ones that are promoted by the presence of obstacles (like scars or alterations in the cardiomyocytes refractory period), around which an action potential can advance; and reflection or phase 2, which are the ones in which re-entries occur without the presence of an obstacle. All these alterations can cause quick, slow or irregular cardiac beats, promoting arrhythmias (Tse, 2016).

2.5. PHARMACOTHERAPY

Pharmacotherapy is defined as the science in which one or more pharmaceutical drugs are used as a non-invasive therapy to prevent and treat diseases and their underlying symptoms and conditions. Specifically, cardiovascular drugs are designed to have an impact on the running of the heart and blood circulation. However, there seem to be other non-cardiovascular drugs that have antiarrhythmic and proarrhythmic effects on patients' hearts due to their influence in some ionic channels altering inward and outward currents during AP. Moreover, as it has been explained in section 2.4, the alteration of some ionic currents can lengthen the APD, which is a proarrhythmic factor.

Having said this, a pharmacological drug that excessively lengthens the APD is proarrhythmic and vice versa. For example, a pharmaceutical drug able to block inward currents such as calcium ones, will be an antiarrhythmic drug because of the resulting APD shortening. Nevertheless, proarrhythmic drugs are the ones that are able to inhibit outward currents, such as potassium ones, delaying the repolarization and thus lengthening the AP duration.

In section 2.2.2 the gating model of ion channels has been explained. It is known that ion channels have several conformational states that are associated with a specific probability of opening and closing of the channel. To sum up, in the gating model of ion channels, these conformational states are understood using a gateway approach in which gates control the ion movement across the channel. Apart from the explained voltage-dependent channels, there are also ligand-dependent channels, whose opening depends on the concentration of a specific molecule because this type of channel has receptors with binding affinity for certain ligands, which are exogenous and endogenous molecules. When the ligand-receptor union happens, the opening and closing probability changes. Moreover, there are ligand-activated and ligand-inactivated gates, in which they tend to open or close when the ligand binds to the receptor, respectively. However, in some channels, there seems to be more than one receptor; this fact is taken into account with the so-called Hill coefficient. Thereby, once all receptors are occupied, the channel opens or closes with an opening and closing rate, respectively. In conclusion, the opening fraction of a ligand-dependent channel depends on the opening and closure rates, Hill coefficient and ligand concentration.

With all this, as a ligand can be a drug, this above-explained approach is used to model how some drugs affect several ion channels and, in turn, the bioelectrical response of the cell. Nevertheless, in the case of pharmaceuticals, the half-maximal excitatory concentration (EC_{50}) and the half-maximal inhibitory concentration (IC_{50}) are used instead of opening and closure rates. EC_{50} and IC_{50} are equivalent to the concentration of a determined drug that is able to excite or inhibit, respectively, 50% of the channels it affects. For drugs, each parameter can be determined by obtaining a dose-response curve using the patch-clamp technique. Moreover, there is another parameter called EFTPC (Effective Free Therapeutic Plasma Concentration) which is used to quantify the drug concentration in plasma that is available to produce therapeutic effects.

Therefore, depending on which channels are affected and how strongly, a drug can be either pro- or anti-arrhythmic, and thus may be the cause of afterdepolarizations, arrhythmias, TdP… or be used as a therapy. In this thesis, the effect of a list of inhibitory drugs and their combination on different cardiomyocyte ion channels will be modelled under different conditions in order to determine their use to treat the effects of HF and HCM on cardiomyocyte bioelectricity (Ferrero, 2022).

2.6. MATHEMATICAL MODELS OF ACTION POTENTIALS

In biomedical engineering, mathematical models in conjunction with computer tools permit the creation of computational models, so-called *in silico*. *In silico* models are used to simulate and study the behaviour of the system they reproduce in hypothetical situations to understand electrophysiology, illnesses, pharmacological therapies, and new treatments, among others (Doke & Dhawale, 2015).

Specifically, cardiac computational models are based on mathematical descriptions with a lot of biophysical and electrophysiological detail, they are therefore a useful quantitative tool used to study drug efficacy and security and their effect on the heart running. For this purpose, these models reproduce ion channels' behaviour in order to accurately represent the multi-scale nature, because everything that happens at the microscopic or cellular level must be able to explain what happens at the macroscopic level.

In this thesis, computer-generated simulations are going to be used as a complementary tool to clinical trials to analyse the effect and efficacy of several drugs on the bioelectrical behaviour of cardiomyocytes in different situations. Therefore, the value of biomarkers defined on the variables of interest of the system are going to be taken into consideration. Consequently, using computational

models, researchers obtain a significant reduction in both, time and cost in the process of developing a new drug, thus obtaining a greater economic and social benefit.

2.6.1. Hodgkin–Huxley (HH) formalism. Electrical model of a cell

Hodgkin–Huxley (HH) formalism is a detailed mathematical model that describes the excitability dynamics of nerve and muscle cells. It considers ion channels as gates that can open or close depending on membrane potential and other stimuli. This model is able to reproduce both the AP of an excitable cell and underlying ion currents. For this purpose, in an electric circuit analogy, Hodgkin and Huxley simplified the cell membrane and all ion channels crossing it, as Figure 2.8 shows (Sigg et al., 2010).

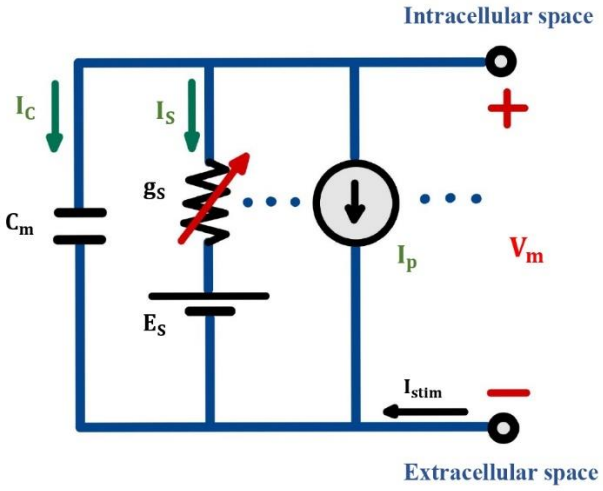

Figure 2.8. Electrical model of a cell. Source: modified from Ferrero (2022).

In the electric circuit analogy, the external stimulation current (I_{stim}) can be carried through the membrane by both, charging the membrane capacity (C_m) and ions' movement through the several mechanisms of transport which form conductive branches in parallel with the capacity. Specifically, the ionic current is divided into two components, ion channels and other mechanisms of transport (Hodgkin & Huxley, 1952).

On the one hand, as ion channels are proteins with selective pores that offer resistance to ions' passage, the term conductance (g_S) is used to express this phenomenon related with the facility of an ion channel for the passage of ions though its pore. Moreover, as has been stated, ion channel gates are the equivalent to protein structures that conform the channels, and which experience conformational changes according to the voltage or ligand concentration. For this reason, in order to represent this phenomenon accurately, in HH formalism voltage and ligand-dependent channels coexist. In short, as the electrical properties of membranes are governed by Ohm's law, each ionic current (I_S) is determined by a driving force, which is considered as an electrical potential difference, and a permeability coefficient with the dimensions of conductance, which are in series conforming the S ion channel's branch. Thus, mathematically, for a specific ion (S), its ion current (I_S) is equivalent to its conductance (g_S) multiplied by the difference between the membrane potential (V_m) and its equilibrium potential (E_S), representing the electric field to which the ions are subjected and the diffusion forces, respectively (Hodgkin & Huxley, 1952; Sigg et al., 2010).

On the other hand, the other mechanisms of transport, like pumps, exchangers and cotransporters, are represented by a current source (I_p).

Therefore, to obtain the equation of the electric circuit mathematically, the first Kirchhoff's law, which states that the sum of currents must be equal to zero, is used. According to this, the sum of the current that crosses the capacitor (I_C), ionic currents across the ion channels (I_S), the currents related with pumps, exchangers and cotransporter (I_p) and external stimulation current (I_{stim}) must be zero (see equation 1).

$$I_C + I_S + I_p + I_{stim} = 0 \qquad (1)$$

Moreover, considering that I_C can be mathematically defined by equation 2 and, as mentioned above, I_S is equal to equation 3 (Hodgkin & Huxley, 1952).

$$I_C = C_m \cdot \frac{dV_m}{dt} \qquad (2)$$

$$I_S = g_S \cdot (V_m - E_S) \qquad (3)$$

Considering equations 1, 2 and 3, equation 4 is obtained.

$$C_m \cdot \frac{dV_m}{dt} + \sum g_S \cdot (V_m - E_S) + I_p + \sum I_{stim} = 0 \qquad (4)$$

Additionally, considering that g_S impedance is modelled according to its dependence on V_m and ligand concentration, thus representing both voltage and ligand-dependent channels, its value is equal to equation 5, in which N_S is the number of S family channels, γ_S is the unit conductance (pS), and f_S is the fraction of open channels or probability of channel opening. Also, with regard to this last parameter, as the open and closed state of the gates is modelled probabilistically based on the principle of independence, if there is no competition between ligands, the f_S can be calculated as the product of the probability of finding each of the gates in the channel open as shown in equation 6 (Ferrero, 2022; Plonsey & Barr, 2007).

$$g_S(V_m, [ligand]) = N_S \cdot \gamma_S \cdot f_S(V_m, [ligand]) \qquad (5)$$

$$f_S(V_m, [ligand]) = f_{V1}(V_m) \cdot f_{V2}(V_m) \cdot \ldots \cdot f_{Vn}(V_m) \cdot f_{L1}([L]) \cdot f_{L2}([L]) \cdot \ldots \cdot f_{Lm}([L]) \qquad (6)$$

Besides the fact that, according to equation 6, a channel is open based on the joint mechanism of all voltage and ligand-dependent gates, these two are modelled differently.

On the one hand, in order to mathematically model the fraction of open voltage-dependent channels, two V_m-dependent parameters, called opening ($\alpha(V_m)$) and closing rate ($\beta(V_m)$), are necessary. Respectively, both represent the average time in which a closed channel becomes open and vice versa. As this process is not linear, it is necessary to use infinitesimal periods to calculate the number of channels that open. For this reason, the fraction of open voltage-dependent channels is defined from the following differential equations, which in turn, allow determining the activation and inactivation curves of a voltage-dependent gate.

First, as we need to determine the infinitesimal changes of open channels, we have to use differentials (dN_o). As equation 7 shows, N_o can be defined by both the product between N_S and f_S and the difference between the closed channels that have opened and the opened channels that have closed.

$$dN_o = d(N_s \cdot f_S) = \langle N_{c \to o} \rangle - \langle N_{o \to c} \rangle \qquad (7)$$

Then, to know how many channels were closed and afterwards have opened and vice versa, we have to multiply the number of closed/opened channels by the opening/closing rate times the infinitesimal time difference, as equations 8 and 9 show.

$$\langle N_{c \to o} \rangle = N_S \cdot (1 - f_S) \cdot \alpha_S \cdot dt \qquad (8)$$

$$\langle N_{o\to c}\rangle = N_S \cdot f_S \cdot \beta_S \cdot dt \qquad (9)$$

Finally, using equations 8 and 9 in equation 7 and considering that N_S is constant, equation 10 is obtained, in which it is evident that f_S depends on time and V_m.

$$N_S \cdot df_S = [(1-f_S)\cdot\alpha_S - f_S\cdot\beta_S]\cdot N_S\cdot dt \rightarrow \frac{df_S}{dt} = (1-f_S)\cdot\alpha_S - f_S\cdot\beta_S \qquad (10)$$

However, this latter equation is transformed to use two more understanding and quantifiable parameters, stationary fraction of open channels (f_∞) and time constant associated with them (τ_f), whose equations are 11 and 12, respectively.

$$f_\infty(V_m) = \frac{\alpha_S(V_m)}{\alpha_S(V_m)+\beta_S(V_m)} \qquad (11)$$

$$\tau_f(V_m) = \frac{1}{\alpha_S(V_m)+\beta_S(V_m)} \qquad (12)$$

Lastly, using 11 and 12, equation 10 is transformed into equation 13.

$$\frac{df_S}{dt} = \frac{f_\infty(V_m) - f_S(t)}{\tau_f(V_m)} \qquad (13)$$

On the other hand, in order to mathematically model the fraction of open ligand-dependent gates, different parameters have to be taken into consideration, ligand concentration ([L]), number of receptors (H) and opening (k_o) and closing (k_c) rates. Applying the same operations as for the voltage-dependent gates but considering equation 14 for the closed channels that have been opened, the infinitesimal changes in the number of opened ligand-dependent gates is determined in equation 15.

$$\begin{aligned}\langle N_{c\to o}\rangle &= N_S\cdot(1-f_S)\cdot[L]_1\cdot V_1\cdot[L]_2\cdot V_2\cdot\ldots\cdot[L]_H\cdot V_H\cdot k_o\cdot dt \\ &= N_S\cdot(1-f_S)\cdot([L]\cdot V)^H\cdot k_o\cdot dt \qquad (14)\end{aligned}$$

$$df_S = [(1-f_S)\cdot[L]^H\cdot V^H\cdot k_o - f_S\cdot k_c]\cdot dt \rightarrow \frac{df_S}{dt} = [L]^H V^H K_o(1-f_S) - k_c f_S \qquad (15)$$

Then, considering that k_o and k_c are not dependent on V_m and ligand concentration is constant, the probability that ligand-dependent gates are opened (f_S) is also constant, so its derivative is zero. Taking all this into account, the consequent operations lead to equation 16, in which the fraction of open ligand-activated gates can be calculated.

$$f_{S,ligand-activated} = \frac{1}{1+\left(\frac{K_m}{[L]}\right)^H} \qquad (16)$$

In the equation 16, K_m is called the semi-activation constant and corresponds to the ligand concentration, [L], which must exist in order for half of the gates to be open. Its value depends on opening and closing rates as equation 17 shows.

$$K_m = \frac{\left(\frac{k_c}{k_o}\right)^{1/H}}{V} \qquad (17)$$

However, there are ligand-inactivated gates too. Therefore, performing the same operations, it is obtained that their opening fractions correspond to that shown in equation 18 (Ferrero, 2022).

$$f_{S,ligand-inactivated} = \frac{1}{1 + \left(\frac{[L]}{K_m}\right)^H} \qquad (18)$$

2.6.2. Drug modelling

Drugs are molecules designed to be capable to join to several receptor molecules, among which are the ion channel receptors. For this reason, drugs' effects can be modelled according to ligand-dependent gates theory that has been already explained in section 2.6.1. As with the ligands, there are excitatory and inhibitory drugs. Excitatory drugs are the ones that directly increase the level of responsiveness of their receptor. On the other hand, inhibitory drugs indirectly reduce the channel activity. Although the latter do not decrease the channel activity directly, they bind to the receptor occupying the same site as a ligand or drug that produces channel activation, thus, they are called inhibitory or antagonistic drugs.

Therefore, all in all, changing the nomenclature of some variables, the equations that govern the fraction of open drug-activated and inactivated channels are the equations 19 and 20, respectively (Ferrero, 2022).

$$f_{S,drug-activated} = \frac{1}{1 + \left(\frac{EC_{50}}{[D]}\right)^H} \qquad (19)$$

$$f_{S,drug-inactivated} = \frac{1}{1 + \left(\frac{[D]}{IC_{50}}\right)^H} \qquad (20)$$

Where [D] is the drug concentration and K_m has been replaced with EC_{50} and IC_{50}, which are the half-maximal excitatory and inhibitory concentration respectively. That means that EC_{50} and IC50 are the equivalent to the drug concentration that excite and inhibit 50% of channels, respectively.

In this way, knowing the effects of a drug on the proportion of open channels (f_S) and the corresponding current functions, it is possible to add the effect of a drug to the model to determine the resulting changes on the cardiomyocyte AP (Amanfu & Saucerman, 2011).

With this purpose, equation 6 can be modified adding the drug effect in the fraction of open channels, resulting then in equation 21 (Ferrero, 2022).

$$f_S(V_m, [L], [D]) = f_{V1}(V_m) \cdot f_{V2}(V_m) \cdot \ldots \cdot f_{Vn}(V_m) \cdot f_{L1}([L]) \cdot f_{L2}([L]) \cdot \ldots \cdot f_{Lm}([L]) \cdot f_{D1}([D]) \cdot f_{D2}([D]) \cdot \ldots \cdot f_{Dk}([D]) \qquad (21)$$

Currently, different versions of AP models using the Hodgkin-Huxley formalism have been published, all of them including the corresponding formulation to simulate the propagation of AP, the ion channels' conductance and gates and transport mechanisms, among others. This leads to a system of differential equations with many state variables and with variation in both time and space, resulting in a truly complex resolution. Therefore, heart electrical activity computational simulations require high-performance computing (HPC) techniques and/or the use of GPUs due to the very high computational cost associated with them. Due to these models being so complex that they require a high consumption of computing resources to be solved analytically, they are usually solved using differential equations approximations. This requires solution mechanisms such as ordinary differential equations (ODEs), which have been implemented in a multitude of computer software, like the one used in this thesis.

CHAPTER 3. OBJECTIVES

Afterdepolarizations and the consequent arrhythmias are common in some stages of heart failure and hypertrophic cardiomyopathy. However, despite the incidence of these pathologies and their fateful effects, the causes of their arrhythmic phenomena are still unknown, and how some drugs act to improve or worsen the patient's condition remains unclear.

The global objective of this Bachelor Thesis is to develop a mathematical model and a computational tool to study the effects of drugs (alone or in combination) in the action potential of human (both male and female) ventricular cardiomyocytes in both healthy and diseased (HCM and HF) conditions, with the aim of assessing their potential anti or proarrhythmic effect.

For all these reasons, the principal objectives of this thesis are the following:

1. To develop and use computational models in order to study the underlying effects of HF and HCM over ionic currents, cardiomyocyte AP and several biomarker parameters.
2. To develop computational simulation models to determine the effects of different drugs under HF and HCM conditions over ionic currents and, in turn, on the cardiomyocyte AP.
3. To develop an interface where users can test how drugs or a combination of them affect AP, intracellular calcium concentration and biomarker parameters taking into consideration several eligible conditions.

Concomitantly, regarding secondary objectives, these can be interpreted as the steps in a pipeline and are as follows:

a. Integrate HF and HCM parameters in a predefined cardiac computational model in order to model their effects under ionic currents and the resulting cardiomyocyte AP.
b. Develop a software script to calculate several parameters (biomarkers) for each AP, such as:
    - APD_{90} and APD_{30}: action potential duration to reach 90% and 30% of repolarization respectively.
    - Triangulation: the difference between APD_{90} and APD_{30}.
    - RMP: resting membrane potential.
    - Amplitude: the measure of the peak voltage difference during an AP.
    - LAT and NLAT: local activation time and its index.
    - $[Ca^{2+}]_i$ TT: the difference between systolic $[Ca^{2+}]_i$ and diastolic $[Ca^{2+}]_i$.
    - $CaTD_{80}$: calcium transient duration to reach 80% of repolarization.
    - Ca_{max} and Ca_{min}: maximum and minimum value of Ca^{2+}.
    - dV_m/dt: the maximum derivative of V_m.
c. Program a script to detect in which simulations alternants and EADs occur.
d. Program a script in which several biomarkers such as APD_{90} prolongation or abnormal triangulation values are calculated because they are determining for identifying arrhythmic risk.
e. Implement programming code in MATLAB® and connect all scripts in order to accomplish several simulations with different conditions in one execution in the most optimal way.

f. Perform simulations with the cardiac computational model taking into account a healthy condition and three states of illness (mild, moderate and severe) for both HF and HCM.
g. Carry out above simulations for women as well as for men.
h. Carry out above simulation for epicardium, endocardium and midmyocardium cells.
i. Carry out above simulations for three heart rates, bradycardia, normal heart rate and tachycardia.
j. Determine in which states and conditions HF and HCM provoke proarrhythmic phenomena.
k. For each of the above conditions, determine which drug reduces the risk of arrhythmia and at which concentration (1xEFTPC, 2xEFTPC or 10xEFTPC).
l. For healthy heart conditions, determine which common drugs provoke alternants, EADs and consequently arrhythmias depending on the heart rate.
m. Determine the most protective drug combination for the heart when the occurrence of EADs is provoked by one drug.
n. Implement all the performed programming code in a user interface made in MATLAB® App Designer.

CHAPTER 4. COMPUTATIONAL MODELLING AND SOFTWARE DEVELOPMENT

The present thesis analyses the proarrhythmic effect of several stages of both HF and HCM taking into account several conditions like patient sex, cell type and heart rate and how a list of common pharmaceutical drugs improve or worsen those conditions. All these aims are going to be accomplished by computational simulation of isolated individual cardiomyocytes (0D simulations).

Computational models used in cardiac modelling are mathematical representations of heart electric, mechanical and/or biochemical activity at the microscopic level, i.e. at the cellular level through the comprehensive understanding of the behaviour of ionic currents. In this way, in this thesis these models are used to simulate and understand the heart running under different conditions and pathologies, allowing then the study of some possible consequent proarrhythmic effects and the possible pharmaceutical therapies.

4.1. PROGRAMMING ENVIRONMENT AND HARDWARE USED

The version R2022b of MATLAB® has been used as programming environment to implement and develop the computational programs in which cardiac electric activity are modelled under different conditions to reach the objectives and analyse the obtained results.

In particular, MATLAB® is a technical computational environment and a programming language developed by MathWorks. Its name derives from "MATrix LABoratory" due to its capacity of carrying out operations related with matrix, which are fundamental in most scientific and engineering calculations. It is based on numerical computation integrating a programming environment with its own language, known as M language. MATLAB® stands out for its high level and interactive environment for algorithm development, data analysis and visualization, scientific and technical problem solving, and user interface creation, among others.

Throughout the development of this thesis, several programmes have been carried out and they will be described later. Those programmes have been done in order to calculate several marker parameters, which are necessary to determine which stages of HF and HCM increase the risk of arrhythmias and how or why they do it, analysing ionic currents and concentrations values. Some parameters have been programmed to be saved in an Excel® file for faster and easier result viewing and control. Moreover, other scripts have been done to represent several AP with some indicators under different conditions to make comparisons with control simulations and determine the underlying proarrhythmic factors. Finally, using the App Designer tool from MATLAB®, a user interface has been created by integrating the above-mentioned programmes together with others in order to obtain a user-friendly interface and as complete and intuitive as possible.

Regarding the hardware, all MATLAB® programmes and some simulations have been done in a laptop equipped with 8GB of RAM and a processor with 6 cores and 12 logical processors. However, as we needed to run a relatively large number of simulations in a loop, the tutor's computer has been

used too, which is equipped with 32GB of RAM and a processor with 6 cores and 12 logical processors, but with a higher clock frequency of the processor, 3.70GHz instead of 2.20GHz.

4.2. COMPUTATIONAL MODEL: ACTION POTENTIAL MODEL

Isolated human ventricular myocyte action potential model developed by Thomas O'Hara et al. (O'Hara et al., 2011) and implemented in MATLAB® language has been used for the development of this thesis. The O'Hara-Rudy model is the state-of-the-art in cardiac cellular electrophysiology modelling and it has been adopted by the FDA (Food and Drug Administration) as the golden standard for *in-silico* study of the cardiotoxicity of drugs. However, this model does not include the influence of sex and type of cell on cardiac AP. For this reason, in this project, O'Hara-Rudy model developed by Carla Bascuñana in her thesis (Bascuñana Gea, 2023), which includes these conditions, is used. Finally, electrophysiology parameters that affect AP under heart failure and hypertrophic cardiomyopathy have been incorporated to Bascuñana's model in order to accomplish the proposed objectives.

4.2.1. O'Hara-Rudy model

The O'Hara-Rudy model is a detailed mathematical model of human ventricular cell, broadly used in cardiac electrophysiology study. It was developed by Colleen E. Clancy and other researchers, and it is based on a combination of *in-vitro* experiments and computational simulations. As it describes electrophysiological phenomena like ionic dynamics through ion channels, it is particularly useful to study cardiac AP, as well as to simulate the consequences of some illnesses and predict the effect of some drugs.

The following Figure 4.1 shows the original diagram of O'Hara-Rudy model based on HH formalism. This model splits the cell in four compartments: the myoplasm (MYO), the junctional sarcoplasmic reticulum (JSR), the network sarcoplasmic reticulum (NSR) and the subspace (SS) representing the space near the T-tubules. Along these compartments, mathematical descriptions of currents that cross the membrane through ion channels, pumps and exchangers are included together with diffusion currents and calcium buffering in the intracellular space and the calcium transient involved in the Calcium Induced Calcium Release (CICR) process. All these currents are listed in the following Table 4.2.

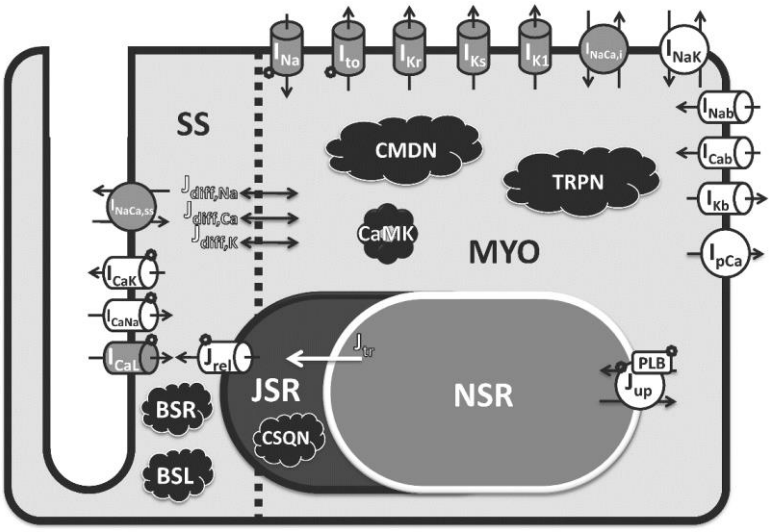

Figure 4.1. Schematic diagram of the human ventricular cardiomyocyte O'Hara-Rudy model. Source: figure taken from O'Hara et al. (2011).

Table 4.1. Currents included in O'Hara model. Source: own elaboration based on O'Hara et al. (2011).

Ion related	Location	Name	Description
K^+ currents	MYO	I_{to}	Transient outward K^+ current
		I_{Kr}	Rapid delayed rectifier K^+ current
		I_{Ks}	Slow delayed rectifier K^+ current
		I_{K1}	Inward rectifier K^+ current
		I_{Kb}	Background K^+ current
		I_{KATP}	ATP-sensitive K^+ current
Na^+ currents	MYO	I_{Na}	Fast component of Na^+ current
		I_{NaL}	Late component of Na^+ current
		I_{Nab}	Background Na^+ current
Ca^{2+} currents from channels and Ca^{2+} buffers	MYO	I_{Cab}	Background Ca^{2+} current
	NSR ↔ JSR	J_{tr}	NSR to JSR Ca^{2+} translocation
	SS	I_{CaL}	L-type Ca^{2+} current
		I_{CaNa}	Na^+ component of L-type Ca^{2+} current
		I_{CaK}	K^+ component of L-type Ca^{2+} current
	Ca^{2+} buffers	CMDN	Calmodulin
		TRPN	Troponin
		CSQN	Calsequestrin
		BSR	Anionic SR binding sites for Ca^{2+}
		BSL	Anionic sarcolemmal binding sites for Ca^{2+}
		CaMK	Ca^{2+}/calmodulin-dependent protein kinase II
Currents related with pumps, exchangers and cotransporters	MYO	$I_{NaCa,i}$	80% of Na^+/Ca^{2+} exchange current
		I_{NaK}	Na^+/K^+ pump current
		I_{pCa}	Sarcolemmal Ca^{2+} pump current
	SS	$I_{NaCa,ss}$	20% of Na^+/Ca^{2+} exchange current
	JSR ↔ SS	J_{rel}	Ca^{2+} through ryanodine receptor
	NSR ↔ MYO	J_{up}	Ca^{2+} uptake into NSR via SERCA2a/PLB
Diffusion fluxes	MYO ↔ SS	$J_{diff,Na}$	Diffusion Na^+ flux from subspace to myoplasm
		$J_{diff,Ca}$	Diffusion Ca^{2+} flux from subspace to myoplasm
		$J_{diff,K}$	Diffusion K^+ flux from subspace to myoplasm

In order to apply sex and cell type conditions and drugs combination effect, the reconfigured code made by Bascuñana Gea (2023) has been used. Moreover, in this code, to obtain realistic values for the depolarization rate of the AP and its propagation velocity, the formulation of fast sodium current (I_{Na}), as well as L-type calcium current (I_{CaL}) have been modelled as Carpio et al. (2019).

In addition, in this thesis, some modifications have been inserted to Bascuñana's code to apply the parameters that allow the modelling of HF and HCM and other parameters to be able to simulate several heart rate conditions. All these changes will be explained in the following sections.

4.2.2. HF and HCM modelling

In order to model the effects that HF and HCM have over cardiac electrical activity, the ionic electrophysiological remodelling in HCM and HF reviewed by Elisa Passini and others in Passini et al. (2016) has been integrated into the model used as a basis (see Table 4.2).

Table 4.2 Percentual changes for each ionic current to integrate the HF and HCM ionic electrophysiological remodelling. Source: table taken from Passini et al. (2016).

Ionic Current	HCM	HF	Ionic Current	HCM	HF
I_{Na}	-	-57%	I_{to}	-70%	-60/73%
I_{NaL}	+165%	+80/200%	I_{K1}	-30%	-32/50%
I_{Nab}	+165%	-	I_{Kr}	-45%	-45%
I_{CaL}	+40%	0/-60%	I_{Ks}	-45%	-57%
τ I_{CaL} fast inactivation	+35%	-	I_{NaK}	-30%	-30/42%
τ I_{CaL} slow inactivation	+20%	-	J_{up}	-25%	-25/50%
I_{NCX}	+30%	+75/200%	J_{Rel}	-20%	-20%

Nevertheless, in the percentual HF changes for some ionic current a range is presented instead of a value, for that reason it was decided to apply the average value of that range as the percentual change. However, when control simulations, without any kind of drug effect, were run, we realised that with those parameters both, HCM and HF, in female as well as male provoked EADs in midmyocardium cells. These results are incongruous with clinical values because not all patients diagnosed with HF or HCM present EADs and the consequent arrhythmias, but depends on the stage of the disease. Taking all this into account, we decided to use the HF ionic remodelling exposed by Juan F. Gomez and others in Gomez et al. (2014) instead. Nonetheless, no consistent results were obtained because with Gomez's parameters no cases of HF had EADs or alternants, which also does not correspond to the clinical picture. For all these reasons, as both HF and HCM have several stages (mild, moderate and severe) we decided to split the parameters given by Passini et al. (2016) in three equidistant values in order to model the three stages of each disease following equation 22 and equation 23 in each of the affected ionic currents.

$$Mild = Healthy + \frac{Severe - Healthy}{3} \qquad (22)$$

$$Moderate = Severe - \frac{Severe - Healthy}{3} \qquad (23)$$

In above equations, $Healthy$ is the value in the basic model and $Severe$ is the unique value given for HCM or the average value of that range given for HF by (Passini et al., 2016). With these modifications, proarrhythmic effects only in severe stages of both pathologies were obtained, which was consistent with the clinic.

4.2.3. Drug modelling

On the other hand, just as the effects of HF and HCM have been integrated in the model, the inclusion of the effects of drugs is also required in order to achieve the objectives of this thesis. The corresponding modifications were done by Carla Bascuñana in her thesis using equations 19 and 20 from section 2.6.2 for each affected current. Therefore, this model can be used for the simulation of the pharmacological effect of different drugs as long as IC_{50} values, Hill coefficients and EFTPC are available. Bascuñana Gea (2023) used a list of 95 drugs classified by TdP risk category (proarrhythmic, antiarrhythmic and intermediate risk) according to Fogli Iseppe et al. (2021). However, in this thesis the classification of drugs into arrhythmogenic and non-arrhythmogenic (dangerous and safe, respectively) is different.

Lancaster & Sobie (2016) indicate that a common molecular mechanism underlying the effect of arrhythmogenic drugs is the blockade of the channels responsible for the I_{Kr} current. As explained in section 2.2.3, I_{Kr} plays a key role in the repolarization of human ventricular cardiomyocyte, so a reduction in this current lengthens the APD, which becomes evident with the increase of the QT interval in the ECG. Moreover, it is well-known that the arrhythmogenicity of I_{Kr} blockade is attenuated by concurrent blockade of Na^+ and Ca^{2+} channels (Lancaster & Sobie, 2016).

In addition, the drug's ability to block or inhibit a current depends on its IC_{50} for that current. The following figures (Figure 4.2 (A) and (B)) illustrate the relationship between two drugs (Amiodarone and Lamivudine) concentration ([Drug]) and the fraction of open channels (f_{open}) for the ones that are affected for those drugs. IC_{50} values for Amiodarone are 30, 270 and 4800 nM and, for Lamivudine are 2054000, 54200 and 1571400 nM for I_{Kr}, I_{CaL} and I_{Na}, respectively. This shows that the higher the IC50 value, the more the f_{open} vs. [Drug] curve moves to the right, requiring a higher drug concentration to have a decreasing or blocking effect on the affected channels.

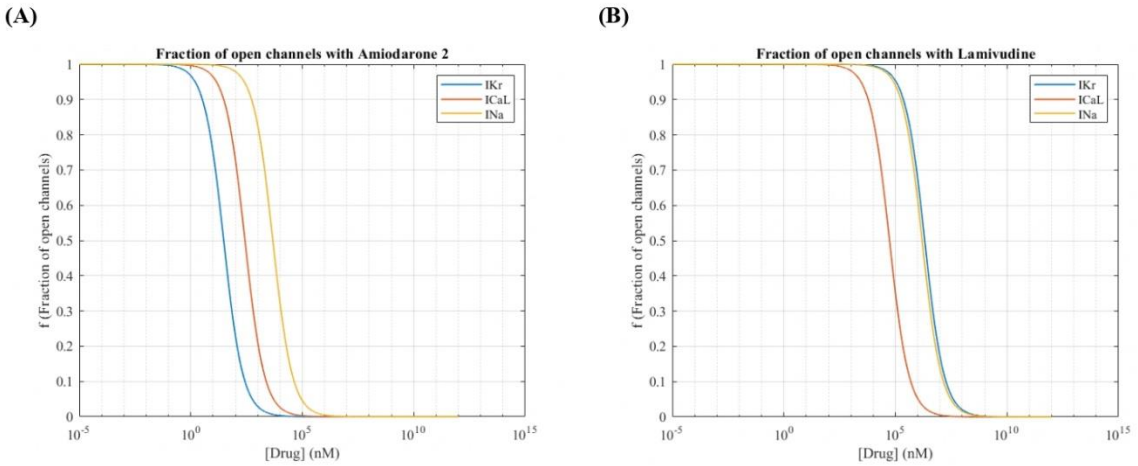

Figure 4.2. Fraction of open channels vs. drug concentration for (A) Amiodarone and (B) Lamivudine considered as an arrhythmogenic and non- arrhythmogenic drug respectively.

Therefore, in this thesis those drugs whose difference $IC_{50}(I_{CaL}) - IC_{50}(I_{Kr})$ is negative, have been considered as non-arrhythmogenic. That is, those drugs for which the following inequality is satisfied $IC_{50}(I_{Kr}) > IC_{50}(I_{CaL})$. In this way, for the same value of [Drug], if the IC_{50} is higher for I_{Kr} than for I_{CaL}, it means that the decrease of proportion of open channels for a particular V_m will be lower for I_{Kr} than for I_{CaL}.

In short, in drugs whose IC_{50} for I_{CaL} is less than for I_{Kr}, during the plateau phase (phase 2 of AP) the blockade of I_{CaL} will be higher than that of I_{Kr}. So, the repolarisation phase, started by the higher

outflow of K^+ relative to the inflow of Ca^{2+}, will begin easily thus shortening the APD, trying to prevent the presence of EADs and the consequent risk of arrhythmias.

4.2.4. Stimulation/pacing protocol

In this thesis, in order to simulate several heart rates, different basic cycle length (BCL) have been used. BCL is the period of time that passes by between two stimulation input currents, and corresponds to RR interval in the ECG, which in turn reflect the heart rate in that moment. The ranges of bpm values for bradycardia, normal frequency and tachycardia have already been exposed in section 2.4, taking into account that ranges, the following specific values have been considered: 45, 75 and 120 bpm for bradycardia, normal frequency and tachycardia respectively. Keeping in mind those values, the fact that the duration of all the simulations is 60000 ms and that the BCL can be calculated following the equation 24, the BCL used are: 1333, 800 and 500 ms for bradycardia, normal frequency, and tachycardia respectively.

$$BCL = \frac{Simulation\ time}{Heart\ rate} \qquad (24)$$

Moreover, apart from the different values from BCL, other parameters have been taken into account when the simulations have been run. These ones are sex (male and female), cell type depending on its location in the heart (endocardium, epicardium and midmyocardium), disease (healthy, HF and HCM) and its severity (mild, moderate and severe), drug (in particular the code is prepared for the combination of the effect of three drugs) and its concentration (EFTPC, 2xEFTPC and 10xEFTPC).

4.3. SOFTWARE DEVELOPMENT

The simulation software is the tool used in order to accomplish the objectives of this thesis, the study of the underlying effects of HF and HCM on cardiac electrophysiology in different conditions and which drugs can reverse arrhythmogenic consequences and how they do it.

For this purpose, the corresponding parameters to the modelling of HF and HCM in a human cardiomyocyte model have been introduced into the software belonging to the Ci^{2}b research group (*Centro de Investigación e Innovación en Bioingeniería*), which has been used as the basis for this study.

The following Table 4.3 shows the different software modules that compound the human ventricular cardiomyocyte model, including both the modified and the new ones elaborated for this project. Next, the development of each module will be explained, emphasising the content of each one, its purpose and the changes applied in order to achieve the proposed objectives.

Table 4.3. Modules that compound the human cardiomyocyte model.

Model	Modules	References
Human cardiomyocyte	main_ORd_MMChACR	Developed by Hara et al. (2011), modified and expanded in this thesis.
	model_Ord_MMChACR	
	calc_parameters_v10	Own elaboration
	drugs_and_pathologies_with_severity_simulations_function	Developed by Bascuñana Gea (2023) and expanded in this thesis
	simulations_to_solve_abnormalities	Own elaboration
	arrhythmic_risk_score_v6	Own elaboration

4.3.1. Main and Model files

Both *main* and *model* modules have not been completely developed in this thesis, but they have been modified in order to incorporate parameters to simulate HF and HCM with three possible stages.

On the one hand, *main* module corresponds to the principal module of the model whose running return the results of the differential equations programmed to simulate the bioelectrical functioning of a ventricular cardiomyocyte in different conditions.

As with most modules, this module requires the input of certain parameters. The first one is the vector *settings*, which contain the basic configuration parameters that are needed for computational calculations. Although these parameters are already defined in the *model* module, the settings vector allows that they are changed to simulate different conditions.

Its principal purpose is calling to the *model* module using ode15s function in order to solve stiff differential equations by making use of the defined functions in *model* module. Ode15s is a numerical method used to solve ordinary differential equations (ODEs) in MATLAB®, hence its name. More specifically, "15" indicates that this method uses a variable step with order 1 to 5 for more accurate approximations and the "s" means that ode15s is efficient for stiff problems, where multiple time scales are present in the system of equations. In this case, ode15s has been used because a cardiac cell model includes processes that occur on different time scales, that means they are stiff models. For instance, the fast membrane depolarization during AP can take place in milliseconds, while ion channels recovery and other regulation processes can occur in slower time scales.

Once all equations are solved, the output variables from main module are three: a vector T_i with time instants in milliseconds, a matrix *StateVars* with the values of 42 state variables for each time instant and a structure *currents* that stores ionic currents and other additional variables. Throughout the thesis, the first two arrays are the ones that are going to be used in order to plot the AP or the intracellular Ca^{2+} concentration as a function of time. These two representations are quite useful for studying the effects of the simulated conditions.

In particular, the changes that have been done in this module are the addition of *pathology* and *severity* to the vector *settings* apart from *celltype* and *male_female* which had already been added by Bascuñana Gea (2023). As the following code shows, the two parameters added correspond to the health condition (healthy, HF or HCM) and the pathology stage to be simulated respectively.

```
function settings = setDefaultSettings(settings)

    if ~isfield(settings, 'TSim'), settings.TSim = 5000; end
    if ~isfield(settings, 'BCL'), settings.BCL = 1000; end

    if ~isfield(settings, 'basic_stim_amp'), settings.basic_stim_amp = -80.0; end
    if ~isfield(settings, 'basic_stim_duration'), settings.basic_stim_duration = 0.5; end
    if ~isfield(settings, 'extra_stim_amp'), settings.extra_stim_amp =
settings.basic_stim_amp; end
    if ~isfield(settings, 'extra_stim_duration'), settings.extra_stim_duration =
settings.basic_stim_duration; end
    if ~isfield(settings, 'CI_extra'), settings.CI_extra = settings.BCL; end


    if ~isfield(settings, 'Ko'), settings.Ko = 5.4; end
    if ~isfield(settings, 'ATPi'), settings.ATPi = 10; end
    if ~isfield(settings, 'ADPi'), settings.ADPi = 15; end
    if ~isfield(settings, 'pHi'), settings.pHi = 7.2; end
    if ~isfield(settings, 'pHo'), settings.pHo = 7.4; end
    if ~isfield(settings, 'fmINaL'), settings.fmINaL = 8; end
    if ~isfield(settings, 'LPC'), settings.LPC = 2; end
    if ~isfield(settings, 'wash_out_norm'), settings.wash_out_norm = 1.0; end
    if ~isfield(settings, 'tau_wash_out'), settings.tau_wash_out = 1000; end

 %Sex --> female = 1 ;  male = 2
    if ~isfield(settings, 'male_female'), settings.male_female = 1; end %
```

```
 %Celltype --> %endocardium = 1, epicardium = 2, midmyocardium = 3
    if ~isfield(settings, 'celltype'), settings.celltype = 1; end

%Pathology --> healthy = 1, HF (Heart Failure) = 2, HCM (Hypertrophic cardiomyopathy) = 3
    if ~isfield(settings, 'pathology'), settings.pathology = 1; end

%Severity --> %mild = 1, moderate = 2, severe = 3
    if ~isfield(settings, 'severity'), settings.severity = 1; end

end
```

On the other hand, *model* module comprises all differential equations necessary for the calculation of the different state variables that make up *StateVars* matrix, such as membrane potential, ionic concentrations, and intracellular currents equations. This means that this module corresponds to both, process modelling and cardiac cellular electrical response.

Because of this, this module was already modified by Bascuñana Gea (2023) in order to extend the formulation of the model to include the effects of the drugs on the bioelectrical functioning of cardiomyocytes, as she explains in the section 4.4.3 of her thesis. However, this module has been further modified to add the pathology effects on electrical activity of cardiomyocytes depending on the stage and other conditions of the subject to be simulated. Next, the above changes will be briefly explained.

The incorporation of HF and HCM depending on their stages has been done using a switch case block as the following code shows.

```
%=============Modifying factors according to Pathology=================
pathology = settings.pathology;
severity = settings.severity;

switch pathology
    case 1 %Healthy
        %The corresponding modifying factors will be equal to 1 (no changes)
    case 2 %HF
        switch severity
            case 1 %mild
                %Here mild HF modifying factors for each current will be defined
            case 2 %moderate
                %Here moderate HF modifying factors for each current will be defined
            case 3 %severe
                %Here severe HF modifying factors for each current will be defined
        end
    case 3 %HCM
        switch severity
            case 1 %mild
                %Here mild HCM modifying factors for each current will be defined
            case 2 %moderate
                %Here moderate HCM modifying factors for each current will be defined
            case 3 %severe
                %Here severe HCM modifying factors for each current will be defined
        end
    otherwise
      %Warning message and the execution will pause
end
```

In relation to the values of the modifying factors presented in comments in the above code, these have been incorporated into the computational model as shown in the code below, which displays the modifying factors for moderate HCM as an example. The modifying factors for the rest of health conditions have been integrated in the same way.

```
       case 2 %Moderate = Severe - (Severe - Health)/3

                modifying_factor_INa = 1;
                modifying_factor_INaL = (1 + 1.65) - (1.65)/3;
                modifying_factor_INab = (1 + 1.65) - (1.65)/3;
```

```
modifying_factor_ICaL = (1 + 0.4) - (0.4)/3;
modifying_factor_tauCaL_fast = (1 + 0.35) - (0.35)/3;
modifying_factor_tauCaL_slow = (1 + 0.2) - (0.2)/3;
modifying_factor_INCX = (1 + 0.3) - (0.3)/3;
modifying_factor_Ito = (1 - 0.7) - (- 0.7)/3;
modifying_factor_IK1 = (1 - 0.3) - (- 0.3)/3;
modifying_factor_IKr = (1 - 0.45) - (- 0.45)/3;
modifying_factor_IKs = (1 - 0.45) - (- 0.45)/3;
modifying_factor_INaK = (1 - 0.3) - (- 0.3)/3;
modifying_factor_Jup = (1 - 0.25) - (- 0.25)/3; %SERCA pump
modifying_factor_JRel = (1 - 0.2) - (- 0.2)/3; %RyRs release

modifying_factor_volume = (1 + 0.9) - (0.9)/3;
```

After the definition of the values of these modifying factors depending on the selected conditions, these are included in each respective current, being included as a multiplying factor in the equation defining that current. These changes are shown in the next code for the I_{Na} as an example, the rest of the currents and multiplying factors have been operated in the same way.

```
INa=modifying_factor_INa*f_drug_1_INa*f_drug_2_INa*f_drug_3_INa*f_pHi_INa*f_LPC_INa*GNa*…
        …(v-ENa)*m^3.0*((1.0-fINap)*h*j+fINap*hp*jp)
```

Finally, once *StateVars* matrix and T_i vector are obtained as a result of solving the equations defined in the module *model* using the numerical method ode15s, these two arrays are used as input parameters in the function *model* in order to obtain the structure *currents* as the output parameter. This structure includes the temporal evolution of several parameters, most of them being ionic currents. Although these parameters are obtained from the combination of different state variables, they are not state variables because they do not ensue from differential equations.

4.3.2. Biomarker measurement

As the main objective of this thesis is the study of the risk of arrhythmias that underlies HF and HCM in different conditions of sex, cell type, heart rate and pathology stage, in this thesis, a script, called *calc_parameters_v10.m*, has been developed in order to calculate several useful biomarkers. Some of these parameters are APD_{90}, the derivative of V_m, resting membrane potential (RMP), calcium transient duration at 80% repolarization (Ca_{TD80}), the difference between systolic $[Ca]_i$ and diastolic $[Ca]_i$ ($[Ca]_i$ TT) and the occurrence of EADs and/or alternans among others.

This script contains a function whose input parameters are the simulation time, *BCL*, T_i and *StateVars* and the output parameters that it returns are a matrix called *parameters*, which returns the value of each biomarker for each beat; a cell array called *results*, which contains certain parameters for each simulation in order to build an Excel file with them; a vector with the temporal derivative of membrane potential; and two cell arrays called *start_final_times* and *start_final_idx*, which contain the times and the indexes in the time array where APD_{90}, APD_{30} and Ca_{TD80} for the last 5 beats start and finish in order to study them easily displaying them in the AP plot.

Throughout the following paragraphs, *calc_parameters_v10.m* is going to be described. Fist, temporal derivative of V_m is calculated for each time point i, as the following code shows. For this purpose, the equation 23 is used and the first value has been initialized to 0 considering that at first V_m does not change. However, as a consequence of limited precision, some entries of T_i are equal, so following the equation 25 some temporal derivatives result in NaN value. For this reason, to handle those cases several options were considered, but finally two options were tested. One option was to interpolate the T_i value at the current time using the previous and next times, but unfortunately it did not work because the same time values were gotten for the limitation in precision. The other option,

and the one used, is to consider for the present value the same value of the temporal derivative of V_m from the previous step.

```
dVm_dt(1,1) = 0;

for i = 2 : size(Vm, 1)
    % Check if the time difference is non-zero
    if (Ti(i) - Ti(i-1)) ~= 0
        dVm_dt(i,:) = (Vm(i) - Vm(i-1))/(Ti(i)-Ti(i-1));
    else % if (Ti(i) - Ti(i-1)) = 0, we will get dVm_dt = NaN and this will cause errors
        % Handle the case where the time difference is zero
        dVm_dt(i,:) = dVm_dt(i-1,:);
    end
end
```

$$\frac{dV_m}{dt}(i) = \frac{V_m(i) - V_m(i-1)}{T_i(i) - T_i(i-1)} \qquad (25)$$

Then, a detector of each action potential, or beat, that is in each simulation has been developed. Different algorithms were tested such as fixed threshold or first derivative analysis. However, as they were not efficient enough for the variability that some simulations show, a window-based algorithm has been developed using temporal derivative of V_m and thresholds backed by thorough and detailed analysis through trial and error (see the code below where the onset of each AP corresponding to each beat is detected).

```
reference_time_AP = BCL;
num_peak = 0; %Counter of number of peaks

for j = 1:length(Ti)
    if j == 1
        %Between 0 and 5ms (we open the window where the peak will be)
        interval_peak_idx = find(Ti >= 0 & Ti <= 5);
        for k=2:length(interval_peak_idx)-1
                    if dVm_dt(interval_peak_idx(k-1)) <= dVm_dt(interval_peak_idx(k)) && …
       …dVm_dt(interval_peak_idx(k))>= dVm_dt(interval_peak_idx(k+1)) %This is the peak
                num_peak = num_peak + 1; %We find a peak
                crossings(num_peak) = interval_peak_idx(k);
                break
            end
        end

    elseif Ti(j-1)<= reference_time_AP && Ti(j)>= reference_time_AP
        interval_peak_idx = find(Ti >= reference_time_AP-1 & Ti <= reference_time_AP+5);
        for k=2:length(interval_peak_idx)-1
                    if dVm_dt(interval_peak_idx(k-1)) <= dVm_dt(interval_peak_idx(k)) && …
       …dVm_dt(interval_peak_idx(k))>= dVm_dt(interval_peak_idx(k+1)) %This is the peak
%Now, we need to know if this peak is a real one, for that it should start by Vm = RMP.
                if Vm(interval_peak_idx(k)-100) < -75
                %If this peaks starts with a Vm < -75mV, will be a real peak
                    num_peak = num_peak + 1; %We find a peak
                    crossings(num_peak) = interval_peak_idx(k);
                    reference_time_AP = reference_time_AP + BCL; %Go over to another window
                    break
                else %There is no peak in the temporal development of dVm_dt
                    reference_time_AP = reference_time_AP + BCL; %Go over to another window
                    break
                end
            end
        end
    end

    if BCL == 1333
        if reference_time_AP >= BCL * 45
            break; %exit the for loop
        end
    elseif BCL == 800
        if reference_time_AP >= BCL * 75
            break; %exit the for loop
        end
    elseif BCL == 500
        if reference_time_AP >= BCL * 120
            break; %exit the for loop
```

```
        end
    else
        if reference_time_AP >= TSim %BCL * TSim/BCL
            break; %exit the for loop
        end
    end
end
```

In the developed algorithm, firstly, a first window from simulation time 0 ms to 5 ms is open in dV_m/dt vector to look for the first peak which will correspond to the onset of first AP. Then, for the rest of the simulation, each generated window starts from 1 ms before the corresponding stimulation time to 5 ms after it, because it is in that time window where the onset of each respective AP should be. Once a peak in the derivative is found in each time window, the corresponding time is considered the onset of a real AP if the value of V_m for 100-time values prior to the time of the peak of the derivative corresponds to the value of RMP, approximately. This value has been defined as -75 mV according to the literature (Tse, 2016) and tutor's experience. Finally, the loop stops when there is no other pacing time according to the simulated heart rate.

However, while the code was tested by running several simulations, we realized that some extreme cases weren't detected correctly, such as the ones that have an APD so long that when the next pacing time arrives the value of V_m doesn't correspond to RMP but there are no EADs either. These cases are captured considering both when not a single beat has been detected or when the number of beats detected does not correspond to the number of beats that should be detected according to simulation time and BCL. Then, beats' detection is actualized, as the following code shows where the onset of each beat is detected for extreme cases. In this code snippet, first, the indexes where stimulation currents take place are defined according to BCL value, and then, for each pacing input, the V_m value is checked, and if its value is more negative than a threshold, that index would be considered as the point where a beat starts. The threshold considered has been -30 mV because in the literature, the voltage range typical for phase 2 EADs has been found to be between 0 and -30 mV (Weiss et al., 2010). Moreover, considering the electrophysiology of cardiomyocytes, when V_m has values below that threshold all the process of excitation-contraction coupling explained in section 2.1.4 take place (Weiss et al., 2010; Liu et al., 2016; Nerbonne & Kass, 2005). For that reason, as in each pacing current time where V_m is below -30 mV, the release of calcium from the cardiac sarcoplasmic reticulum occurs so the contraction can be produced, and also the following calcium uptake by SERCA2a pump, the corresponding pacing index can be considered as an onset of an AP.

```
%Initialize values:
stimulations_time_values = [0:BCL:Ti(end)];
stimulations_time_values = stimulations_time_values(1:end-1);%We delete the stim in Ti(end)
stimulations_idx = zeros(1,length(stimulations_time_values));
num_peak = 0;
for s = 1:length(stimulations_time_values)
    stimulations_idx(s) = find(Ti>=stimulations_time_values(s), 1);
    if Vm(stimulations_idx(s)) < -30
        num_peak = num_peak + 1;
        crossings(1, num_peak) = stimulations_idx(s);
    end
end
```

Afterwards, based on the detected onsets of each AP, the simulation is split into the individual AP detected, trying to consider all possible scenarios as the code below shows. In this code snippet V_m, T_i and $[Ca]_i$ are split into the corresponding values for each detected PA.

```
%Based on peaks_indices, we can split AP:
%Extract individual action potentials based on peaks_indices
Vm_splited = cell(1, num_beats_detected);
Ti_splited = cell(1, num_beats_detected);
```

```
Cai_splited = cell(1, num_beats_detected);

%But, if we have only one AP because a prolonged EAD is generated,
%we need to set a conditional in order to avoid errors
if num_beats_detected == 1
   Vm_splited{1} = Vm;
   Ti_splited{1} = Ti;
   Cai_splited{1} = Cai;

   results{1,33} = 'Permanent EADs';
   warning ("We have only one AP --> permanent EADs")
else
    for i = 1:num_beats_detected
        if i == 1
            %First action potential
            Vm_splited{i} = Vm(1:crossings(i+1)-1);
            Ti_splited{i} = Ti(1:crossings(i+1)-1);
            Cai_splited{i} = Cai(1:crossings(i+1)-1);
        elseif i == num_beats_detected
            % Last action potential
            Vm_splited{i} = Vm(crossings(i):end);
            Ti_splited{i} = Ti(crossings(i):end);
            Cai_splited{i} = Cai(crossings(i):end);
        else
            Vm_splited{i} = Vm(crossings(i):crossings(i + 1) - 1);
            Ti_splited{i} = Ti(crossings(i):crossings(i + 1) - 1);
            Cai_splited{i} = Cai(crossings(i):crossings(i + 1) - 1);
        end
    end
end
```

Then, in the following code, each biomarker is detected for each detected beat, and then they are saved in the matrix called *parameters*. The first two parameters are APD_{90} and APD_{30}, which are the time taken for a cardiomyocyte's AP to reach 90% and 30% repolarization respectively. As the following code shows, both are calculated for each beat b considering the starting time where the corresponding dV_m/dt reaches its maximum and the ending time when the voltage falls below the voltage level at 90% and 30% repolarization, respectively.

```
%----------APD90 (parameter 1) and APD30 (parameter 2)-----------------

%Calculate the voltage level at 90% repolarization.
threshold_APD90 = (1-0.9) * (maxVoltage - minVoltage) + minVoltage;
%Calculate the voltage level at 30% repolarization.
threshold_APD30 = (1-0.3) * (maxVoltage - minVoltage) + minVoltage;

%Find the time when the voltage exceeds the threshold
for i = 1:length(Vm_beat)
    %We open a time window in order to get the max dVm_dt but
    %whithin the first 5 ms of the dVm_dt splited.
    interval_dVm_dt_peak_idx = find(time_beat >= time_beat(1)&time_beat<=time_beat(1)+15);
    [max_dVm_dt_value, max_dVm_dt_point] = max(dVm_dt(interval_dVm_dt_peak_idx));
    start_time_APD(1,b) = time_beat(max_dVm_dt_point);
    start_time_APD_idx(1,b) = find(Ti == start_time_APD(1,b),1);

    % Find the time when voltage falls below the threshold_APD30 after reaching it
    for j = length(Vm_beat):-1:max_dVm_dt_point
        if Vm_beat(j-1) >= threshold_APD30 && Vm_beat(j) <= threshold_APD30
            final_time_APD30(1,b) = time_beat(j);
            APD30 = final_time_APD30(1,b) - start_time_APD(1,b);
            final_time_APD30_idx(1,b) = find(Ti == final_time_APD30(1,b),1);
            break;
        end
    end

    % Find the time when voltage falls below the threshold_APD90 after reaching it
    for j = max_dVm_dt_point:length(Vm_beat)
        if Vm_beat(j-1) >= threshold_APD90 && Vm_beat(j) <= threshold_APD90
            final_time_APD90(1,b) = time_beat(j);
            APD90 = final_time_APD90(1,b) - start_time_APD(1,b);
            final_time_APD90_idx(1,b) = find(Ti == final_time_APD90(1,b),1);
            break;
```

```
        end
    end
    break;
end
```

The following 7 parameters, triangulation, RMP, amplitude, local activation time (LAT) and its index (NLAT), maximum and minimum value of $[Ca]_i$ and $[Ca]_i$ TT, are calculated. Triangulation is calculated following the equation 26. The value of RMP is equal to the minimum value of voltage for each beat. The amplitude parameter is calculated as the difference between the maximum and minimum value of voltage. LAT is the first value of the time vector for each beat and NLAT is the respective index. And $[Ca]_i$ TT is calculated as the difference between the maximum and minimum value of $[Ca]_i$.

$$Triangulation = APD_{90} - APD_{30} \qquad (26)$$

Finally, Ca_{TD80} is calculated as the period that takes place from the time [Ca]i exceeds the level of calcium ions at 80% of the maximum concentration until it falls below that level as the following code, in which Ca_{TD80} is calculated for each beat b, shows.

```
%Calculate the level of calcium ions at 80% of the maximum concentration.
threshold_CaTD80 = (1-0.8) * (maxCai - minCai) + minCai;

%Find the time when the Cai exceeds the threshold
for i = 1:length(Cai_beat)
    if Cai_beat(1) >= threshold_CaTD80
        start_time_CaTD80(1,b) = time_beat(i);
        start_time_CaTD80_idx(1,b) = find(Ti == start_time_CaTD80(1,b),1);
        % Find the time when Cai falls below the threshold_Cai after reaching it
        for j = length(Cai_beat):-1:2
           if Cai_beat(j-1) >= threshold_CaTD80 && Cai_beat(j) <= threshold_CaTD80
               final_time_CaTD80(1,b) = time_beat(j);
               CaTD80 = final_time_CaTD80(1,b) - start_time_CaTD80(1,b);
               final_time_CaTD80_idx(1,b) = find(Ti == final_time_CaTD80(1,b),1);
               break;
           end
        end
        break;
    elseif Cai_beat(i) >= threshold_CaTD80 && Cai_beat(i-1) <= threshold_CaTD80
        start_time_CaTD80(1,b) = time_beat(i);
        start_time_CaTD80_idx(1,b) = find(Ti == start_time_CaTD80(1,b),1);
        % Find the time when Cai falls below the threshold_Cai after reaching it
        for j = length(Cai_beat):-1:i
           if Cai_beat(j-1) >= threshold_CaTD80 && Cai_beat(j) <= threshold_CaTD80
               final_time_CaTD80(1,b) = time_beat(j);
               CaTD80 = final_time_CaTD80(1,b) - start_time_CaTD80(1,b);
               final_time_CaTD80_idx(1,b) = find(Ti == final_time_CaTD80(1,b),1);
               break;
           end
        end
        break;
    end
end
```

Moreover, apart from the above parameters, there are some values that are saved in the cell array called results such as the number of detected APs, if APD_{90}, APD_{30} and Ca_{TD80} have been detected or not, the value of maximum $[Ca]_i$, $[Ca]_{i\ TT}$ and APD90 for the last five APs detected, and also if there are alternans and EADs and the number of them.

In order to automatically know the presence of alternans and/or EADs in the simulations run, the following calculations were also programmed in the script called *calc_parameters_v10.m*. On the one hand, to detect the occurrence of alternans, the difference between the maximum and minimum APD_{90} of the last 5 APs is calculated, because in the last APs the values obtained are in the stationary phase. First, it was considered that if that difference is greater or equal to 80 ms, that means that there are alternans, which is a pro-arrhythmical factor. However, the literature is stricter, considering

thresholds significantly lower than 80 ms, such as 4 ms (Jing et al., 2012), 10 ms (Pastore & Rosenbaum, 2000), 20 ms or it is commonly set at around 5% to 20% of the mean APD. In order to not be too much lenient nor too strict, the threshold finally considered has been 40 ms, which corresponds approximately to 14% of the mean APD.

On the other hand, EADs' detection was a little bit more complex, as the code below shows. Only the occurrence of EADs is searched in the last 5 APs and, as in the APs' detector, all thresholds used are based on thorough and detailed trial-and-error analysis on a wide range of simulations run.

```
%EADs detection
%We are going to check the EADs from starting_point_last_APs_idx
Vm_lasts_APs = Vm(starting_point_lasts_APs_idx:end);
Ti_lasts_APs = Ti(starting_point_lasts_APs_idx:end);
% Initialize variables
stimulations_time_values = [Ti_lasts_APs:BCL:Ti(end)];
stimulations_time_values = stimulations_time_values(1:end-1);
stimulations_idx = zeros(1,length(stimulations_time_values));
for s = 1:length(stimulations_time_values)
    stimulations_idx(s) = find(Ti_lasts_APs>=stimulations_time_values(s), 1);
end

counter_num_EADs = 0;
EADs_idx = [];

for j = 2:length(Vm_lasts_APs)-1
    % Check if the voltage is increasing
    if Vm_lasts_APs(j - 1) <= Vm_lasts_APs(j) && Vm_lasts_APs(j) >= Vm_lasts_APs(j + 1)
        % Increment the count of transitions
        counter_num_EADs = counter_num_EADs + 1;
        EADs_idx(counter_num_EADs) = j;
    end
end
true_EADs_idx = EADs_idx(1);

%Now we are going to delete local increments
%We open a window between stimulations:
for stim = 1:length(stimulations_idx)
    if stim ~= length(stimulations_idx)
        window_between_stims = [stimulations_idx(stim):stimulations_idx(stim+1)];
    else
        window_between_stims = [stimulations_idx(stim):length(Ti)];
    end
    for idx = 2:length(EADs_idx)
        if ismember(EADs_idx(idx), window_between_stims)
            if ismember(true_EADs_idx(end), window_between_stims)
                if abs(EADs_idx(idx) - true_EADs_idx(end)) >= 400 %500 %1000
                 % Add the element to the new array only if the difference is >= 400 idices
                    true_EADs_idx = [true_EADs_idx, EADs_idx(idx)];
                elseif abs(EADs_idx(idx) - true_EADs_idx(end)) <= 400 && Vm(EADs_idx(idx))…
                …> Vm(true_EADs_idx(end))
                %We want the greater Vm of the two indices which difference is < 400 indices
                    true_EADs_idx(end) = [];
                    true_EADs_idx = [true_EADs_idx, EADs_idx(idx)];
                end
            else
                true_EADs_idx = [true_EADs_idx, EADs_idx(idx)];
            end
        end
    end
end

%If there are peaks in the first 250 ms of each AP --> delete them because
%they will be peaks from depolarization phase or local peaks
idx_to_delete = [];
for i = 1:length(range_lasts_APs_idx)
    range_idx_to_delete = [find(Ti >= Ti(range_lasts_APs_idx(i)),1):find(Ti >=
Ti(range_lasts_APs_idx(i))+250,1)];
    range_idx_to_delete = range_idx_to_delete - range_lasts_APs_idx(1);
    %Find the indexes in the original array corresponding to the values of the new array.
    idx_true_EADs_ismember_of_range = find(ismember(true_EADs_idx, range_idx_to_delete));
    idx_to_delete = [idx_to_delete, idx_true_EADs_ismember_of_range];
end
```

```
true_EADs_idx(idx_to_delete) = [];

%Now, we are going to delete the ones that are not peaks provoked by
%EADs but they are peaks because of the stimulation current input (not
%considering as crossings because Vm was > -30mV)but Vm does not have
%an increasing tendency before that current what means that they would
%repolarize if it weren't for the incoming stimulus stream:
%Initialize variables:
idx_to_delete_complete = [];
for k = 1:length(stimulations_idx)
    if ~ismember(stimulations_idx(k), crossings)
        % We will open a window from 5 idx before the stimulation_idx to
        % stimulation_idx:
        window_size = 5;
        start_idx = max(1, stimulations_idx(k) - window_size);
        Vm_window = Vm_lasts_APs(start_idx:stimulations_idx(k)-1); %define the window
        Vm_diff = diff(Vm_window); %we calculate the different between consecutive points
        % Check if all differences are positive or 0 (no difference) to know if there is a
         % increasing tendency:
        is_increasing = all(Vm_diff >= 0);

        if is_increasing
            %Nothing happens, that would be an EAD
        else %If is not increasing --> delete because it is not an EAD
            %We open a window that has all the idx between
            %stimulations_idx(k) and the 250 ms more
            window_250_since_stim_idx = [find(Ti_lasts_APs >= …
               …Ti_lasts_APs(stimulations_idx(k)),1):find(Ti_lasts_APs >= …
               …Ti_lasts_APs(stimulations_idx(k))+250,1)];
      %Find the indexes in the original array corresponding to the values of the new array.
            idx_true_EADs_ismember_of_window_250_since_stim = find(ismember(true_EADs_idx,
window_250_since_stim_idx));
            idx_to_delete_complete = [idx_to_delete_complete,
idx_true_EADs_ismember_of_window_250_since_stim];
        end
    end
end

true_EADs_idx(idx_to_delete_complete) = [];
true_EADs_idx = true_EADs_idx + starting_point_lasts_APs_idx-1;
```

EADs' detection is performed as follows. First, in the first loop, every increasing dynamic is captured. In this way we detect both the moment that depolarization starts and also the small spikes or positive deviation in AP tracing, after the initial repolarization phase, which are the EADs. However, some local increments are detected too, so in the second loop, if, in the same simulation window, two increasing dynamics are close enough, the one corresponding to the smaller V_m is considered as a local increment and not a possible EAD, otherwise both increments detected are included as a possible EAD. Then, in the last loop, the increasing intervals related with depolarization phase are also deleted in order to detect only the positive deviations related with EADs if there are any. Finally, while the results were being reviewed, some cases that do not have EADs, the code considered that they do have EADs. Therefore, the last loop of the code showed in the above code is added. This detection error is due to the fact that the mistakenly considered EADs result from stimulation currents that were not considered as an onset of AP, because the corresponding V_m was above -30 mV, but there is not any ascending trend showing the beginnings of EADs. For this reason, in the last loop, the stimulation times that are not an onset of AP are analysed, and if they present a previously ascending trend, the following detected peak will be considered as an EAD, otherwise it will not.

4.3.3. Driver file

Moreover, apart from above scripts, *drugs_and_pathologies_with_severity_simulations_function* is a function based on the module *SimulacionMultiple* from Bascuñana Gea (2023) and created to launch the simulations with the selected conditions. For this purpose, some loops are programmed in

order to run all the simulations according to the selected conditions. For each combination of conditions to be simulated, the module *main* and the script *calc_parameters* are called to calculate relevant biomarkers. Afterwards, an Excel file, called *parameters_results.xlsx*, is created displaying the values saved in the cell array *results*, that has already been explained in section 4.3.2. This Excel file is extremely useful because it allows to obtain and analyse the effects of diseases and drugs efficiently without the need to analyse each simulation one by one.

Finally, this function is called from the file *simulations_to_solve_abnormalities.m* where there are two modalities, manual simulation in order to determine the conditions to be simulated one by one, or the execution of loop simulations to determine the effect of some drugs on specific conditions selected according to the occurrence of EADs and/or alternans in other simulations. As the following code shows, the table obtained from Excel file (*parameters_results.xlsx*) is iterated over to detect the cases where EADs and/or alternans occur. Then, in those cases, combination of drugs is applied to solve or mitigate the pro-arrhythmic phenomena.

```
sim_results = readtable(sim_results_Excel_file_path, 'Sheet', sheet);
abnormality_rows_counter = 0;

for row = 1:height(sim_results)
    sim_results_row = sim_results(row,:);
    if strcmp(abnormality, 'EADs')
        if strcmp(sim_results_row.EADs, 'EADs')
                abnormality_rows_counter = abnormality_rows_counter + 1;
                rows_with_abnormality(1,abnormality_rows_counter) = row;
        end
    elseif strcmp(abnormality, 'Alternans')
        if strcmp(sim_results_row.Alternances, 'Alternans')
            if strcmp(sim_results_row.EADs, 'No EADs')
                abnormality_rows_counter = abnormality_rows_counter + 1;
                rows_with_abnormality(1,abnormality_rows_counter) = row;
            end
        end
    end
```

4.3.4. Arrhythmic risk calculation

Moreover, to make the analysis of the results of each simulation easier, another script has been done *a posteriori* of the programme's executions in which 8 biomarkers are calculated in order to identify the arrhythmic risk that each simulated condition has. These 8 biomarkers that determine the arrhythmogenicity are the following. The first one consists of if the time derivative of membrane potential is greater than 0 during the resting phase, the arrhythmogenicity increases. The second one, is related to the prolongation of APD_{90} with respect to control simulation, when it is greater than 20%, it elevates the probability of arrhythmia occurrence. The third one refers to the resting membrane potential value of each action potential, if it is greater than -50 mV, the risk of arrhythmia rises. The fourth and the fifth are related to a failure in cellular stimulations, resulting in peaks that are either too low (less than a 0mV) or too high (more than 50 mV), if either of the two occur, the propensity for arrhythmia augments. The sixth and seventh refer to the occurrence of alternans or EADs respectively, the detection of one or both of them increases the arrhythmogenicity. Finally, the eighth biomarker refers to the triangulation, if its value is greater than 140 ms, the probability of arrhythmia occurrence raises. Out of all of these biomarkers, the most determining for identifying arrhythmic risk are the prolongation of APD90, the occurrence of alternants and/or EADs and the triangulation value.

With the purpose of determining these biomarkers, first in *arrhythmic_risk_score_v6.m* the APs of steady-state (SS) phase are detected, if there are no APs detected, that means that there are permanents EADs, otherwise the occurrence of EADs is also calculated as it has been explained in section 4.3.2. If there are no EADs, the rest of the biomarkers are calculated, but before some specific

cases are captured (see the code below). These cases have APs so large that they don't reach neither the RMP (-75 mV) before the next stimulation input nor the V_m is below the threshold of -30 mV in each pacing time. Therefore, those abnormal beats are not detected as individual APs. However, those abnormalities are not detected as EADs either because the depolarization occurs due to stimulation current. For these reasons, in the following code snippet, if the number of individual APs detected is lower than it should be during SS phase according to the BCL value, some observations are added as strings in order to analyse these special cases individually.

```
num_beats_detected_ss = length(crossings);
%And we calculate the number of beats that should be:
TSim = Ti(end); %60000 ms
real_num_beats_ss = TSim/BCL - TSim/BCL * start_time_ss /TSim;

if BCL == 800 %1333 if start_time_ss = 40000
    if num_beats_detected_ss ~= round(real_num_beats_ss)-1
        %Because just before start_time_ss a beat has just been
        %depolarized so we have to rest 1 to real_num_beats_ss
        arrhythmic_factor{i,15} = num_beats_detected_ss;
        arrhythmic_factor{i,16} = 'Not all beats are detected.';
    else
        arrhythmic_factor{i,15} = num_beats_detected_ss;
    end
else
    if num_beats_detected_ss ~= round(real_num_beats_ss)
        arrhythmic_factor{i,15} = num_beats_detected_ss;
        arrhythmic_factor{i,16} = 'Not all beats are detected.';
    else
        arrhythmic_factor{i,15} = num_beats_detected_ss;
    end
end
```

Afterwards, the percentage of the prolongation of APD_{90} value based on control APD_{90} value is calculated as equation 27 and the following code shows.

$$\Delta APD_{90}(\%) = \frac{APD_{90}(Sim) - PD_{90}(Control)}{APD_{90}(Control)} \cdot 100 \qquad (27)$$

For $APD_{90}(Sim)$ and $APD_{90}(Control)$ values the mean of the last five APD_{90} values is considered. As there are some control simulations (the ones with pathology in a severe stage) in which permanent EADs occur, there is no reliable APD_{90} value for them, so we consider it as infinite (10^6 ms).

```
APD90_prolongation = ((last_APD90s-last_APD90s_control)/last_APD90s_control)*100;

if APD90_prolongation > 20 %The drug conditions worsen the control ones
    arrhythmic_factor{i,3} = 'Enlarged'; %arrhythmic risk increase
elseif APD90_prolongation < -20 %The drug conditions improve the control ones
    arrhythmic_factor{i,3} = 'Shortened'; %arrhythmic risk decrease
else %There is no nighlighting change between drug and control conditions
    arrhythmic_factor{i,3} = 'No APD changes';
end
```

Then, for the calculation of alternans, the same protocol as the one used in *calc_parameters_v10* was considered. And next, the triangulation and RMP value are checked. After that, the resting phase of the last beat is detected to analyse the time derivative of membrane potential during that period.

```
%-------------------------------dVm/dt>0 in resting phase----------------------------------
%As I want to detect the resting phase from the last AP both before
%and after the occurrence of the last AP:

if length(crossings) == 1
    arrhythmic_factor{i,2} = 'Resting phase cannot be found';
else
    idx_to_analyse = [find(Ti >= Ti(crossings(end-1)) + APD90(end-1),1):crossings(end), …
        … find(Ti >= Ti(crossings(end)) + APD90(end),1):length(Ti)];

    %Now, we analyse the dVm/dt of the resting phase.
    if dVm_dt(idx_to_analyse) > 0
```

```
        %In spite of being in the resting phase, Vm is increasing at some point
        arrhythmic_factor{i,2} = 'dVm/dt>0 at rest';
    else
        arrhythmic_factor{i,2} = 'No alterations';
    end
end
```

Specifically, as the above code shows, the resting phase is considered from the previous APD_{90} ending to the beginning of the last AP, and from the last APD_{90} ending to the end of the simulation. Afterwards, if the time derivative of V_m is positive at some point of the resting phase, it will be noticed. Finally, the peak value is analysed in order to detect failures in cellular stimulation.

In *arrhythmic_risk_score_v6.m* a loop that iterates over individual samples is implemented, so all these biomarkers are calculated for each .mat file that is saved in a specific folder whose path is copied by the user at the beginning of the script. These biomarkers are saved in a cell array called *arrhythmic_factor*, using one row for each simulation file. Once the loop finishes, the cell array is used to create a .xlsx file where all biomarkers, parameters' values and observations that are determining for identifying the risk of arrhythmia are saved.

4.3.5. Development of a Graphic User Interface (GUI)

Interface design

Additionally, in this thesis, a user interface has been developed using a software developer tool from MATLAB®, called AppDesigner. This is an intuitive interface, whose main objective is to offer a useful simulation environment to analyse the results of the simulations visualizing and comparing them with the control simulations and results of other simulations with different conditions. With it, the user is able to study the effect of different health conditions together with the corresponding pharmacological effect of some drugs on the bioelectrical activity of human ventricular cardiomyocytes.

The interface presents several windows. The first window that pops up when the shortcut icon is clicked is shown in Figure 4.3. It is an informative window about the files that are needed and where they must be in order to run the application. All the necessary files have been uploaded to the Cloud and the user can access them by clicking on DDBB shared link button.

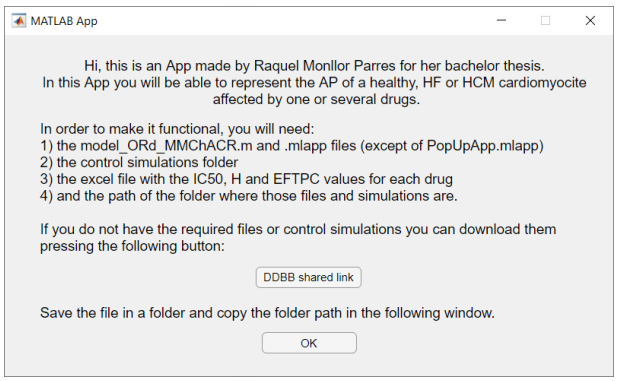

Figure 4.3. Information window about the requirements and how to start using the interface.

Then, once the OK button is clicked, the main window will appear. As Figure 4.4 shows, the main window has an organized layout which facilitates the visualization and data analysis.

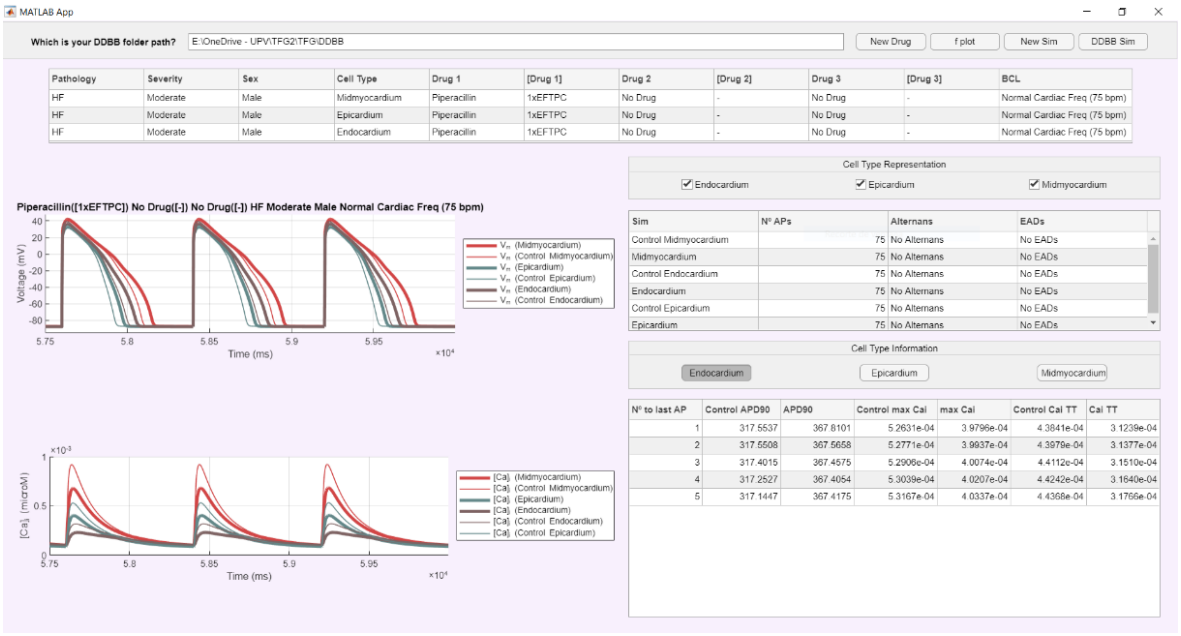

Figure 4.4. Main window of user interface.

At the top, there is a text box for copying there the local folder path where the above-mentioned files have been uploaded. Moreover, through two graphs areas the V_m and $[Ca]_i$ against time are represented for each simulation selected. In addition, the window includes three tables. The one at the top specifies the displayed simulations' conditions, in order, pathology and its stage, sex, cell type, drugs and their respective concentrations and the heart rate. The one on the centre right displays the number of AP detected in the selected simulation and the fact if alternans and/or EADs occur. Below is the third table showing the APD_{90}, maximum [Ca]i and $[Ca]_i$ TT values for the last 5 beats detected. Moreover, there are also three checkboxes and three buttons in order to select the simulation to be displayed and the corresponding values according to the type of cell (endocardium, epicardium and midmyocardium), respectively. Finally, next to the text box, there are four buttons displayed to access the other 4 screens developed shown in Figure 4.5.

The first button, labelled as *New Drug*, goes to another window shown in Figure 4.5 (A). In this one, the user can enter the name, IC_{50} values and Hill coefficients for each channel and EFTPC corresponding to the new drug to be registered. The second button, labelled as *f plot*, leads to the window shown in Figure 4.5 (B) where one of the registered drugs can be selected in the dropdown menu in order to display in the graph the fraction of open channels for each current affected by the selected drug against the drug concentration. The third button, called *New Sim*, carries the user to the window shown in Figure 4.5 (C), where the user can select one by one the conditions to be simulated and then plot it in the main window. And, finally, the fourth button, called *DDBB Sim*, goes to the window shown in Figure 4.5 (D) where the dropdown menus display the different combinations of conditions that have already been run and the user can represent in the main window.

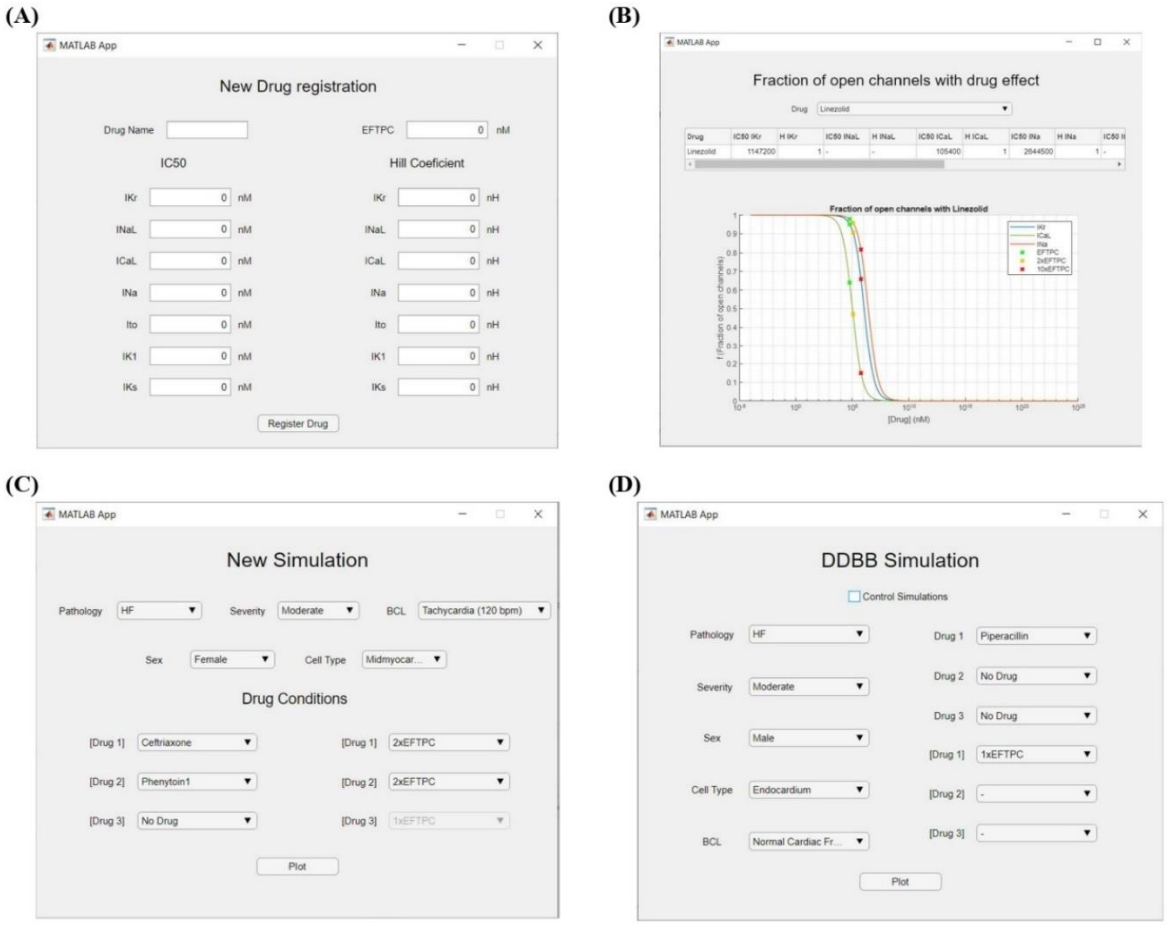

Figure 4.5. 4 alternative windows which can be accessed through the main window. (A) New drug registration window. (B) The window where the fraction of open channels with a selected drug effect against the medication concentration is displayed. (C) New simulation window. (D) The window where the user accesses to the simulations uploaded to the DDBB.

Additionally, throughout the interaction with the interface, some pop-ups can emerge to notify the user of some processes, if their request is being carried out or the fact that an error has taken place (see Figure 4.6).

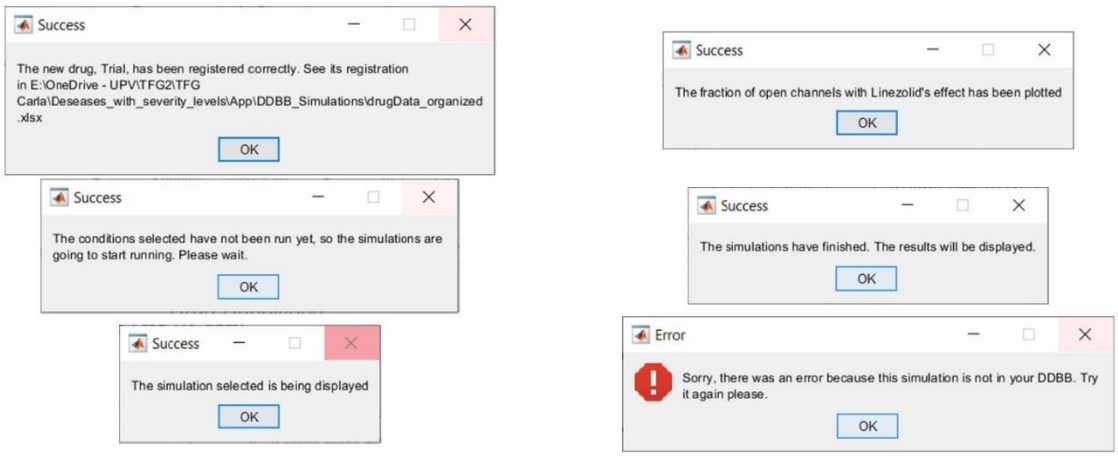

Figure 4.6. User-interface interaction though success and error pop-ups.

User manual

These are the steeps to follow to use the interface correctly.

1. Open MATLAB®, go to APPS tab and then click on Install App. Once a pop-up of the file explorer has emerged, search the .mlappinstall file and install the app.
2. Once the app shortcut icon is clicked, the above-mentioned information window will pop up. As some files are needed, the user can download them by clicking on the *DDBB shared link* button to access to the folder in the Cloud where the necessary files are uploaded. Download the files and save them in a local folder. Be careful because the path of that folder must be copied in the following window. Click the OK button.
3. When the OK button of the information window is clicked, the main window emerges. In order to enable the buttons, the local folder path must be copied into the top text box. Only then, the user will be able to interact with the interface.
4. Now, depending on what is the user's objective, the interaction changes.
    a. If the user wants to register new drug parameters in order to simulate their effect on the bioelectrical activity of human ventricular cardiomyocytes, the user must click on the *New Drug* button in the main window. Then, new drug registration window emerges and once the drug name, all IC50 values, Hill coefficients and EFTPC are entered in the corresponding text and number boxes, the user must click in the button labelled as *Register Drug*. Finally, a pop-up emerges notifying in which directory is the Excel file where new drugs are registered with the rest of the already registered ones.
    b. If the user wants to analyse how a drug affects each channel individually, they can click in the *f plot* button in the main window. Then, a new window will emerge where the user can select, in the dropdown menu, the drug that they want to analyse. Once a drug is selected, the fraction of open channels with the selected drug effect against that drug concentration will be displayed in the central graph automatically.
    c. If the user wants to simulate different conditions manually selected in order to analyse their effect as a whole, they must click on *New Sim* button in the main window. A new window will emerge with several dropdown menus in which the user can select the conditions to be simulated one by one manually. Once the conditions are selected, click on the button labelled as *Plot* and the simulations will start. It is necessary to comment that although the user selects a specific cell type, all cell types will be simulated in order to be able to compare results when they are displayed, that means that three simulations will be run, one per each cell type. When the simulations finish, they will be displayed in the main window automatically. Moreover, if the selected conditions have been already run, the interface will notify the user about it and display the results without re-execution.
    d. If the user wants to study the results of a simulation already run and stored in the database, they must click on *DDBB Sim* button. DDBB Simulation window will emerge with a checkbox and several dropdown menus, which are dynamically populated from database. The checkbox allows to change the database folder to access control simulations (no drug effects) in case the user wants them to be represented individually. Once conditions are selected, click on the button labelled as *Plot*, and the results will be displayed in the main window.
5. Once the results are displayed in the main window, either because a new simulation that has just been run or one that was saved in the database has been represented, the user can select the type of cell on which to analyse effects using check boxes labelled as endocardium,

epicardium and midmyocardium. Moreover, using the buttons with the same name, they can change the data displayed in the table below.

To finish, it is important to know that the name of the Excel file where drug parameters are saved (*drugData_organized.xlsx*) should not be changed because the internal code of the interface would not find it and would give an error.

CHAPTER 5. RESULTS

This work is a continuation of Carla Bascuñana's thesis (Bascuñana Gea, 2023), about the combination of drugs and its effects over healthy human ventricular cardiomyocytes. However, specifically, the principal objective of this thesis is to include more conditions such as three different heart rates (bradycardia (45 bpm), normal heart rate (75 bpm) and tachycardia (120 bpm)) and two pathologies (HF and HCM) and their severities (mild, moderate, and severe). For all these reasons, in the present CHAPTER 5 "RESULTS" the focus will be on the effects of pathologies without drugs for each condition (sex, cell type, heart rate and disease severity). And then, for the ones that have arrhythmogenic abnormalities, like the occurrence of EADs, the combination of drugs will be considered in order to analyse which drugs solve or palliate those arrhythmogenicities. Moreover, all drugs will be simulated in healthy conditions as Bascuñana Gea (2023) did but considering the different heart rates with a view to determine the heart rate impact on the cardiomyocyte response in specific conditions.

Another difference is that the drugs considered as proarrhythmic and the ones considered as antiarrhythmic are different with respect to those considered in Carla Bascuñana's work, as mentioned in section 4.2.3. Considering this difference, 28 drugs have been defined as non-arrhythmogenic (see Table 5.1) and the rest, 67 drugs, as arrhythmogenic (see Table 5.2).

Table 5.1. Table that includes the drugs of the DDBB considered as non-arrhythmogenic in this thesis.

Anti-arrhythmogenic drugs			
Piperacillin	Ribavirin	Nitrendipine1	Ranolazine_CiPA
Lamivudine	Ceftriaxone	Diazepam	Mibefradil2
Metronidazole	Nifedipine2	Diltiazem 2	Mibefradil1
Pentobarbital	Phenytoin1	Saquinavir	Duloxetine
Linezolid	Voriconazole	Diltiazem CiPA	Verapamil_CiPA
Raltegravir	Nifedipine1	Diltiazem 1	Verapamil1
Mitoxantrone	Sitagliptin	Nitrendipine2	Verapamil2

Table 5.2. Table that includes the drugs of the DDBB considered as arrhythmogenic in this thesis.

Arrhythmogenic drugs					
Pimozide2	Astemizole	Bepridil CiPA	Cibenzoline	Dofetilide 1	Ajmaline
Bepridil 2	Prenylamine	Thioridazine 1	Droperidol	Sunitinib	Risperidone2
Pimozide1	Haloperidol 1	Phenytoin2	Amitriptyline	Donepezil	Cilostazol
Amiodarone 2	Thioridazine 2	Solifenacin	Sertindole2	Methadone	Sotalol
Dofetilide CiPA	Clozapine	Terodiline	Mexiletine CiPA	Risperidone1	Moxifloxacin
Desipramine	Propafenone	Quetiapine	Cisapride1	Mexiletine	Procainamide
Terfenadine2	Halofantrine	Imipramine	Propranolol	Quinidine CiPA	Paliperidone
Terfenadine_CiPA	Haloperidol 2	Loratadine	Quinidine 2	Dasatinib	Diphenhydramine
Bepridil 1	Fluvoxamine	Quinidine 1	Nilotinib	Dofetilide 2	Telbivudine
Terfenadine1	Chlorpromazine1	Sertindole1	Ondansetron_CiPA	Ibutilide	Disopyramide
Amiodarone 1	Paroxetine	Chlorpromazine_CiPA	Flecainide	Sparfloxacin	Sotalol CiPA
Cisapride_CiPA					

It is noticeable that some drugs are repeated and differ because they are named with "1", "2" or "CiPA", the first two cases are due to different drug data being published by different research during the review done by Fogli Iseppe et al. (2021). As real data is unknown, both publications are taken

into consideration. As for the name "CiPA", it is an acronym that refers to the initiative "Comprehensive in Vitro Proarrhythmia Assay". This is an international initiative proposed by the Food and Drugs Administration (FDA), which analyses the drugs' effects on several ion channels in a standardized and mechanistic way. Its main purpose is to achieve a computational model capable of predicting the risks that a human myocardial cell can suffer by the effect of considered drugs.

5.1. SIMULATION OF PATHOLOGY EFFECT AND SEVERITY WITHOUT DRUGS

In order to analyse the effect of HF and HCM considering three stages of severity (mild, moderate and severe), 126 control (without drug) simulations were needed, being the first 18 the ones that do not consider the effect of the diseases (healthy condition), and the remaining 108 the ones that do contemplate it.

The procedure consisted of using the file *simulations_to_solve_abnormalities.m* but considering manual modality (variable *manual_simulation* equal to 'Yes') and then, in the parameters choice section, the three healthy conditions and their severity, both sexes, the three cell types and the three heart rates (set from the *BCL_values*) are configured. However, all variables related to drugs must have a value of 1, which means "No drug".

Once the simulations have been run, Table 5.3 and Table 5.4 have been created in order to have healthy biomarkers' values on hand as a reference to be able to properly analyse the data, make comparisons and get consistent conclusions.

Table 5.3. Biomarkers' values for the different conditions under healthy cardiac tissue.

No.	Cell type	Sex	Heart rate	APD_{90} (ms)	RMP (mV)	Peaks value (mV)	Triangulation (ms)
1	Endocardium	Female	Bradycardia	302.3	-88.0	38.8	106.2
2			Normal	282.5	-87.9	38.1	104.2
3			Tachycardia	254.6	-87.7	37.2	98.2
4		Male	Bradycardia	286.4	-88.1	37.9	102.4
5			Normal	270.2	-87.9	37.3	100.2
6			Tachycardia	245.3	-87.7	36.7	95.4
7	Midmyocardium	Female	Bradycardia	387.5	-87.8	41.9	142.4
8			Normal	355.3	-87.6	42.6	136.8
9			Tachycardia	318.8	-87.2	42.4	126.2
10		Male	Bradycardia	373.4	-87.8	40.4	133.6
11			Normal	342.0	-87.6	41.1	129.4
12			Tachycardia	307.6	-87.2	41.5	119.6
13	Epicardium	Female	Bradycardia	251.6	-88.0	33.1	75.0
14			Normal	236.7	-87.8	32.7	73.4
15			Tachycardia	220.2	-87.6	32.2	70.4
16		Male	Bradycardia	242.6	-88.0	32.5	73.2
17			Normal	228.0	-87.9	32.1	71.8
18			Tachycardia	212.7	-87.6	31.8	69.2

Table 5.4. The average ± standard deviation of APD_{90}, RMP, peaks values and triangulation (APD_{90}- APD_{30}) for each condition of cell type, sex and heart rate.

Conditions		APD_{90} averages (ms)	RMP averages (mV)	Peaks averages (mV)	Triangulation average (ms)
Cell type	Endocardium	273.54 ± 21.16	-87.90 ± 0.15	37.67 ± 0.71	101.10 ± 3.98
	Midmyocardium	347.43 ± 30.94	-87.53 ± 0.26	41.64 ± 0.83	131.33 ± 8.07
	Epicardium	231.95 ± 14.47	-87.82 ± 0.16	32.40 ± 0.47	72.17 ± 2.13
Sex	Female	289.93 ± 56.19	-87.74 ± 0.26	37.67 ± 4.19	103.64 ± 27.36
	Male	278.68 ± 53.96	-87.76 ± 0.25	36.81 ± 3.89	99.42 ± 24.66
Heart rate	Bradycardia	307.31 ± 60.93	-87.94 ± 0.12	37.42 ± 3.83	105.47 ± 28.76
	Normal	285.75 ± 52.90	-87.78 ± 0.17	37.30 ± 4.29	102.63 ± 27.19
	Tachycardia	259.86 ± 44.25	-87.52 ± 0.24	36.99 ± 4.45	96.50 ± 23.86

Specifically, the analysis of the APD_{90} is relevant in order to determine which is the cell type, sex and heart rate that have the greatest APD_{90} which in turn means a greater arrhythmia risk, as prolonged repolarization is associated with pro-arrhythmia. As Table 5.4 shows, midmyocardium is the cell type with the higher value of APD_{90} with an average of 347.4 ms, female is the sex whose APD_{90} are more extended with an average value of 289.9 ms and finally, regarding to heart rate, bradycardia (45 bpm) has a value of 263.4 ms, greater than the ones for normal heart rate and tachycardia. These values are coherent according to the literature (Prajapati et al., 2022; Guérard et al., 2014; Kim et al., 2013).

In particular, in the absence of pathology, the action potential duration is inversely proportional to the heart rate. Specifically, a slow heart rate (bradycardia) is given by the activity of parasympathetic nervous system which, though acetylcholine (ACh) release, reduces the activity of L-type calcium channels and activates the acetylcholine-dependent inward-rectifier K^+ current, that should drive to an APD shortening. However, as the pacing rate is lower in bradycardia, the activation of calcium channels is more prolonged, which results in a more sustained calcium inward, and also, as potassium channels are not subdued to continuous and fast activations, they are able to deactivate more slowly. Therefore, the repolarization is prolonged due to both, calcium and potassium currents are less strong and more sustained.

In short, a female midmyocardium with bradycardia has an APD_{90} of 387.5 ms, as Table 5.3 shows and is the most prolonged APD_{90} value in heathy conditions.

Then, in order to analyse the effect of both pathologies on myocardial tissue, the occurrence of EADs was the first arrhythmogenic biomarker taken into consideration. As Table 5.5 shows, of all 108 drug-free simulations with pathology effect, 10 have EADs, being in one case permanent EADs, which means that in steady-state phase the cell never repolarizes.

Table 5.5. Summary table of control cases in which EADs occur. Those with a cross (×) in the 'EADs' column means that they have EADs, and the one with permanent EADs has "Permanent" written in it.

No.	Cell type	Sex	Pathology	Severity	Heart rate	EADs
1	Midmyocardium	Female	HF	Severe	Bradycardia	×
2					Normal	×
3			HCM	Severe	Bradycardia	×
4					Tachycardia	**Permanent**
5					Normal	×
6		Male	HF	Severe	Bradycardia	×
7					Normal	×
8			HCM	Severe	Bradycardia	×
9					Tachycardia	×
10					Normal	×

It is noticeable that both pathologies in a severe stage provoke EADs in midmyocardium, whatever the sex and heart rate, except in the case of severe HF with tachycardia. This makes sense since midmyocardium cells are the ones with the highest APD_{90} by default, so if the effect of the most severe stage of an arrhythmogenic pathology is added, the APD prolongation is such that it favours the occurrence of EADs. In particular, the exception of non-occurrence of EADs in cases of severe HF in tachycardiac heart rate is consistent too because the pacing times are too close between them to permit the occurrence of EADs. However, as explained below, their APD duration is so long that they do not reach the RMP value before the subsequent excitation currents.

Example of one case of the occurrence of EADs and another in which permanent EADs occur are shown in the Figure 5.1 together with the corresponding control (without pathology nor drug).

(A) (B)

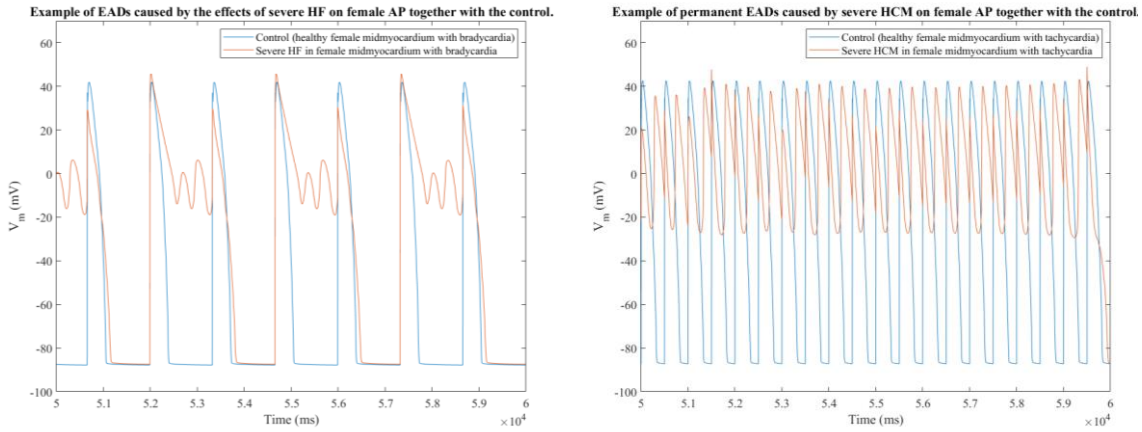

Figure 5.1. Examples of the occurrence of (A) EADs and (B) Permanent EADs. In (A) the abnormality (EADs) occurs when severe HF affects female midmyocardium with bradycardia. However, in (B) the abnormality (permanent EADs) occurs when severe HCM affects female midmyocardium with tachycardia. Both pathological conditions (red) are represented together with the control (blue), healthy female midmyocardium with bradycardia and tachycardia respectively.

As EADs is a phenomenon that occurs during repolarization phase, in which calcium and potassium currents are the ones that are most activated, it is interesting to analyse what happens with them during the occurrence of EADs. For this reason, Figure 5.2 has been created. On it, several currents have been displayed to understand its progression over time.

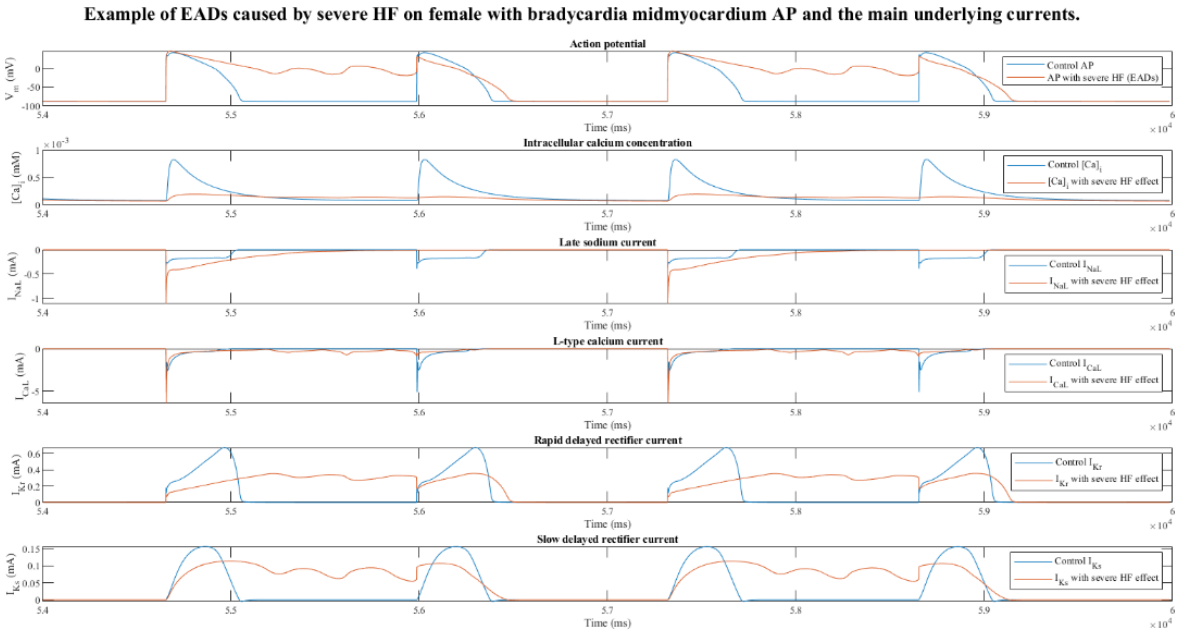

Figure 5.2. Occurrence of EADs in female midmyocardium with bradycardia caused by severe HF and its effects on Vm, intracellular calcium concentration, and some currents such as late sodium current, L-type calcium currents and rapid and slow delayed rectifier potassium currents.

It can be appreciated that, when EADs occur, all displayed parameters are altered as well. First, intracellular calcium concentration remains at low levels throughout the course of time, which in turn affects excitation-contraction coupling complicating cell contraction and the proper pumping of the heart. Next, it can be seen that late sodium current presents a peak in those excitation times when EADs occur increasing then the positive charges into the cell and maintaining positive V_m. Then, L-

type calcium current has greater peaks when EADs occurs than control, which, in turn, hinder the correct repolarization. Moreover, it remains activated during all EADs progression provoking the maintenance of high V_m values. Finally, delayed rectifier potassium currents, as I_{CaL}, are activated during all arrhythmogenic mechanism (EADs) as well. The fight between inward calcium by I_{CaL} and outward potassium by I_{Kr} and I_{Ks} is the responsible for the AP waves that characterize the occurrence of EADs.

Furthermore, as EADs is an abnormality sufficiently arrhythmogenic, the remaining arrhythmogenic biomarkers were calculated with those conditions that did not cause EADs (98), of which fortunately none had alternans, nor either of both failures in cellular stimulation, nor an ascendent time derivative during resting phase. However, as mentioned above, when severe HF affects tachycardic midmyocardium in both male and female the duration of each AP is so long that they do not reach RMP values before the subsequent pacing current, for that reason, these two cases, represented in Figure 5.3, have a higher RMP than -50 mV.

(A) (B)

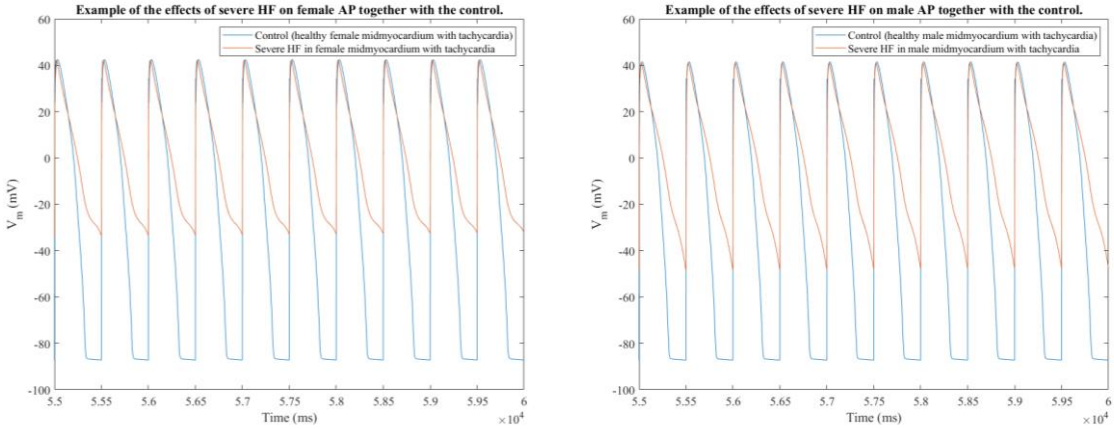

Figure 5.3. Examples of the effects of severe HF on (A) female and (B) male midmyocardium with tachycardia together with their respective controls. High RMP values can be observed.

Moreover, many of the 98 conditions with disease but without the presence of EADs present an enlarged APD and an altered triangulation value. Specifically, 93 present a prolongation of APD_{90} higher than 20% with regard to the respective control, and 64 have a triangulation value higher than 140 ms.

Due to the large number of cases analysed and the limited number of pages for this thesis, the following Table 5.6 shows an excerpt of the results obtained for the two above-mentioned arrhythmogenic biomarkers, even so, the rest of the table is attached in the Appendix 8.1.

Additionally, Figure 5.4 shows an example of a simulation with both biomarkers altered, the repolarization phase of the simulated conditions lengthens in the time axis, thus having a higher APD than the control.

Table 5.6. An excerpt of the results obtained for the remaining 98 drug-free simulations where the APD_{90} prolongation and the triangulation value are analysed. The rest of the table is attached in Appendix 8.1. The conditions in which a prolongation of APD_{90} and/or altered triangulation value is given are marked with a ×.

No.	Cell type	Sex	Pathology	Severity	Heart rate	APD_{90} Prolongation	Triangulation > 140
1	Endocardium	Female	HF	Mild	Bradycardia	×	×
2					Tachycardia	×	
3					Normal	×	×
4				Moderate	Bradycardia	×	×
5					Tachycardia	×	×
6					Normal	×	×
7				Severe	Bradycardia	×	×
8					Tachycardia	×	×
9					Normal	×	×
10			HCM	Mild	Bradycardia	×	
11					Tachycardia	×	
12					Normal	×	
13				Moderate	Bradycardia	×	×
14					Tachycardia	×	×
15					Normal	×	×
16				Severe	Bradycardia	×	×
17					Tachycardia	×	×
18					Normal	×	×
.							
.							
.							
86	Midmyocardium	Male	HF	Mild	Bradycardia	×	×
87					Tachycardia	×	×
88					Normal	×	×
89				Moderate	Bradycardia	×	×
90					Tachycardia	×	×
91					Normal	×	×
92				Severe	Tachycardia	×	×
93			HCM	Mild	Bradycardia	×	×
94					Tachycardia		×
95					Normal	×	×
96				Moderate	Bradycardia	×	×
97					Tachycardia	×	×
98					Normal	×	×

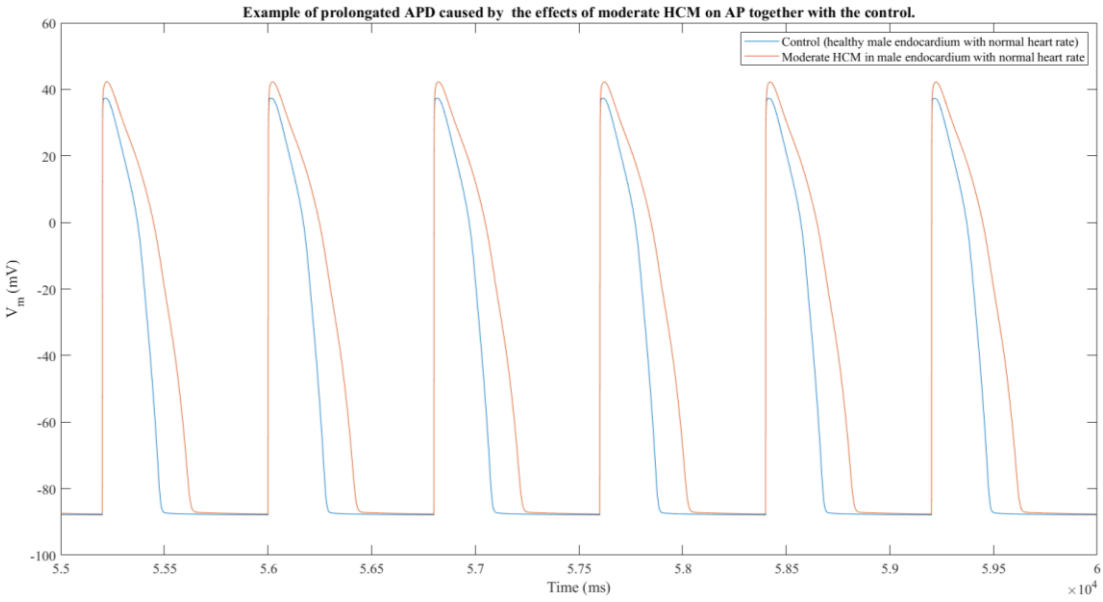

Figure 5.4. Example of the effect of moderate HCM on male endocardium AP with normal heart rate together with the control. A noticeable APD prolongation can be appreciated.

It should be noted that the simulation that reproduces the severe HF conditions in female midmyocardium with tachycardia is not detected as having a prolongation in the APD. However, as Figure 5.3 (A) shows and as mentioned above, it does have such prolongation. This is one of the limitations of the code that can be improved in future modifications. This is due to the fact that the APD_{90} is calculated considering the maximum and minimum value of V_m in each AP, for that reason, as in this simulation not only does V_m not reach values of RMP, but also the minimum value that it reaches in steady-state phase is roughly -32 mV, the APD_{90} is calculated with thresholds whose usage can be questionable in order to detect APD_{90} prolongations consistently in this particular case, which is the only one. Taking all these factors into account, the code can be improved in order to correctly calculate the APD_{90} in cases such as this where the V_m values during repolarization remain well above the RMP.

Analysing the rest of the data results, some patterns have been discovered. The first one is that, except for the above-mentioned case, the four unique conditions where there is no APD_{90} prolongation are the ones with the effect of mild HCM in the epicardium and midmyocardium when the heart rate corresponds to tachycardia values. Additionally, all the cases in which triangulation value is not altered the severity of pathologies follows a pattern. In endocardium, only mild HF and HCM do not provoke a triangulation value over the threshold. However, in epicardium both mild and moderate severities for both pathologies preserve the triangulation value. In midmyocardium all conditions result in an altered triangulation value.

5.2. ANTI-ARRHYTHMOGENIC DRUGS EFFECT TO SOLVE ABNORMALITIES

As mentioned above, once drug-free conditions considering pathologies' effects have been analysed, the occurrence of abnormalities has been attempted to be palliated by adding the effect of anti-arrhythmogenic drugs one per one considering three drug concentrations (1xEFTPC, 2xEFTPC and 10xEFTPC). As there are 28 drugs considered as non-cardiotoxic and 10 drug-free conditions exhibit EADs, 840 simulations have been run.

The procedure followed consisted of using the file *simulations_to_solve_abnormalities.m* but without considering manual modality (variable *manual_simulation* equal to 'No'). Then, the path where there the corresponding Excel file *parameters_results.xlsx* of control simulations is, has to be refilled. Also, as the first drug effect wanted to be simulated, the variable *drugSimWith* must be 'Drug_1' as explained in the code. Next, as the abnormality that wants to be alleviated is the occurrence of EADs, the variable *abnormality* must be 'EADs'. Finally, as there are 28 anti-arrhythmogenic drugs with three different concentrations, in the corresponding part of the code, the variables related to drugs must be *ndrug1_1* equal to 2, *ndrug1_2* equal to 29 in order to apply the effect of the first 28 drugs except for the first one that corresponds to no drug, and then, for simulating the effect of the three concentration, the variables *ncon1_1* and *ncon1_2* must be 1 and 3 respectively.

From them a lot of information has been obtained, but the focus is on those where the occurrence of EADs disappears. Of all simulations, 251 no longer exhibit EADs and the responsible drugs and the respective concentrations are shown in Table 5.7. The rest of simulated drugs do not have enough antiarrhythmic effect in order to palliate EADs. Figure 5.5 shows an example of the treatment of EADs thanks to the effect of an anti-arrhythmogenic drug.

Table 5.7. Summary of the effective drugs and their concentrations to palliate EADs occurrence caused by severe HF or HCM in midmyocardium. The cases where EADs are mitigated are marked with a ✓.

Effective drugs for the treatment of EADs caused by pathologies (✓)											
Drug	[Drug]	Female					Male				
		HF		HCM			HF		HCM		
		Bradycardia	Normal	Bradycardia	Normal	Tachycardia	Bradycardia	Normal	Bradycardia	Normal	Tachycardia
Diltiazem 1	1xEFTPC										✓
	2xEFTPC							✓			✓
	10xEFTPC	✓	✓	✓	✓	✓	✓	✓	✓	✓	✓
Diltiazem 2	1xEFTPC							✓			✓
	2xEFTPC					✓	✓	✓	✓	✓	✓
	10xEFTPC	✓	✓	✓	✓	✓	✓	✓	✓	✓	✓
Diltiazem CiPA	1xEFTPC	✓	✓	✓	✓	✓	✓	✓	✓	✓	✓
	2xEFTPC	✓	✓	✓	✓	✓	✓	✓	✓	✓	✓
	10xEFTPC	✓	✓	✓	✓	✓	✓	✓	✓	✓	✓
Lamivudine	1xEFTPC							✓			✓
	2xEFTPC		✓			✓	✓	✓	✓	✓	✓
	10xEFTPC	✓	✓	✓	✓	✓	✓	✓	✓	✓	✓
Linezolid	1xEFTPC						✓	✓		✓	✓
	2xEFTPC	✓	✓			✓	✓	✓	✓	✓	✓
	10xEFTPC	✓	✓	✓	✓	✓	✓	✓	✓	✓	✓
Metronidazole	1xEFTPC					✓	✓	✓	✓	✓	✓
	2xEFTPC	✓	✓			✓	✓	✓	✓	✓	✓
	10xEFTPC	✓	✓	✓	✓	✓	✓	✓	✓	✓	✓
Mibefradil 2	1xEFTPC										✓
	2xEFTPC										✓
	10xEFTPC		✓			✓	✓	✓	✓	✓	✓
Mitoxantrone	1xEFTPC										
	2xEFTPC										✓
	10xEFTPC										✓
Nifedipine 1	1xEFTPC		✓			✓	✓	✓	✓	✓	✓
	2xEFTPC	✓	✓	✓	✓	✓	✓	✓	✓	✓	✓
	10xEFTPC	✓	✓	✓	✓	✓	✓	✓	✓	✓	✓
Nifedipine 2	1xEFTPC										✓
	2xEFTPC							✓			✓
	10xEFTPC	✓	✓	✓	✓	✓	✓	✓	✓	✓	✓
Nitrendipine 1	1xEFTPC										✓
	2xEFTPC							✓			✓
	10xEFTPC	✓	✓	✓	✓	✓	✓	✓	✓	✓	✓
Nitrendipine 2	1xEFTPC	✓	✓	✓	✓	✓	✓	✓	✓	✓	✓
	2xEFTPC	✓	✓	✓	✓	✓	✓	✓	✓	✓	✓
	10xEFTPC	✓	✓	✓	✓	✓	✓	✓	✓	✓	✓
Pentobarbital	1xEFTPC										✓
	2xEFTPC										✓
	10xEFTPC										✓
Phenytoin 1	1xEFTPC										✓
	2xEFTPC							✓			✓
	10xEFTPC	✓	✓			✓	✓	✓	✓	✓	✓
Piperacillin	1xEFTPC										
	2xEFTPC										
	10xEFTPC	✓	✓		✓		✓	✓		✓	✓
Saquinavir	1xEFTPC										✓
	2xEFTPC										✓
	10xEFTPC					✓	✓	✓		✓	✓
Verapamil CiPA	1xEFTPC										
	2xEFTPC										
	10xEFTPC							✓			
Verapamil 2	1xEFTPC										
	2xEFTPC										
	10xEFTPC							✓		✓	

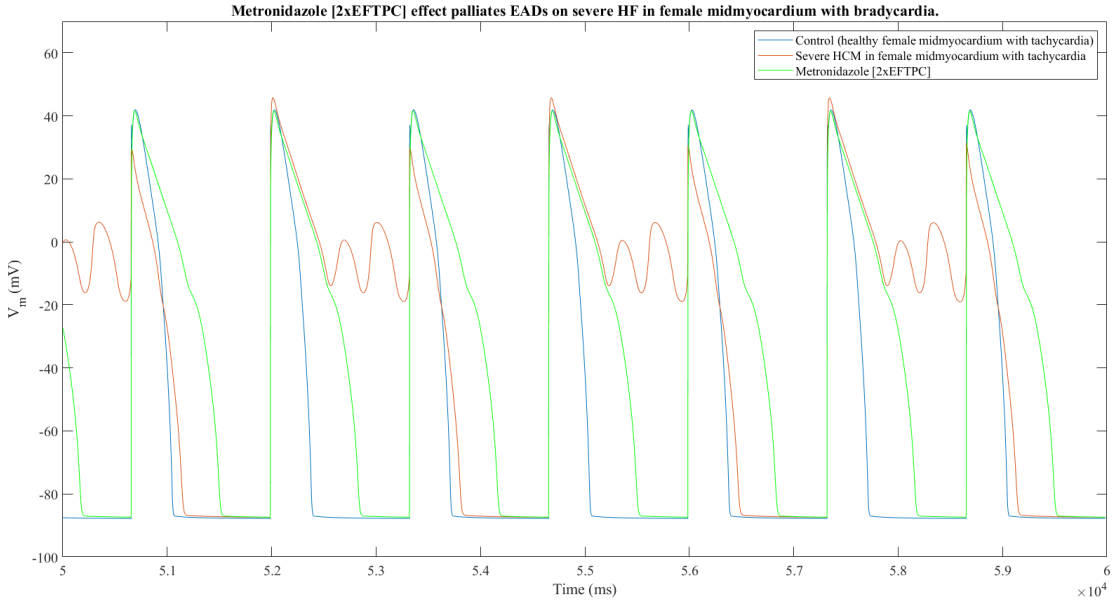

Figure 5.5. Example of antiarrhythmic drug, Metronidazole, that with a concentration of 2xEFTPC achieves treating EADs caused by severe HF in female midmyocardium with bradycardia.

According to results, there are 18 effective drugs to treat EADs, however in some of them this effectiveness occurs with a drug concentration equal to 10 folds EFTPC which can lead to toxicity and adverse side effects. For this reason, the drugs that are going to be considered will be the ones that are effective with a concentration equal to EFTPC or at most twice that value, thus shortening the list to 15 drugs that palliate EADs in a total of 119 cases. Of these 15 drugs, there are some that are the same drug but with different parameters depending on the research, as mentioned at the beginning of this chapter, so there are actually 11 different drugs that are effective for treating EADs with a concentration suitable for dosing: Diltiazem, Lamivudine, Linezolid, Metronidazole, Mibefradil, Mitoxantrone, Nifedipine, Nitrendipine, Pentobarbital, Phenytoin and Saquinavir. Nevertheless, not all of them are appropriate for treating cardiac pathologies like HF and HCM. For instance, Lamivudine and Saquinavir are antiretroviral drugs, Linezolid and Metronidazole are antibiotics, Mitoxantrone is an anthracenedione antineoplastic agent that avoids malignant tumour cells proliferation through the disruption of DNA synthesis and repair in both healthy and cancer cells, Pentobarbital is a short-acting barbiturate used to control convulsions, as a sedative and a preanesthetic that has been forbidden in some countries because of its poor safety, habituation, and lack of an antidote, and Phenytoin is an anti-convulsive.

In short, only 4 of those 11 drugs, Diltiazem, Mibefradil, Nifedipine and Nitrendipine are calcium channel blockers, which are currently prescribed for treating high blood pressure, angina and some cardiac rhythm disorders, except for Mibefradil which was voluntarily withdrawn from the market by the company that developed it due to the possibility of adverse interaction, some of them fatal, when combined with other drugs. In addition, as Phenytoin works as a voltage-gated sodium channel blocker, it affects cardiac sodium channels too, therefore it also has effects as an anti-arrhythmic agent.

Moreover, it is necessary to filter those drugs which are able to treat EADs with a concentration equal to the EFTPC value. The four drugs listed above as viable for treating EADs are effective with EFTPC.

But, in addition, in order to determine the viability to prescribe these medicines chronically, their specific uses, warnings and precautions and side effects have to be taken into account. According to

the online information centre for authorised medicines (CIMA "*Centro de Información online de Medicamentos Autorizados"*) of the Spanish Agency for Medicines and Health Products (AEMPS for its acronym in Spanish), Diltiazem, Nifedipine and Nitrendipine are calcium antagonists currently prescribed for hypertension (HBP) in all three cases, and angina in the case of Diltiazem and Nifedipine, so that all three are usually prescribed chronically. However, Diltiazem is not recommended in cases of severe bradycardia (heart rate less than 40 bpm), Nifedipine should be used with caution in patients with heart failure, and Nitrendipine should be used with caution with patients with decompensated HF. Nevertheless, as they are calcium antagonist, they inhibit the calcium ion flux in myocardium tissue and smooth muscle of coronary arteries and peripheral vessels, dilating thus the coronary arteries improving the oxygen supply to the myocardium. At the same time, they reduce vascular peripheral resistance decreasing thus the cardiac afterload, improving heart efficiency, and reducing HF symptoms (Agencia Española de Medicamentos y productos sanitarios, 2023; Agencia Española de Medicamentos y productos sanitarios, 2020; Agencia Española de Medicamentos y productos sanitarios, 2018).

Regarding Phenytoin, it is an antiepileptic effective in the treatment of some types of epilepsy. As it promotes the diffusion of sodium from the neurons, it tends to balance the hyperexcitability threshold caused by overstimulation or environmental changes that reduce the membrane sodium gradient. As a result, the propagation of seizure activity is inhibited. Unfortunately, cases of bradycardia and asystole have commonly been associated with Phenytoin intoxication but also with therapeutic dose (Agencia Española de Medicamentos y productos sanitarios, 2021 - a). In short, as the effects of Phenytoin overdose are serious, such as trembling, nystagmus, ataxia and dysarthria, among others and it has a narrow therapeutic margin (Agencia Española de Medicamentos y productos sanitarios, 2019), together with the fact that it is not prescribed to treat cardiac diseases but neurological disorders, Phenytoin is ruled out as a possible alternative to treat EADs caused by failure and hypertrophy.

In the end, three drugs, **Diltiazem, Nifedipine** and **Nitrendipine,** have been selected as an effective pharmacological treatment of EADs and, as a result, the cases in which they are effective with a concentration equal to EFTPC are limited to 32 conditions, summarised in Table 5.8.. It is noted that Diltiazem CiPA and Nitrendipine 2 are able to palliate the occurrence of EADs in all conditions. And, in particular, Nifedipine 1 is effective in all the cases in which EADs are produced by the effect of severe HF and HCM in males, but only in the ones caused by severe HF in female with normal heart rate and severe HCM in female with tachycardia. In addition, the EADs provoked by severe HCM in male midmyocardium with tachycardia are alleviated by all 3 drugs in all their sets of parameters obtained from the data base.

Table 5.8. Summary of the conditions (✓) in which viable drugs with a concentration equal to EFTPC are effective and viable for treating EADs caused by pathologies.

Effective drugs [1xEFTPC] for the treatment of EADs (✓)										
Drug	Female					Male				
	HF		HCM			HF		HCM		
	Bradycardia	Normal	Bradycardia	Normal	Tachycardia	Bradycardia	Normal	Bradycardia	Normal	Tachycardia
Diltiazem 1										✓
Diltiazem 2							✓			✓
Diltiazem CiPA	✓	✓	✓	✓	✓	✓	✓	✓	✓	✓
Nifedipine 1		✓			✓	✓	✓	✓	✓	✓
Nifedipine 2										✓
Nitrendipine 1										✓
Nitrendipine 2	✓	✓	✓	✓	✓	✓	✓	✓	✓	✓

5.3. EFFECTS OF DRUGS ON HEALTHY MYOCARDIUM

5.3.1. One drug effect on healthy myocardium

As mentioned at the beginning of CHAPTER 5 "RESULTS", all drugs were simulated also under healthy conditions considering the different heart rates, in order to determine the heart rate impact on the cardiomyocyte response in specific conditions.

As in section 5.1, the procedure consists of using the file *simulations_to_solve_abnormalities.m* with manual modality (variable *manual_simulation* equal to 'Yes'). However, in this case, in the parameters choice section, no pathology conditions (variables *npat* equal to 1), both sexes, the three cell types and the three heart rates (set from the *BCL_values*) are configured. In addition, the variables related to drug 1 must be 2 and 96 for *ndrug1_1* and *ndrug1_2* respectively, in order to add the effect of all the drugs for which parameters are available and then, the values 1 and 3 for *ncon1_1* and *ncon1_2* respectively, to simulate three drug concentrations.

Once the effect of 95 drugs with three concentrations on both sexes, three cell types and three heart rates have been simulated, giving a total of 5130 simulations, the obtained results have been analysed. Healthy conditions do not provoke any kind of arrhythmia, however, some drugs with certain concentrations under particular conditions enhance the probability of arrhythmia, disrupting some biomarkers associated with arrhythmogenicity. For instance, in Table 5.9 the conditions under which the occurrence of EADs is provoked (179 cases) are shown.

Table 5.9. The occurrence of EADs (×) caused by the effect of some drugs under healthy conditions (without pathology).

EADs (×) caused by the effect of some drugs on healthy cardiac tissue																				
Drug	[Drug]	Female									Male									
		Endocardium			Midmyocardium			Epicardium			Endocardium			Midmyocardium			Epicardium		
		Bradycardia	Normal	Tachycardia	Bradycardia	Normal	Tachycardia	Bradycardia	Normal	Tachycardia	Bradycardia	Normal	Tachycardia	Bradycardia	Normal	Tachycardia	Bradycardia	Normal	Tachycardia
Ajmaline	2xEFTPC				×	×	×							×		×			
	10xEFTPC				×	×	×							×	×	×			
Bepridil 1	10xEFTPC						×												
Bepridil 2	10xEFTPC				×	×	×							×	×	×			
Bepridil CiPA	10xEFTPC				×	×	×							×	×	×			
Cisapride CiPA	10xEFTPC				×		×												
Dofetilide 2	10xEFTPC				×	×	×							×	×	×			
Dofetilide CiPA	10xEFTPC				×	×	×							×		×			
Droperidol	10xEFTPC				×	×	×							×		×			
Flecainide	10xEFTPC				×	×	×							×	×	×			
Halofantrine	10xEFTPC				×		×									×			
Ibutilide	1xEFTPC				×	×	×							×	×	×			
	2xEFTPC				×	×	×							×	×	×			
	10xEFTPC	×	×		×	×	×			×				×	×	×			
Prenylamine	10xEFTPC				×	×	×									×			
Propafenone	10xEFTPC				×	×	×									×			
Quinidine 1	1xEFTPC				×	×	×							×		×			
	2xEFTPC				×	×	×							×	×	×			
	10xEFTPC				×	×	×								×	×			
Quinidine 2	1xEFTPC				×	×	×							×		×			
	2xEFTPC				×	×	×							×	×	×			
	10xEFTPC				×	×	×							×	×	×			
Quinidine CiPA	1xEFTPC				×	×	×									×			
	2xEFTPC				×	×	×							×	×	×			
	10xEFTPC			×	×	×	×	×	×	×			×	×	×	×		×	×
Ranolazine CiPA	10xEFTPC						×												
Terfenadine 2	2xEFTPC				×		×												
	10xEFTPC				×	×	×							×	×	×			
Terodiline	10xEFTPC						×												
Thioridazine 1	1xEFTPC						×												
	2xEFTPC				×	×	×							×		×			
	10xEFTPC				×	×	×							×	×	×			
Thioridazine 2	1xEFTPC				×	×	×							×	×	×			
	2xEFTPC				×	×	×							×	×	×			
	10xEFTPC			×	×	×	×						×	×	×	×			
Verapamil 2	10xEFTPC						×												

It is notable that the results indicate that the midmyocardium is by far the most affected cell type and particularly if the sex is female. These results are consistent because it has been already mentioned that midmyocardium and female are two conditions with an extended APD_{90} compared to endocardium and epicardium and male, respectively. What is unexpected is that the most affected heart rate is tachycardia, which is the one that has the shortest default APD_{90} compared to normal heart rate and bradycardia. Nevertheless, these results are coherent too because the heart rate has intense consequences on intracellular Ca^{2+} dynamics. Specifically, tachycardia increases the Ca^{2+} influx/efflux ratio, which in turn increases the cell Ca^{2+} content considering that I_{CaL} is enhanced and SERCA2a is stimulated by the adrenergic response. However, although the feedback system guarantees the prevention of progressive Ca^{2+} overload, adrenergic stimulation and tachycardia are a breeding ground for stressing the Ca^{2+} handling system. Therefore, if any of the components that affect intracellular Ca^{2+} dynamics, such as pro-arrhythmic drugs, tachycardia is most likely to lead to an instability of SR, which in turn has a crucial influence in several arrhythmogenic phenomenon, like afterdepolarizations (DADs and EADs), alternans and repolarisation variability in general (Zaza et al., 2018).

Moreover, as Table 5.9 shows there are 22 drugs which provoke EADs (Ajmaline, Bepridil 1, 2 and CiPA, Cispride CiPA, Dofetilide 2 and CiPA, Droperidol, Flecainide, Halofantrine, Ibutilide, Prenylamine, Propafenone, Quinidine 1, 2 and CiPA, Ranolazine CiPA, Terfenadine 2, Terodiline, Thioridazine 1 and 2 and Verapamil 2), which prove their arrhythmogenicity.

Nevertheless, there are many others that are also arrhythmogenic as they alter some of the other biomarkers such as APD_{90} prolongation. Unfortunately, to analyse all the data collected in depth is practically impossible with the limit of pages that this thesis has; however, all the results are attached in the appendix 8.1 and can be analysed in future works.

In particular, in this project the focus has been on those drugs that provoke EADs and mainly the ones that provoke them with 1xEFTPC and 2xEFTPC. Even so, it must be mentioned that simulating higher concentrations such as 10xEFTPC or even 30xEFTPC is important, because some people reach these plasma concentrations due to the way they metabolize the drug or even due to the interactions with other biomolecules. Taking this into consideration, 8 of the 22 above-mentioned drugs cause the occurrence of EADs with concentrations equal to 1xEFTPC and 2xEFTPC, and these are Ajmaline, Ibutilide, Quinidine 1, Quinidine 2, Quinidine CiPA, Terfenadine 2, Thioridazine 1 and Thioridazine 2, of which there are actually 5 different drugs, Ajmaline, Ibutilide, Quinidine, Terfenadine and Thioridazine. All of them considered as dangerous at the beginning of this chapter for being potentially the cause of some arrhythmogenic mechanisms.

On the one hand, although Ajmaline, Ibutilide and Quinidine are antiarrhythmic agents, their ability to disrupt biomarkers that indicate an increased propensity for arrhythmias is consistent, because the three of them prolong the cardiac action potential, contributing to a QT interval prolongation in the ECG, potentially leading to TdP. On the other hand, in spite of the fact that Terfenadine is an antihistaminic for treating allergic affections, it is not currently used because it prolongs the QT interval inciting cardiac arrhythmias as well. Finally, Thioridazine is an antipsychotic, which is usually used as the last option when other treatments have failed because it causes severe cardiac arrhythmias. This was the reason why the manufacturer stopped commercialising it, however, generic drugs are still in the market.

Lastly, it is important to highlight that Ajmaline is considered as a safe drug in the data base where the drugs IC_{50}, hill coefficients and EFTPC values have been gotten. Nevertheless, in the re-classification carried out in this thesis, the comparison (IC_{50} for I_{CaL} vs. IC_{50} for I_{Kr}) used as filter to sort the drug as arrhythmogenic or non-arrhythmogenic demonstrate that, as the IC_{50} of Ajmaline for I_{CaL} is greater than the IC_{50} of Ajmaline for I_{Kr}, the blockade of I_{Kr} will be higher than the blockade of I_{CaL}, so there will be a higher inflow of Ca^{2+} compared to the outflow of K^{+}, prolonging the plateau

and repolarization phase, and in turn lengthening the APD. In Figure 5.6 shows the difference between the effect of Ajmaline with a concentration of 1xEFTPC and 2xEFTPC under the same conditions (female midmyocardium with tachycardia).

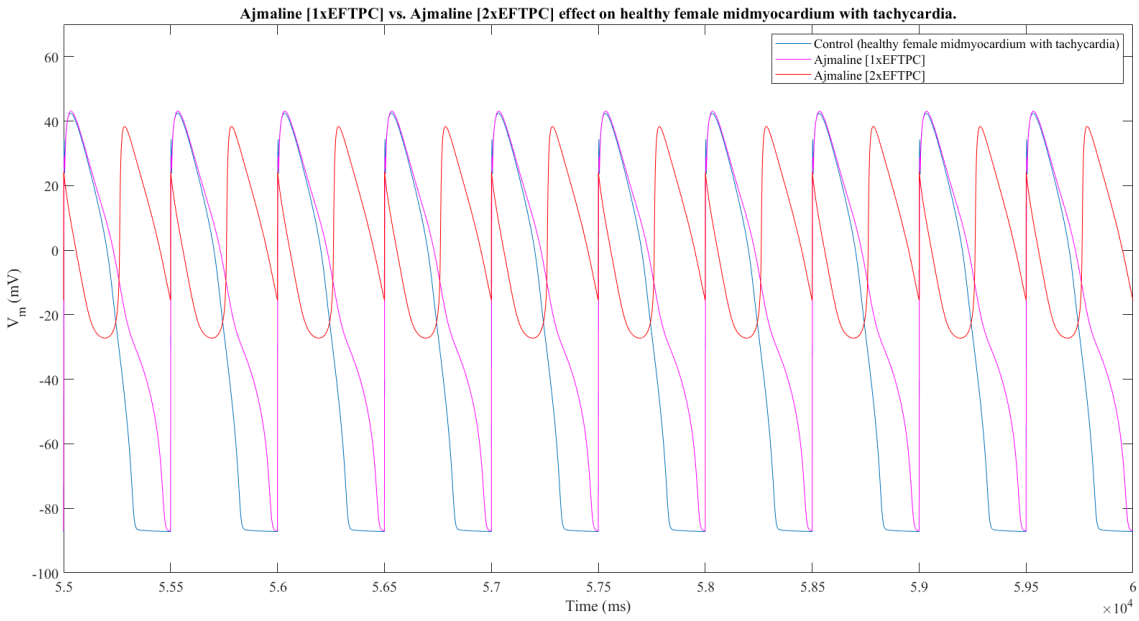

Figure 5.6. Female midmyocardium with tachycardia under Ajmaline effect with a concentration equal to 1xEFTPC (blue) which does not provoke EADs and 2xEFTPC (red) which causes the occurrence of EADs.

Furthermore, putting the 179 cases above mentioned aside, the remaining 4951 simulations were analysed taking into consideration the rest of biomarkers. On the one hand, of the remaining 7 biomarkers, the increase of V_m during the resting phase and failures in cellular stimulation are never given under the effects of drugs. On the other hand, unfortunately, all other biomarkers are altered in some particular cases. First, regarding an elevated RMP, there are 9 cases in which it is greater than -50 mV as a consequence of 7 drugs effects (Ajmaline, Ibutilide, Quinidine 1, 2 and CiPA and Thioridazine 1 and 2) as Table 5.10 shows.

Table 5.10. Summary of the cases with one drug effect that does not provoke EADs but in which RMP is altered having a value greater than -50 mV.

No.	Drug name	[Drug]	Cell type	Sex	Heart rate	RMP (mV)
1	Ajmaline	10xEFTPC	Endocardium	Female	Tachycardia	-39.61
2	Ibutilide	2xEFTPC	Endocardium	Female	Tachycardia	-47.07
3		10xEFTPC	Endocardium	Female	Tachycardia	-30.05
4				Male	Tachycardia	-42.25
5	Quinidine 1	10xEFTPC	Endocardium	Male	Tachycardia	-36.90
6	Quinidine 2	10xEFTPC	Endocardium	Female	Tachycardia	-46.12
7	Quinidine CiPA	10xEFTPC	Endocardium	Female	Normal	-30.02
8	Thioridazine 1	10xEFTPC	Endocardium	Male	Tachycardia	-39.17
9	Thioridazine 2	2xEFTPC	Endocardium	Female	Tachycardia	-47.70

In these cases, the V_m remains high during all the repolarization phase, never reaching an adequate RMP, which implies an increased risk of arrhythmia. It was to be expected that all the responsible drugs are some of the ones that have previously been proved as the cause of the occurrence of EADs. However, it is noticeable that endocardial tissue is the only one affected in this case and specifically, in most cases, female with tachycardia. These results are consistent due to the high frequency of

pacing currents in the tachycardic heart rate hampers that V_m reach normal RMP in cases where there is a prolongation of repolarization phase.

Next, with respect to changes in APD_{90}, of all 4951 cases, 3570 have no changes (72.11%), 1377 have an enlarged APD_{90} (27.81%) and 4 have a shortened APD_{90} (0.08%). Considering the cases that have an enlarged action potential, there are 55 drugs that provoke that effect as Table 5.11 shows.

Table 5.11. An excerpt of the cases with one drug effect on healthy conditions (no pathology) that does not provoke EADs, but they have a prolongation of APD_{90} greater than 20% regarding to the corresponding control simulation. The rest of the table is attached in the Appendix 8.1.

No.	Drug name	[Drug]	Sex	Cell type	Heart rate	APD_{90} value (mV)
1	Ajmaline	1xEFTPC	Female	Endocardium	Bradycardia	464.38
2					Tachycardia	367.46
3					Normal	425.26
4				Epicardium	Bradycardia	394.16
5					Tachycardia	322.07
6					Normal	359.29
7				Midmyocardium	Bradycardia	611.52
8					Tachycardia	462.22
9					Normal	534.48
10			Male	Endocardium	Bradycardia	442.08
11					Tachycardia	355.24
12					Normal	407.45
13				Epicardium	Bradycardia	379.27
14					Tachycardia	309.99
15					Normal	345.39
16				Midmyocardium	Bradycardia	564.97
17					Tachycardia	434.59
18					Normal	495.42
.						
.						
.						
1361	Verapamil 2	10xEFTPC	Female	Endocardium	Bradycardia	555.20
1362					Tachycardia	423.27
1363					Normal	502.32
1364				Epicardium	Bradycardia	479.31
1365					Tachycardia	393.22
1366					Normal	441.34
1367				Midmyocardium	Bradycardia	659.54
1368					Normal	598.22
1369			Male	Endocardium	Bradycardia	536.30
1370					Tachycardia	411.44
1371					Normal	485.99
1372				Epicardium	Bradycardia	462.85
1373					Tachycardia	379.35
1374					Normal	425.32
1375				Midmyocardium	Bradycardia	624.19
1376					Tachycardia	484.99
1377					Normal	568.12

However, most of them have that dangerous effect with a concentration equal to 10xEFTPC which corresponds with overdose. For this reason, to be more consistent with the reality that, a priori, patients do not reach overdose concentration because they have professional monitoring of their treatment, only the drugs that cause APD prolongation at concentrations equal to 1xEFTPC or 2xEFTPC are considered, thus reducing the number of drugs from 55 to 26, all of them classified as arrhythmogenic drugs except for 5 drugs, Piperacillin, Ranolazine CiPA and Verapamil 1, 2 and

CiPA. Although these results can be worrying, taking into account that their effect has been simulated under healthy conditions, is quite understanding that if they have some effects on calcium and/or potassium currents, the plateau and repolarization phase are affected by prolonging even though the drugs are considered to be anti-arrhythmogenic. Nevertheless, they are going to be analysed one per one.

First, **Piperacillin** is a broad-spectrum penicillin antibiotic which is not absorbed orally, but it must be given by intravenous or intramuscular injection (Agencia Española de Medicamentos y productos sanitarios, 2021 - b). It is considered to have an intermediate risk by the data base where the drugs' parameters have been gotten. Fortunately, it is not a drug for chronic use, it does not provoke arrhythmogenic effects with EFTPC and, in addition, its effect on APD prolongation is not greater than 32%, what means that its dangerous effects are not much greater than the threshold. Second, **Ranolazine** is used to treat heart related chest pain such as chronic angina. However, it is considered to have an intermediate risk by the original data base due to its effect on APD consists of a balance between the I_{Kr} and I_{NaL} inhibition, thus provoking possible QT prolongation (Rayner-Hartley & Sedlak, 2016). Nevertheless, Ranolazine is an effective drug for managing chronic angine and it is well tolerated by patients with this condition. And, lastly, **Verapamil** is a calcium channels blocker used to treat HT, angina and cardiac rhythms disorders. Although it blocks I_{CaL} channels initially promoting a faster repolarisation, it also affects I_{Kr} current (Pepine et al., 1998). Specifically, according to the parameters values gotten for Verapamil 1, 2 and CiPA, the difference between IC_{50} for I_{CaL} and for I_{Kr} is not so prominent, therefore, its effect of reducing APD is not so evident.

Ultimately, if its corresponding curve of fraction of open channels vs. drug concentration (see the example of Verapamil 1 in Figure 5.7) of all these 5 drug cases is analysed, although the corresponding difference between IC_{50} for I_{CaL} and for I_{Kr} keeps to the condition given for those drugs considered as anti-arrhythmogenic, due to their effect on both channels being very similar (curves with very similar values), the inhibition that they can generate on both currents is so similar that their effect on the plateau and repolarization phases can lead to both lengthening and narrowing of APD.

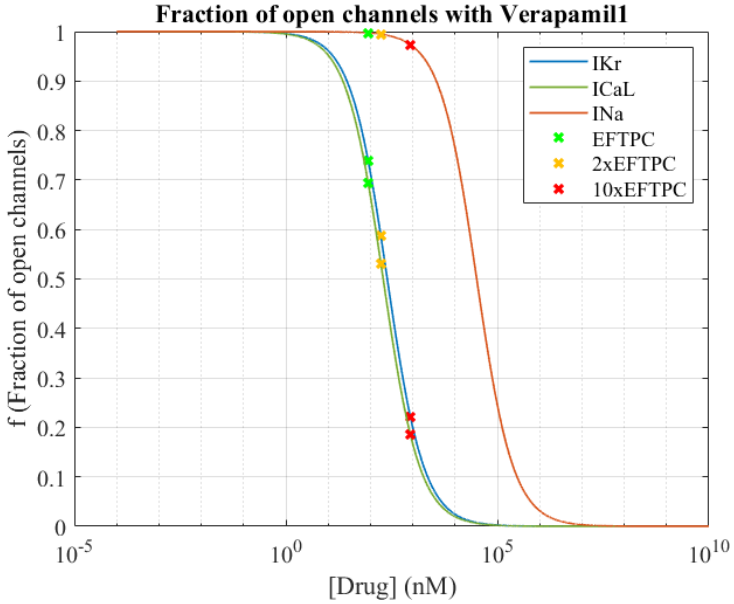

Figure 5.7. Fraction of open channels with Verapamil 1 whose values of IC50 for I_{Kr}, I_{CaL} and I_{Na} are 3405100 nM, 1226000 nM and 2433800 nM respectively, all Hill coefficients are equal to 1 nH and its EFTPC is 1378000 nM.

The following Figure 5.8 shows the effect of these 5 drug cases that, although they are considered as anti-arrhythmogenic, they prolong the APD_{90} regarding the corresponding control.

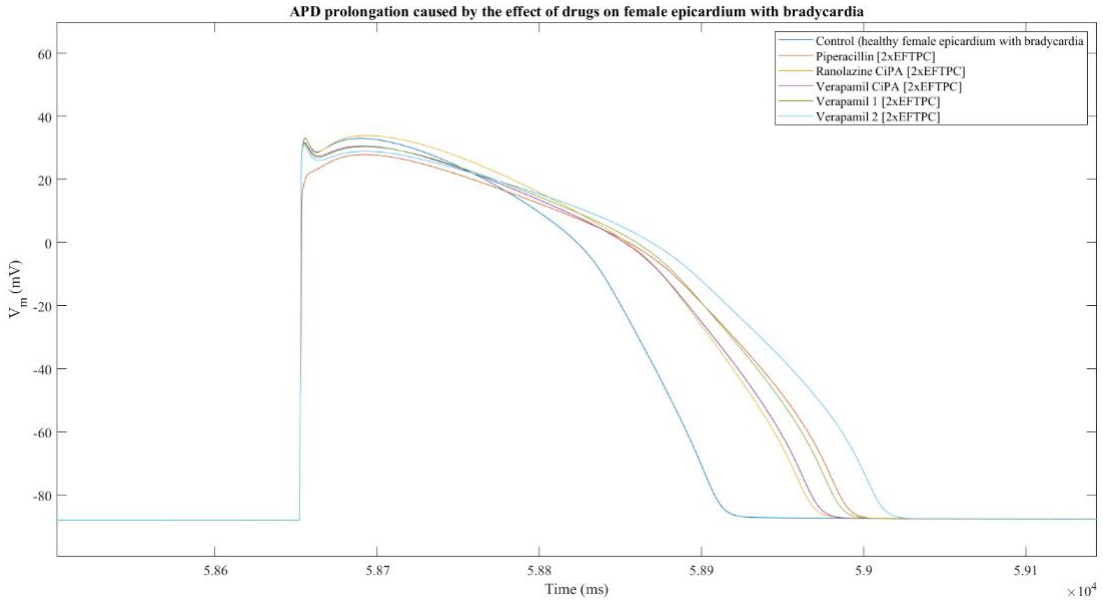

Figure 5.8. APD prolongation due to Piperacillin, Ranolazine CiPA, Verapamil CiPA, Verapamil and Verapamil 2 all of them with a concentration equal to [2xEFTPC]. The effect of these drugs has been added to a female epicardium with bradycardia (control).

Regarding alternans, of all 4951 total cases without EADs, 18 cases have alternans (0.36%) which are shown in Table 5.12. It is noticeable that there is no sex- or cell type-dependent relationship, but there is a heart rate-dependent relation with alternans, being the cases with tachycardia the most affected ones.

Table 5.12. Drugs with the corresponding concentration and the healthy conditions in which alternans occur.

No.	Drug name	[Drug]	Sex	Cell type	Heart rate
1	Ajmaline	10xEFTPC	Female	Endocardium	Tachycardia
2			Male	Endocardium	Tachycardia
3	Ibutilide	10xEFTPC	Male	Endocardium	Bradycardia
4				Epicardium	Tachycardia
5	Piperacillin	10xEFTPC	Female	Midmyocardium	Tachycardia
6			Male	Midmyocardium	Tachycardia
7	Quinidine 1	10xEFTPC	Female	Endocardium	Tachycardia
8			Male	Endocardium	Tachycardia
9	Quinidine 2	10xEFTPC	Female	Epicardium	Tachycardia
10			Male	Endocardium	Tachycardia
11	Quinidine CiPA	2xEFTPC	Female	Endocardium	Tachycardia
12		10xEFTPC	Female		Normal
13			Male	Endocardium	Normal
14	Thioridazine 1	10xEFTPC	Female	Endocardium	Tachycardia
15				Epicardium	Tachycardia
16			Male	Endocardium	Tachycardia
17	Thioridazine 2	2xEFTPC	Female	Endocardium	Tachycardia
18		10xEFTPC		Epicardium	Tachycardia

In Figure 5.9 two examples of these 18 cases are displayed. That heterogeneity between consecutive AP waveforms that characterises alternans is one of the mechanisms that increases the arrhythmia susceptibility. There are several hypotheses around the underlying mechanism of alternans, one of

them is that the disruptions in calcium currents can lead to some perturbations in intracellular Ca^{2+} concentration which, in turn, impact on excitation-contraction coupling (Kulkarni et al., 2019). Therefore, as Figure 5.10 proves, $[Ca^{2+}]_i$ alternans are the responsible of action potential morphology alternation. As all the drugs listed in Table 5.12 have an inhibitory effect on calcium currents, especially in I_{CaL}, they are able to provoke some disturbances in intracellular calcium concentration that can lead to alternances in membrane voltage. Fortunately, the cases with alternans are not many and most of them are due to drug effect with an overdose concentration.

(A) (B)

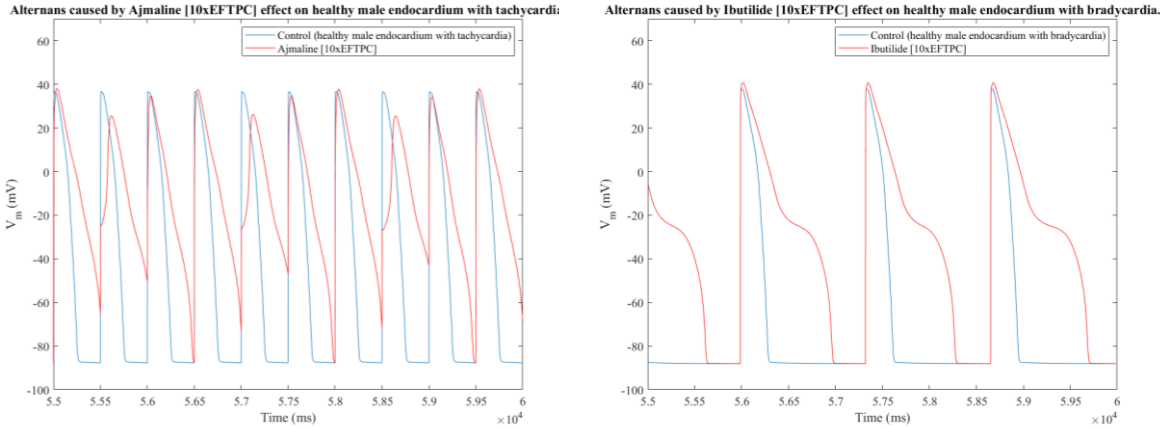

Figure 5.9. Two examples of alternans caused by (A) Ajmaline [10xEFTPC] and (B) Ibutilide [10xEFTPC] effect on healthy male endocardium with tachycardia and bradycardia respectively.

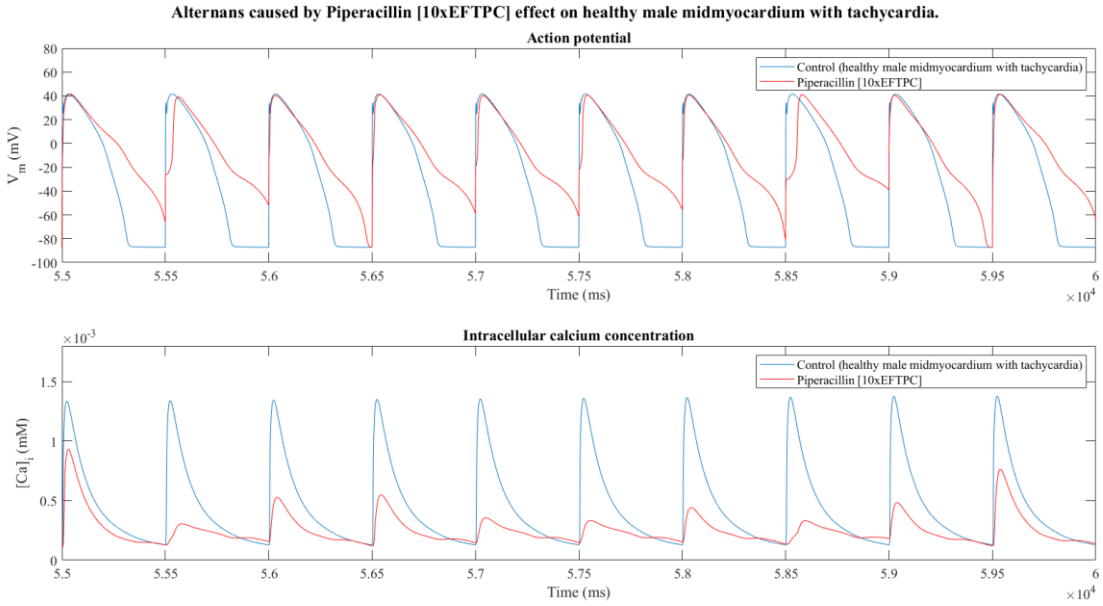

Figure 5.10. Membrane potential and intracellular calcium concentration vs. time. Drug interaction with calcium currents provokes alternans in intracellular calcium concentration which, in turn, promotes alternans in the action potential morphology.

Finally, analysing the cases with a triangulation value greater than 140 ms, of all 4951 total cases without EADs, 1543 have the triangulation value sufficiently altered to increase the risk of arrhythmia, as shown in Table 5.13.

Table 5.13. An excerpt of the cases with one drug effect on healthy conditions (no pathology) that does not provoke EADs, but they cause an altered triangulation value ($APD_{90} - APD_{30}$), being greater than 140. The rest of the table is attached in the Appendix 8.1.

No.	Drug name	[Drug]	Sex	Cell type	Heart rate	Triangulation (ms)
1	Ajmaline	1xEFTPC	Female	Endocardium	Bradycardia	197.2
2					Tachycardia	168.0
3					Normal	189.0
4				Epicardium	Bradycardia	141.6
5				Midmyocardium	Bradycardia	304.4
6					Tachycardia	246.6
7					Normal	271.8
8			Male	Endocardium	Bradycardia	187.6
9					Tachycardia	161.6
10					Normal	179.6
11				Midmyocardium	Bradycardia	267.4
12					Tachycardia	221.0
13					Normal	240.6
.						
.						
.						
1538	Voriconazole	1xEFTPC	Female	Midmyocardium	Bradycardia	144.0
1539		2xEFTPC	Female	Midmyocardium	Bradycardia	145.4
1540		10xEFTPC	Female	Midmyocardium	Bradycardia	156.2
1541					Normal	150.2
1542			Male	Midmyocardium	Bradycardia	146.0
1543					Normal	141.8

Analysing the data, midmyocardium is the cell type whose triangulation values are the highest under the effect of drugs, 867 of 1543, which represent the 56.19% of the total cases with one drug effect, but without EADs (see Table 5.14). These results are consistent due to the fact that, as Table 5.4 shows, midmyocardium has the greatest triangulation values per se, so the addition of any kind of effect on repolarization currents can provoke an alteration in triangulation values that exceeds the threshold of 140 ms. In particular, the case of healthy female midmyocardium with bradycardia is the one with the highest triangulation value (142.4 ms as Table 5.3 shows), which is, in turn, over the threshold, which means that midmyocardial cells of a female with bradycardia have a higher risk of suffering arrhythmias. This value and the above results are consistent with each other too because the specific condition whose triangulations values are most affected by drugs effects is female midmyocardium with bradycardia, 230 of 1543, which in turn represent 14.91% of the total cases with one drug effect but without EADs.

Table 5.14. Relative frequency distribution table by condition in cases without the occurrence of EADs but with altered triangulation value caused by the effect of one drug.

Conditions	Frequency	Rel. Freq. (%)
Total	**1543**	100.00%
Cell type		
Endocardium	453	29.36%
Midmyocardium	867	56.19%
Epicardium	223	14.45%
Sex		
Female	850	55.09%
Male	693	44.91%
Heart rate		
Bradycardia	629	40.76%
Normal	536	34.74%
Tachycardia	378	24.50%

Considering this information, it is interesting to analyse which drugs alter the triangulation parameter in male epicardium, which are the two conditions in which triangulation value in healthy conditions without drugs is the lowest (see Table 5.3). There are 26 drugs that are able to alter this biomarker until dangerous values and the underlying mechanism is shown in Figure 5.11. It is observable that, on the one hand, a "second" plateau occurs in the action potential along with the repolarization phase which in turn provokes both, a prolongation in APD and an alteration in triangulation value due to the mentioned "second" plateau increments APD_{90} regarding APD_{30}. On the other hand, it can be seen that for the time in which the second plateau is generated, there is a slight increase in the intracellular calcium concentration. All this evidence points to the fact that there is a reactivation of calcium currents which counteract the outward potassium currents, thus generating the so-called "second" plateau and preventing the normal course of repolarization phase.

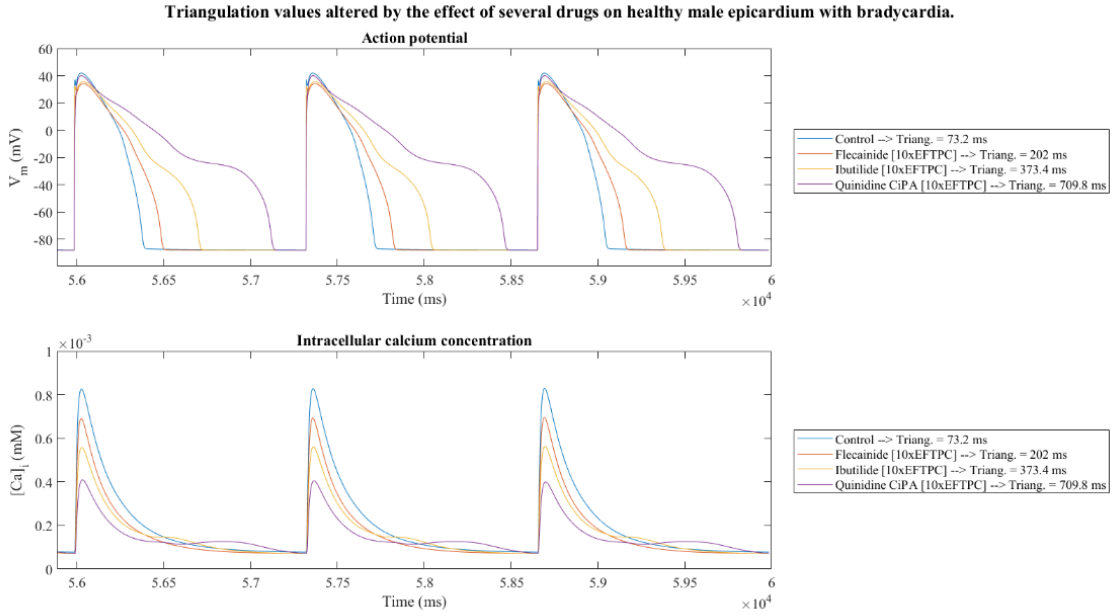

Figure 5.11. Membrane potential and intracellular calcium concentration vs. time. Drug interaction with calcium currents and excitation-contraction coupling provokes a small increment of intracellular calcium concentration during repolarization which, in turn, promotes an abnormal action potential morphology.

5.3.2. Combination of drugs on healthy myocardium

Finally, a second drug has been simulated in those cases in which one drug had caused EADs. As there were 179 cases with no pathology in which the occurrence of EADs was provoked by the effect of one drug, adding the effect of a second drug, considered as anti-arrhythmogenic, with its respective three concentrations would require the execution of 15036 more simulations, which was not viable due to the computation time. For this reason, it was decided that the addition of a second safe drug would be carried out in those cases of drug induced EADs at a concentration of 1xEFTPC or 2xEFTPC at most (69 cases). The concentrations chosen were those because of 10xEFTPC is an overdose that is more unlikely than EFTPC or 2xEFTPC. Thus, the total number of simulations to be run were 5796, which is a more viable amount.

In order to configure the script *simulations_to_solve_abnormalities.m* the procedure is similar to the one carried out in section 5.2 but with the corresponding Excel file path and defining the variable *drugSimWith* as 'Drug_2'.

Once the simulations were run, in order to establish the influence of heart rate with the efficiency of drug combination to solve EADs caused by an arrhythmogenic drug, some percentages have been

calculated. As Table 5.15 shows, of the total 5796 simulations executed to analyse the drug effectiveness to palliate EADs provoked by another drug, 2184 were run with tachycardia conditions, 1596 with normal heart rate and 2016 with bradycardia. Of these, 181, 415 and 690 simulations respectively, do not present the occurrence of EADs. These values correspond to 8.29%, 26.00% and 34.23% of the total simulations executed per each heart rate, respectively.

Table 5.15. Relative frequency distribution table by condition of both, the total cases with two drugs effects and the cases without the occurrence of EADs thanks to the effect of the second drug.

Conditions	Frequency	Rel. Freq. (%)	Freq. No EADs	Rel. Freq. No EADs (%)
Total	**5796**	100.00%	1286	22.19%
Cell type				
Endocardium	0	0.00%	0	0.00%
Midmyocardium	5796	100.00%	1286	22.19%
Epicardium	0	0.00%	0	0.00%
Sex				
Female	3276	56.52%	677	20.67%
Male	2520	43.48%	609	24.17%
Heart rate				
Bradycardia	2016	34.78%	690	34.23%
Normal	1596	27.54%	415	26.00%
Tachycardia	2184	37.68%	181	8.29%

These values, together with the conclusions discussed in section 5.3.1, indicate that not only does tachycardia provoke a greater probability of the occurrence of EADs, but also the favourable response to some anti-arrhythmogenic drugs is lower. Therefore, to sum it up, according to the results, the lower the heart rate is, the greater the ability to handle arrhythmogenic mechanisms like EADs. It would be significant to analyse the causes behind this phenomenon.

In addition, taking into account the limits of this thesis, it strikes as impossible to analyse all the large amount of data collected. For this reason, in this case, the main aim has been analysing the combinations of drugs that treat EADs in female midmyocardium with tachycardia, because these have been the ensemble of conditions which has been affected by all the drugs considered as the ones that provoke EADs (see Table 5.9). Of all the 1176 possibilities that palliate the occurrence of EADs through the combination of one drug conditions that provoke EADs with the drugs considered anti-arrhythmogenic, only 102 combinations palliate EADs caused on female midmyocardium with tachycardia, as Table 5.16 shows.

There are 15 drugs capable of palliating EADs caused by the effect of one arrhythmogenic drug, of which 11 are different: Diltiazem, Lamivudine, Linezolid, Metronidazole, Mibefradil, Mitoxantrone, Nifedipine, Nitrendipine, Phenytoin, Piperacillin and Saquinavir. Most of them are effective with a concentration equal to 10xEFTPC, which means an overdose so not all of them can be used to palliate EADs although they are able to do it. The usage and effect of each one has already been explained in section 5.2, except for Piperacillin which is explained in section 5.3.1, but its possible chronic use remains to be explained. Considering that it is an antibiotic, the possibility of bacterial antibiotic resistance and its route of administration make it impossible for Piperacillin to be considered as an option to be prescribed chronically. Therefore, Piperacillin is ruled out to be administrated together with a dangerous arrhythmogenic drug in order to palliate its side effects.

Table 5.16. Combination of drugs that palliate EADs provoked by one drug effect on female midmyocardium with tachycardia. Note that there are more cases with arrhythmogenic drugs than the ones showed in this table, this is because the missing ones do not have any possible combination to palliate the occurrence of EADs. The complete table can be checked in the Appendix 8.1.

Combinations of drugs that palliate EADs (✓)											
Anti-arrhythmogenic drugs		Arrhythmogenic drugs that cause EADs in female endocardium with tachycardia									
		Ajmaline	Ibutilide	Quinidine 1		Quinidine 2	Quinidine CiPA		Terfenadine 2	Thioridazine 1	
		2xEFTPC	1xEFTPC	1xEFTPC	2xEFTPC	1xEFTPC	1xEFTPC	2xEFTPC	2xEFTPC	1xEFTPC	2xEFTPC
Diltiazem 1	1xEFTPC									✓	
	2xEFTPC								✓	✓	
	10xEFTPC								✓	✓	
Diltiazem 2	1xEFTPC								✓	✓	
	2xEFTPC								✓	✓	
	10xEFTPC	✓							✓	✓	
Diltiazem CiPA	1xEFTPC								✓	✓	
	2xEFTPC								✓	✓	
	10xEFTPC	✓				✓			✓	✓	
Lamivudine	1xEFTPC								✓	✓	
	2xEFTPC								✓	✓	
	10xEFTPC	✓				✓			✓	✓	
Linezolid	1xEFTPC								✓	✓	
	2xEFTPC								✓	✓	
	10xEFTPC								✓	✓	
Metronidazole	1xEFTPC								✓	✓	
	2xEFTPC								✓	✓	
	10xEFTPC			✓							
Mibefradil2	1xEFTPC									✓	
	2xEFTPC									✓	
	10xEFTPC								✓	✓	
Mitoxantrone	10xEFTPC									✓	
Nifedipine 1	1xEFTPC								✓	✓	
	2xEFTPC								✓	✓	
	10xEFTPC	✓		✓		✓	✓		✓	✓	✓
Nifedipine 2	1xEFTPC									✓	
	2xEFTPC								✓	✓	
	10xEFTPC								✓	✓	
Nitrendipine 1	1xEFTPC									✓	
	2xEFTPC								✓	✓	
	10xEFTPC								✓	✓	
Nitrendipine 2	1xEFTPC	✓		✓		✓	✓		✓	✓	✓
	2xEFTPC	✓		✓		✓	✓		✓	✓	✓
	10xEFTPC	✓	✓	✓		✓	✓	✓	✓	✓	✓
Phenytoin 1	1xEFTPC									✓	
	2xEFTPC									✓	
	10xEFTPC								✓	✓	
Piperacillin	10xEFTPC	✓		✓	✓	✓			✓	✓	✓
Saquinavir	2xEFTPC									✓	
	10xEFTPC								✓	✓	

As it can be comprehended analysing the results obtained, the occurrence of EADs caused by the effect of Terfenadine and Thioridazine can be palliated by all the drugs that have some positive effect. However, as mentioned in section 575.3.1, the first is not currently used and the second is used as the last option due to its cardiac side effects, so, definitely their usage is quite limited. In addition,

without considering the necessity to alleviate the effect of these two whose usage is so restricted, the unique drug capable of palliating the occurrence of EADs caused by an arrhythmogenic drug with a concentration equal to 1xEFTPC or 2xEFTPC is Nitrendipine.

In short, as it has been discussed in section 5.2, Diltiazem, Nifedipine and Nitrendipine can be administrated chronically to solve the occurrence of EADs caused by a pathology, as proved in section 5.2, or by an arrhythmogenic drug as discussed in this section. However, as **Nitrendipine** is the only one which is effective without an overdose, it has been considered as the most effective and viable drug to treat EADs caused by some arrhythmogenic drug administrated to female patients with tachycardia, as Figure 5.12 shows.

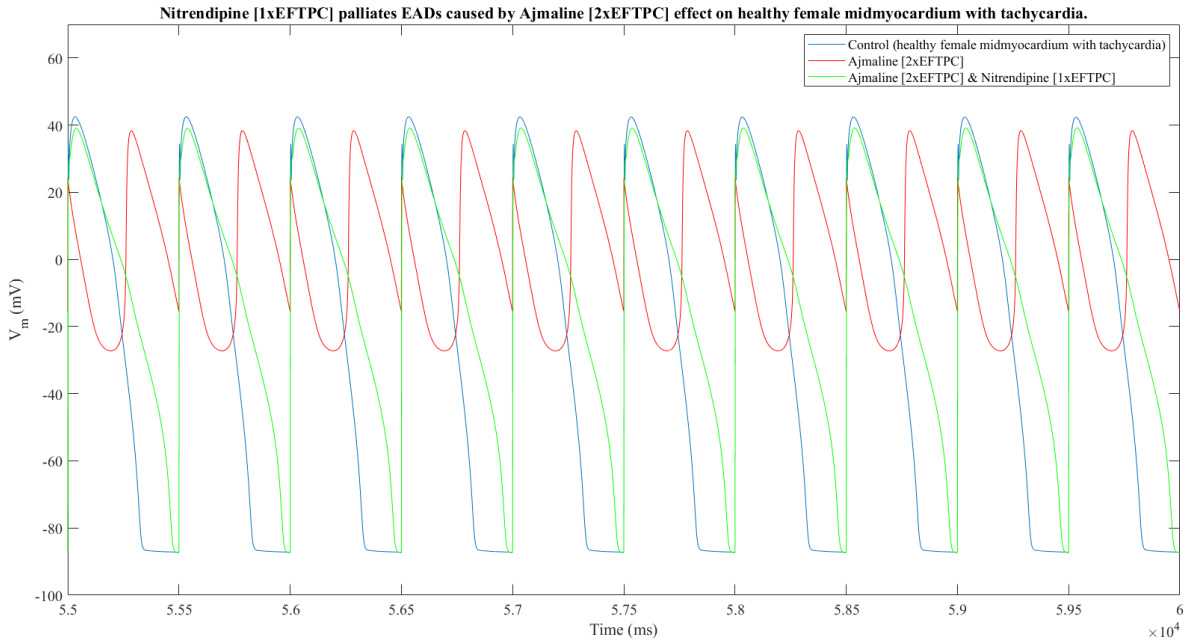

Figure 5.12. The effect of Nitrendipine [1xEFTPC] combined with Ajmaline [2xEFPTC] on female midmyocardium with tachycardia is able to palliate the EADs caused by the latter.

It would be interesting to analyse which drugs are effective for treating the occurrence of EADs caused by one drug effect on different conditions from female midmyocardium with tachycardia; however, this is beyond the boundaries of this thesis.

5.4. THE CASE OF DILTIAZEM

5.4.1. Basic concepts

As it has been already explained, Diltiazem is a non-dihydropyridine calcium-channel blocker derived from benzothiazepine, mainly used to treat HT, angina pectoris and some cardiac arrhythmias. Although it has several mechanisms of action, the principal one is inhibiting the calcium influx into myocardium and vascular smooth muscle (National Center for Biotechnology Information, 2024 - a).

Specifically, Diltiazem blocks voltage-dependent calcium channels by inhibiting the ion-control gating mechanisms, although it is thought that it also interferes with calcium release by SR. Therefore, the overall low calcium level provokes a decrease in myocardial and vascular smooth muscle, leading to a dilation of the main coronary and systemic arteries which, in turn, decreases

peripheral arterial resistance, improves oxygen supply to the cardiomyocites and decreases cardiac output.

Diltiazem is absorbed by the small intestine and is carried to the liver where, thanks to some enzymes of cytochrome P450 (CYP450) such as CYP3A4, it is oxidated and metabolized, converting Diltiazem into several metabolites such as desacetildiltiazem (DAD). Finally, Diltiazem's metabolites are mainly excreted by the kidneys through urine and faeces.

The molecular formula of Diltiazem is $C_{22}H_{26}N_2O_4S$, whose structure is shown in Figure 5.13.

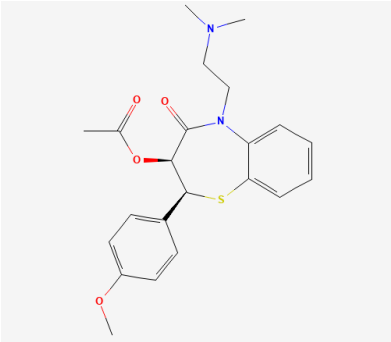

Figure 5.13. Chemical structure of Diltiazem. Source: taken from National Center for Biotechnology Information (2024 - a)

5.4.2. Diltiazem 1 vs. Diltiazem 2 vs. Diltiazem CiPA

In the data base, where drugs' parameters have been acquired, three different sets of parameters for Diltiazem were compiled, Diltiazem 1, 2 and CiPA. This occurs due to, after the literature research carried out by Fogli Iseppe et al. (2021), authors found three different research papers in which IC_{50} values, Hill coefficients and EFTPC were not the same. In particular, it is necessary to mention that Diltiazem 1 and 2 affect the same number of channels, I_{Kr}, I_{CaL} and I_{Na} (see Figure 5.14). However, the data collected for the CiPA initiative for this drug determines that not only does Diltiazem CiPA have an influence on the last three mentioned channels but also on I_{NaL} and I_{to} as Figure 5.15 shows.

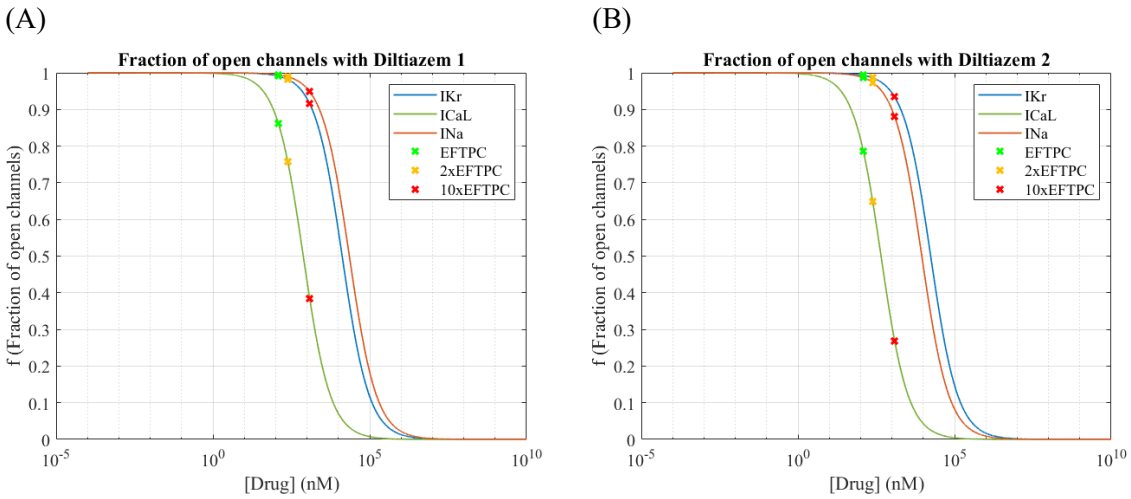

Figure 5.14. Fraction of open channels with (A) Diltiazem 1 whose values of IC_{50} for IKr, ICaL and INa are 13200 nM, 760 nM and 22400 nM respectively, all Hill coefficients are equal to 1 nH and its EFTPC is 122 nM and (B) Diltiazem 2 whose values of IC50 for IKr, ICaL and INa are 17300 nM, 450 nM and 9000 nM respectively, all Hill coefficients are equal to 1 nH and its EFTPC is 122 nM.

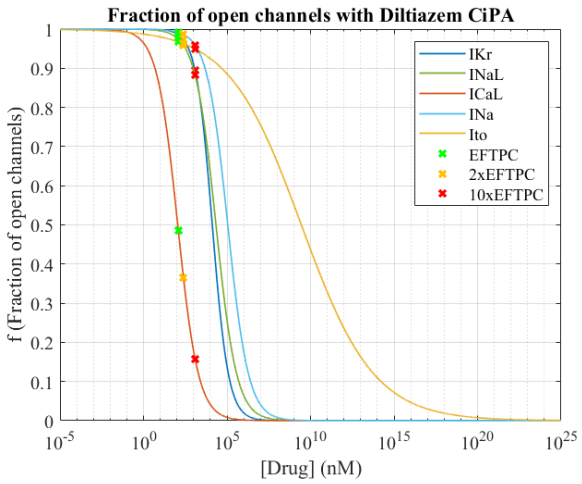

Figure 5.15. Fraction of open channels with Diltiazem CiPA whose values of IC_{50} for IKr, INaL, ICaL, INa and Ito are 13150 nM, 21868.5 nM, 112.1 nM, 110859 nM and 2820000000 nM respectively, Hill coefficients are 0.9 nH for I_{Kr}, 0.7 nH for I_{NaL}, I_{CaL} and I_{Na} and 0.2 nH for I_{to} and its EFTPC is 122 nM.

In the three cases, **Diltiazem CiPA** offers a greater inhibition of L-type calcium channels at EFTPC than Diltiazem 1 and 2, which can explain the higher effectiveness of Diltiazem CiPA in alleviating the occurrence of EADs caused by pathologies with only a concentration equal to EFTPC (see Table 5.8).

5.5. THE CASE OF NIFEDIPINE

5.5.1. Basic concepts

As previously mentioned, Nifedipine is, unlike Diltiazem, a dihydropyridine L-type calcium channel blocking agent used for treating HT and angina pectoris (National Center for Biotechnology Information, 2024 - b). Like Diltiazem, Nifedipine is able to inhibit the extracellular calcium ion influx into myocardium and vascular smooth muscle cells, as a result there is a reduction of intracellular calcium concentration. As a consequence, a decreasing of myocardial and vascular smooth muscle cells contractility is produced, which in turn causes a dilation of the main coronary and systemic arteries. This vasodilatation promotes blood pressure to decrease, palliating HT symptoms. In addition, incidentally, Nifedipine also inhibits the drug pump P-glycoprotein which can improve the efficiency of some antineoplastic agents due to this pump being overexpressed in some multi-drug resistant tumours.

Nifedipine molecular formula is $C_{17}H_{18}N_2O_6$, whose structure is shown in Figure 5.16.

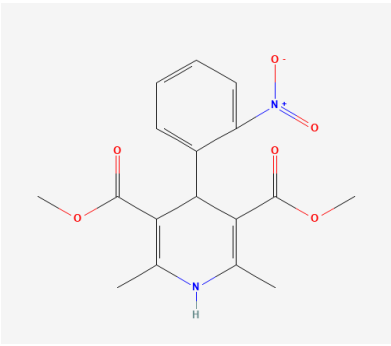

Figure 5.16. Chemical structure of Nifedipine. Source: taken from National Center for Biotechnology Information (2024 - b)

5.5.2. Nifedipine 1 vs. Nifedipine 2

In this case, Nifedipine has two different sets of parameters compiled in the data base, Nifedipine 1 and Nifedipine 2. Both of them affect the same channels, I_{Kr}, I_{CaL} and I_{Na}, however as their influence in each of them is different (see Figure 5.17), so is their effectiveness.

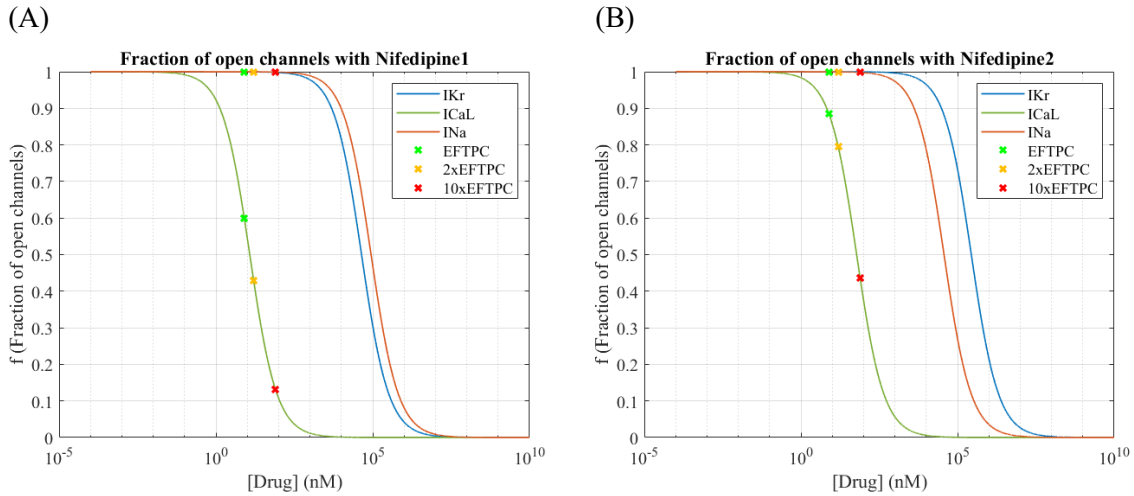

Figure 5.17. Fraction of open channels with (A) Nifedipine 1 whose values of IC_{50} for IKr, ICaL and INa are 44000 nM, 12 nM and 88500 nM respectively, all Hill coefficients are equal to 1 nH and its EFTPC is 8 nM and (B) Nifedipine 2 whose values of IC50 for IKr, ICaL and INa are 275000 nM, 60 nM and 37000 nM respectively, all Hill coefficients are equal to 1 nH and its EFTPC is 7.7 nM.

It is noticeable that the inhibition of I_{CaL} with EFTPC is greater with Nifedipine 1 than with Nifedipine 2 effect, which is consistent with the results in which Nifedipine 1 has a higher cardioprotective effect than Nifedipine 2 because, as shown in Table 5.8 and Table 5.16, Nifedipine 1 is more effective in a large amount of cases.

5.6. THE CASE OF NITRENDIPINE

5.6.1. Basic concepts

As mentioned above, Nitrendipine is, like Nifedipine, a dihydropyridine calciumantagonist used for treating HT and chronic stable angina. It works inhibiting the influx of extra calcium ions across the cell membrane of myocardium and vascular smooth muscle (National Center for Biotechnology Information, 2024 - c).

Nitrendipine also follows hepatic metabolism mediated cytochrome P450 (CYP450). After oral ingestion, Nitrendipine is absorbed by passive diffusion in the small intestine and metabolized in the liver. CYP450 enzymes convert Nitrendipine into its pharmacological inactive metabolites. Afterwards, the resulting metabolites are released into the bloodstream and reach the systemic circulation. Then, metabolites of Nitrendipine are transported through the circulatory system to organism tissues. Finally, the metabolites are filtered by the renal glomerulus, and they are excreted through the urine.

The mechanism of action of Nitrendipine is based on its affinity with inactivated L-type calcium channels, reducing the probability of these channels, thus reducing calcium influx. That is, Nitrendipine alters calcium channels morphology, interferes with the calcium release from the SR, and/or inhibits ion-control gating mechanisms. All these processes result in a decrease in intracellular calcium concentration which, in turn, affect the function of the myocardial smooth muscle cells inhibiting their contractile processes. As a result, the reduction of the contractility of myocardial

smooth muscle cells promotes a dilation of both, coronary and systemic arteries, which, in turn, decreases peripheral resistance decreasing the systemic blood pressure and afterload and increases the oxygen supply to the myocardial tissue.

Nitrendipine is a small molecule whose chemical formula is $C_{18}H_{20}N_2O_6$ and its structure is shown in Figure 5.18.

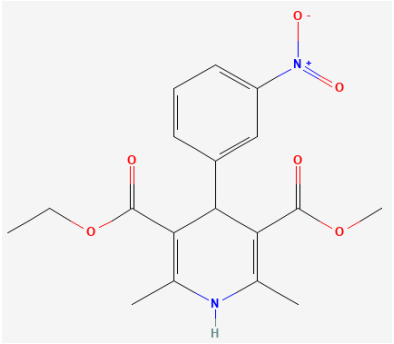

Figure 5.18. Chemical structure of Nitrendipine. Source: taken from National Center for Biotechnology Information (2024 - c).

5.6.2. Nitrendipine 1 vs. Nitrendipine 2

Two different sets of parameters for Nitrendipine were compiled in the data base, Nitrendipine 1 and Nitrendipine 2. In this case, although EFTPC for Nitrendipine 1 and 2 is almost the same, 3 and 3.02 nM, respectively, their influence on every ionic current is not, as can be appreciated in Figure 5.19. Nitrendipine 2 offers a greater inhibition of L-type calcium channels than Nitrendipine 1, which can explain the higher effectiveness of Nitrendipine 2 in reducing the occurrence of EADs.

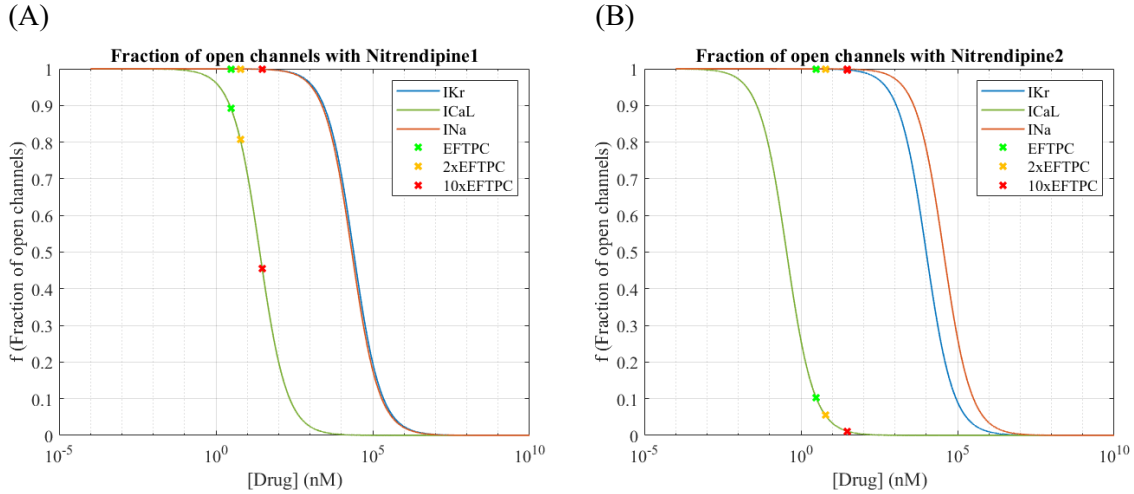

Figure 5.19. Fraction of open channels with (A) Nitrendipine 1 whose values of IC_{50} for IKr, ICaL and INa are 24600 nM, 25 nM and 21600 nM respectively, all Hill coefficients are equal to 1 nH and its EFTPC is 3nM and (B) Nitrendipine 2 whose values of IC_{50} for IKr, ICaL and INa are 10000 nM, 0.35 nM and 36000nM respectively, all Hill coefficients are equal to 1 nH and its EFTPC is 3.02 nM

This evidence is consistent with the results obtained because the cardioprotective effect of Nitrendipine 2 is more evident than Nitrendipine 1 as shown in Table 5.8 and Table 5.16.

Having carried out the relevant analysis, it is concluded that Diltiazem CiPA, Nifedipine 1 and Nitrendipine 2 act as cardioprotective drugs in many pathological cases in which proarrhythmic events, such as EADs, happen. Therefore, one of the objectives of this project is fulfilled, which is

to find a viable drug that is capable of alleviating the occurrence of EADs under several conditions as Figure 5.20 shows, with **Nitrendipine 2** being the most effective in a higher number of cases.

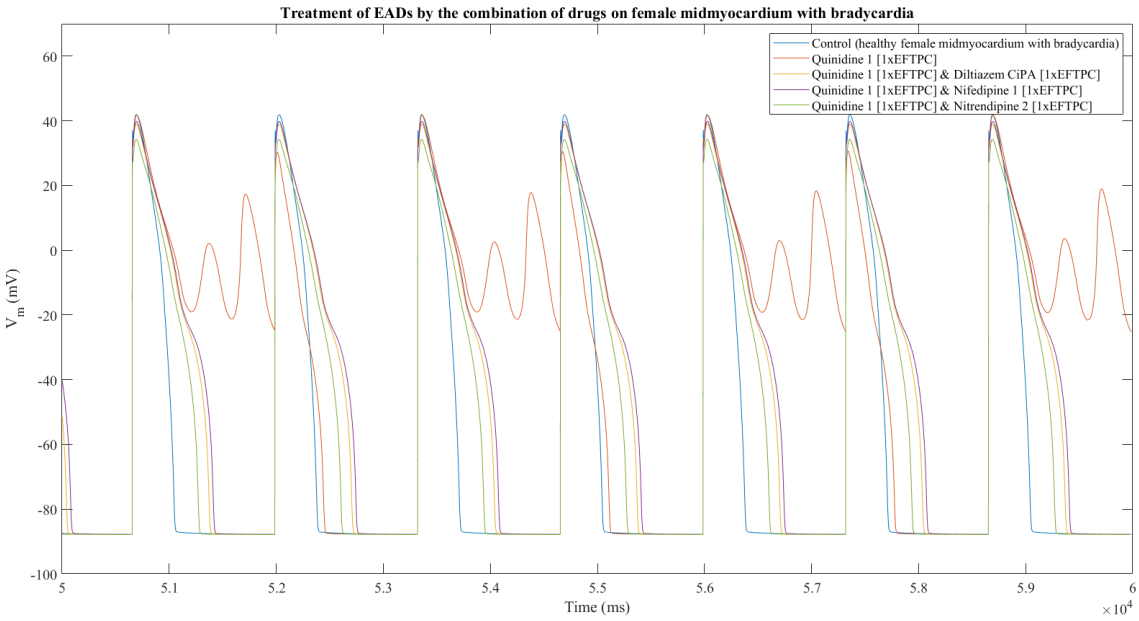

Figure 5.20. Treatment of EADs caused by the arrhythmogenic drug Quinidine 1 (red) at a concentration equal to EFTPC under female midmyocardium with bradycardia conditions. The occurrence of EADs is treated with a second anti-arrhythmogenic drug Diltiazem CiPA [1xEFTPC] (orange), Nifedipine 1 [1xEFTPC] (purple) and Nitrendipine 2 [1xEFTPC] (green). All of them together with the control (blue).

CHAPTER 6. CONCLUSIONS

The principal objectives of this Bachelor Thesis were, first, the development and usage of computational models in order to study how two pathologies (HF and HCM) affect ionic currents across the cell membrane of cardiomyocytes, which, in turn, has several pathological effects on cardiac action potential and the occurrence of several arrhythmogenic mechanisms such as early afterdepolarizations (EADs). The results prove that both pathologies with almost all stages of severity promote arrhythmogenic mechanisms, although some of them are more dangerous than others. In particular, EADs are caused by severe HF and HCM in midmyocardium of both sexes and heart rates with the exception of severe HF in female and male midmyocardium with tachycardia.

Moreover, as a result, the second principal objective, which was the research of the most effective drugs for palliating the effects of these pathologies, was accomplished as well. Once the effect of some anti-arrhythmogenic drugs has been added in those conditions in which EADs occur as a consequence of pathologies, the results suggest that:

- Diltiazem CiPA and Nitrendipine 2 with a concentration equal to EFTPC are able to palliate the occurrence of EADs in all cases.
- Nifedipine 1 with EFTPC is effective in almost all of the affected conditions except for severe HF in female midmyocardium with bradycardia and severe HCM in female midmyocardium with bradycardia and normal heart rate.

In addition, in order to analyse the effect of sex, cell type and heart rate on arrhythmogenic mechanisms, the combination of both, anti and pro-arrhythmogenic drugs, has been added to healthy myocardial cells' functioning. The main results demonstrate that female midmyocardium with tachycardia is the set of conditions with greater arrhythmogenicity and was therefore the most affected by drugs that tend to prolong the APD.

Finally, the third principal objective, which was the development of a user interface, in order to plot action potential and intracellular calcium concentration and display several parameters of the conditions selected, was fulfilled too. The interface was developed using AppDesigner from MATLAB® and it was used to visualize some relevant cases.

To accomplish all these objectives, a pipeline (secondary objectives) was planned, and thanks to their fulfilment, a huge number of results have been obtained. After analysing and visualizing the most relevant results, more conclusions have been drawn, as listed below.

6.1. CODE PROGRAMMING WORK

The first secondary objectives (a, b, c, d and e steps of the pipeline) were related with code programming in order to, on the one hand, integrate HF and HCM parameters to model their effects on cardiomyocyte AP and, on the other hand, develop two scripts to calculate both some relevant parameters, such as APD_{90}, and the most determinant biomarkers, such as the occurrence of EADs, to identify the risk of arrhythmia. To this purpose, the equations that describe the bioelectrical activity of the heart in ventricular human model, formulated by O'Hara et al (O'Hara et al., 2011) were

adapted applying the corresponding factors that models the effect of pathologies on ionic currents and fluxes according to Passini et al. (Passini et al., 2016).

Moreover, relating to calculation of biomarkers and parameters, two scripts were developed. The first one, *calc_parameters_v10.m*, calculates some parameters based on the signals, currents and concentrations obtained from the simulations of the modified ventricular cardiomyocyte model. The second one, *arrhythmic_risk_score_v6.m*, uses the calculated parameters in order to calculate some biomarkers that are useful for identifying the arrhythmic risk of the simulations under study. These two scripts allowed the results to be analysed in a faster and more quantitative way, as it was not necessary to visualize each simulation one by one, but rather the code automatically calculates the most relevant parameters and biomarkers to know which is the arrhythmic risk for each set of conditions.

In addition, other code lines were developed in order to systematically execute all the required computational simulations for studying the effectiveness of anti-arrhythmogenic drugs to palliate the occurrence of EADs caused by both arrhythmogenic drugs or pathologies.

6.2. PROARRHYTHMIC PHENOMENA CAUSED BY HF AND HCM

Regarding the secondary objective j "Determine in which states and conditions HF and HCM provoke proarrhythmic phenomena", once the model was ready, the effect of mild, moderate and severe HF and HCM on male or female endocardium, midmyocardium or epicardium with bradycardia, normal heart rate and tachycardia was simulated. Moreover, in order to have a reference, all above-mentioned conditions were simulated without pathology effect as well. Thereby fulfilling secondary objectives f, g, h and i.

From this set of results, it has been concluded that female midmyocardium with bradycardia was the set of conditions in which parameter values show an increased tendency for arrhythmia. In addition, in relation with the occurrence of EADs caused by pathologies, both pathologies in severe stage provoke EADs in midmyocardium, whatever the sex and heart rate, except in the case of severe HF effect on male and female midmyocardium with tachycardia, in which there are no EADs but the APD_{90} prolongation is such that it is quite proarrhythmic too. Additionally, mild HCM in male and female epicardium and midmyocardium with tachycardia are the unique conditions in which there is no APD_{90} prolongation. Regarding the alteration of triangulation value, this seems to be independent of heart rate because the cases in which it is not affected follow a pattern that have nothing to do with the heart rate value but everything to do with the cell type. In endocardium, only mild stage does not disrupt triangulation value untill abnormal levels. However, in epicardium both mild and moderated severities preserve triangulation value. And, lastly, in midmyocardium triangulation value was modified in all conditions.

6.2.1. Anti-arrhythmogenic drugs that palliate the HF and HCM arrhythmogenic effect.

Once the effect of 28 drugs considered as anti-arrhythmogenic was added individually in those conditions in which severe HF or HCM provoke the occurrence of EADs, the results were analysed and there were three drugs, Diltiazem CiPA, Nifedipine 1 and Nitrendipine 2, that were able to palliate this precursor of arrhythmia in all or most cases. All three have proved effective with a concentration equal to 1xEFTPC. Taking these results into consideration, the secondary objective k has also been accomplished.

6.3. EFFECT OF ANTI AND PRO-ARRHYTHMOGENIC DRUGS ON HEALTHY MYOCARDIUM AND HEART RATE INFLUENCE.

Regarding secondary objective l, the 95 drugs with three concentrations were simulated for each condition of sex, cell type and heart rate and the results prove that female, midmyocardium and tachycardia were the sex, the cell type and the heart rate most negatively affected by the effect of drugs respectively.

There were 22 drugs that provoke EADs: Ajmaline, Bepridil 1, 2 and CiPA, Cispride CiPA, Dofetilide 2 and CiPA, Droperidol, Flecainide, Halofantrine, Ibutilide, Prenylamine, Propafenone, Quinidine 1, 2 and CiPA, Ranolazine CiPA, Terfenadine 2, Terodiline, Thioridazine 1 and 2 and Verapamil 2 but not all of them with an EFTPC concentration. The ones that cause EADs with a concentration equal to 1xEFTPC or 2xEFTPC, which are the most likely to occur in patients, are Ajmaline, Ibutilide, Quinidine 1, Quinidine 2, Quinidine CiPA, Terfenadine 2, Thioridazine 1 and Thioridazine 2. Fortunately, it is well known to health professionals that Ajmaline, Ibutilide and Quinidine contribute to QT interval prolongation, Terfenadine was withdrawn from the market and Thioridazine is usually used as the last option to alleviate psychosis.

Regarding the rest of the disrupted biomarkers, Ajmaline, Ibutilide, Quinidine 1, 2 and CiPA and Thioridazine 1 and 2 disrupt the resting membrane potential (RMP) of some cases most of them being female endocardium with tachycardia.

In relation with APD_{90} prolongation, there were 26 drugs that lengthen the duration of the AP with a concentration equal to 1xEFTPC and/or 2xEFTPC, 5 of them considered as anti-arrhythmogenic. These results have been analysed carefully and it has been concluded that as they affect both L-type calcium channels and rapid delayed rectifier potassium channels similarly, they are able to both, lengthening and narrowing APD depending on other conditions such as the influence of sex, cell type or heart rate, their interaction with other molecules or even their metabolization.

In relation to alternans, it seems that there is not a pattern dependent on sex or cell type, however, the most affected heart rate is tachycardia. Ajmaline, Ibutilide, Piperacillin, Quinidine 1, 2 and CiPA, and Thioridazine 1 and 2 are able to produce alternans, fortunately most of them with a concentration equal to 10xEFTPC. As has been analysed, this ability is due to their interaction with calcium channels, provoking an alteration in intracellular calcium progression which, in turn, affects excitation-contraction coupling.

Finally, regarding triangulation values over the threshold, female midmyocardium with bradycardia is the set of conditions with the highest triangulation values. So, in this case, bradycardia is the heart rate with the highest number of cases affected with an abnormal triangulation value. After analysing the action potential, it is concluded that altered triangulation values are due to the occurrence of the so-called “second plateau” prolonging APD_{90} but not APD_{30}.

6.4. CARDIOPROTECTIVE EFFECT OF COMBINATION OF DRUGS

Once a second anti-arrhythmogenic drug effect is added in those cases in which the occurrence of EADs is due to the effect of a first drug, the data indicates that not only does tachycardia provoke a greater probability of the occurrence of EADs, but also the favourable response to some anti-arrhythmogenic drugs is lower.

Moreover, in relation with the penultimate secondary objective, the most effective drugs when they are combined with another one that provokes EADs are Diltiazem CiPA, Nifedipine 1 and

Nitrendipine 2, being the last one the only one that has the greater effectiveness with the lowest concentration.

Therefore, to sum it up, according to the results, the lower the heart rate is, the greater the ability to handle arrhythmogenic mechanisms like EADs. And the most cardioprotective agents are Diltiazem CiPA, Nifedipine 1 and Nitrendipine 2.

6.5. USER INTERFACE DEVELOPMENT

Finally, in order to accomplish the last secondary objective, closely related to the third principal objective, a software that functions as a user interface, in order to run new conditions with or without drugs or pathologies, and to visualize action potential and intracellular calcium concentration throughout the time, together with the most important parameters has been developed. Thanks to it, the model can be used in a more user-friendly manner because it is quite versatile and intuitive. Moreover, it has an option to represent the fraction of open channels according to drug concentration, and new drug parameters can be added as well. In this project the interface has been used so as to plot the simulations that needed to be visualised.

CHAPTER 7. LIMITATIONS AND FUTURE PERSPECTIVES

Although the results and conclusions generated from this thesis fulfil the main objectives proposed, during the execution of the project and once it has been completed, certain limitations have become apparent which can be palliated with future works as explained below.

First, the model is not completely comprehensive. The computational model developed in this thesis only takes into account the effects of sex, cell type, heart rate, health condition and drugs on heart and, in particular, on human ventricular cardiomyocytes. That is, this model cannot predict if a drug will provoke sinus tachycardia or bradycardia because the SA node has not been modelled. Also, the model does not simulate the effect of mentioned conditions on other organs, so the interactions between the heart and other organs in the presence of drugs cannot be predicted. This limitation is inherent in all mathematical models, which by default are not completely comprehensive.

Second, the simulation time. As 11892 simulations have been executed, the time needed to do it has been quite long (in the order of weeks), and as the code was programmed not to stop and run every simulation block at once, the block dedicated to the simulation of the drug combination in healthy myocardium took more than a month. For all these reasons, a computer with higher features than the laptop on which the whole project was initially planned to be carried out was necessary. In the future the code can be optimized and executed in a computer with even better hardware such as CPU, RAM, GPU and even with an SSD instead of the external HDD hard disk used.

Third, the storage. Each simulation file takes up an average of 0.138 GB, as a total amount of 11892 simulations have been executed, the storage needed to save all of them has been roughly 1641.1 GB, for that reason an external hard disk was bought.

Fourth, taking into account the two limitations commented above, neither the effect of drugs in order to palliate other arrhythmic biomarkers apart from EADs can be simulated nor the combination of drugs in pathological conditions nor even the combination of a third drug in healthy conditions. Therefore, in the future, these simulations can be executed and analysed, due to the fact that the code is prepared for it.

Moreover, an arrhythmic score value was proposed to be calculated for each case in order to determine the arrhythmogenicity of each pathology and each drug in a quantitative way. However, to calculate that score, running multiple simulations with more population to avoid underestimation is the optimal. Some researchers have proved that a population of 3000 simulations per each case with the same conditions is preferable; nevertheless, related to the above limitations, in reality, that would be impossible, because the total number of simulations would amount to 37692000 simulations. In future projects, the calculation of this score with a population greater than 1 may be of great scientific interest in order to quantitatively analyse the risk of arrhythmias that are enhanced or attenuated by the use of certain drugs.

Finally, another limitation that has been considered is about the software development tool used, AppDesigner from MATLAB®. As it is a design environment, all the tools and objects that can be used are pre-designed, so the interface design was limited by what the software offered. Therefore, the development of the user interface though raw code using other programming languages such as Java, Python or C# (C sharp), could be promising in order to design a more versatile interface with multiple options.

CHAPTER 8. APPENDIX

8.1. LINKS TO DOCUMENTS AND RESULTS OBTAINED

Below are the links to download the computational model, GUI installation package, the GUI development files and the Excel files with the results collected.

- Computational model
- GUI installation package and GUI files
- Results

First, the link "Computational model" redirects to a folder with the same name, in which there are 8 files which correspond to the files shown in Table 4.1 together with the Excel "drugData_organized.xlsx", in which IC_{50}, Hill coefficients and EFTPC values for each drug are collected.

Next, in the folder redirected by "GUI installation package" link there are only two files, the so-called "Cardiomyocyte_AP_interface.mlappinstall" is the file required when you install a new App inside MATLAB® interface, and "Cardiomyocyte_AP_interface.prj" is a file that MATLAB® creates during the packaging process and contains information about the app. In addition, inside the "GUI files" folder, there are 6 important files, which are the ones where the user interface has been developed: "PopUpApp.mlapp", "MainApp.mlapp", "NewDrugRegApp.mlapp", "f_plotApp.mlapp", "NewSimApp.mlapp" and "DDBBSimApp.mlapp" in which the windows corresponding to the Figure 4.3, Figure 4.4 and Figure 4.5 (A), (B), (C) and (D), respectively, have been programmed. The remaining file, "model_ORd_MMChACR.m" is required in order to carry out the simulations inside the user interface, so it is not a proper app development file.

Finally, in the folder called "Results" are two Excel files, the "Budget.xlsx" file is the one where the complete budget is calculated and the "Results.xlsx" file is where all the parameters and biomarkers values provided by the simulations executed are cleaned up. Specifically, in the worksheet "APD prolong & triang" from "Results.xlsx" there is the complete Table 5.6, in the worksheet "OneDrug_NoEADs_enlargedAPD_TABL" from "Results.xlsx" there is the complete Table 5.11, and, finally, in the worksheet "OneDrug_NoEADs_Triang_TABLE" from "Results.xlsx" there is the complete Table 5.13. The rest of the tables are spread over the resting worksheets of the workbook "Results.xlsx".

8.2. SUSTAINABLE DEVELOPMENT GOALS (SDGs)

As commented in CHAPTER 1 "MOTIVATION, BACKGROUND AND JUSTIFICATION", this thesis contributes to the achievement of three Sustainable Development Goals (SDGs), goal 3 "Good health and well-being", goal 5 "Gender equality" and goal 10 "Reduced inequalities". The degree to which the work relates to each of the SDGs is shown in Table 8.1 below.

Table 8.1. Degree of alignment of the present bachelor's thesis with the Sustainable Development Goals (SDGs)

SDGs	High	Medium	Low	Not Applicable
SDG 1. No poverty.				✗
SDG 2. Zero hunger.				✗
SDG 3. Good health and well-being.	✓			
SDG 4. Quality education.				✗
SDG 5. Gender equality.	✓			
SDG 6. Clean water and sanitation.				✗
SDG 7. Affordable and clean energy.				✗
SDG 8. Decent work and economic growth.				✗
SDG 9. Industry, innovation and infrastructure.		✓		
SDG 10. Reduced inequalities.	✓			
SDG 11. Sustainable cities and communities.				✗
SDG 12. Responsible consumption and production.			✓	
SDG 13. Climate action.				✗
SDG 14. Life below water.				✗
SDG 15. Life and land.				✗
SDG 16. Peace, justice and strong institutions.				✗
SDG 17. Partnerships for the goals.				✗

Next, the justification of each degree of alignment will be explained.

8.2.1. SDG 3. Good health and well-being.

Throughout the development of this project one of the principal objectives has been to study the effect of drugs on human ventricular cardiomyocytes, in order to analyse both, their level of cardiotoxicity in relation to their potential to produce arrhythmias, and their cardioprotective effect for treating the occurrence of some arrhythmogenic mechanisms. For this reason, this project promotes the achievement of the third SDG "Good health and well-being", in particular the target 3.8 "Achieve universal health coverage, including financial risk protection, access to quality essential health-care services and access to safe, effective, quality and affordable essential medicines and vaccines for all.", as it attempts to study the most effective drugs for specific health conditions.

8.2.2. SDG 5. Gender equality.

In addition, due to sex (female and male) being one of the conditions taken into account in order to simulate the heart action potential and the possible pharmaceutical therapies for some pathological scenarios, during this project the differences between female and male regarding the intrinsic cardiac bioelectrical characteristics and their response to treatment have been considered. The inclusion of sex factors in the thesis supports women's holistic health, thereby promoting the achievement of the fifth SDG "Gender equality", specifically the target 5.6 "Ensure universal access to sexual and reproductive health and reproductive rights as agreed in accordance with the Programme of Action of the International Conference on Population and Development and the Beijing Platform for Action and the outcome documents of their review conferences.". Moreover, by addressing female differences in biomedical research, this project combats the discrimination implicit in medical research that has traditionally been dominated by studies on men. Thinking about this, the target 5.1 "End all forms of discrimination against all women and girls everywhere" is promoted as well.

8.2.3. SDG 10. Reduced inequalities.

Furthermore, another principal objective of this project is the study of HF and HCM effects on human ventricular cardiomyocytes, two pathologies that affect the quality of life of a large part of the population, and tries to seek an effective pharmacological treatment for each stage of severity. For this reason, this project tries to combat the inequalities suffered by people with HF and HCM whose well-being and opportunities are reduced because of their health condition, promoting in turn the tenth SDG "Reduced inequalities", in particular, the target 10.3 "Ensure equal opportunity and reduce inequalities of outcome, including by eliminating discriminatory laws, policies and practices and promoting appropriate legislation, policies and action in this regard".

8.2.4. SDG 9. Industry, innovation and infrastructure.

Additionally, as this project develops and uses computational models in order to simulate the effect of pathologies and drugs on the cardiac bioelectricity, it means an advance in biomedical research, promoting in turn, the scientific and technological innovation by introducing new methodologies and technologies in cardiac research. In view of the above, the present thesis partly promotes SDG 9 "Industry, innovation and infrastructure", specifically the target 9.5 "Enhance scientific research, upgrade the technological capabilities of industrial sectors in all countries, in particular developing countries, including, by 2030, encouraging innovation and substantially increasing the number of research and development workers per 1 million people and public and private research and development spending".

8.2.5. SDG 12. Responsible consumption and production.

Finally, when computational models are used for studying drug effects, the reduction of the need for animal experimentation is promoted, which is a more ethical and responsible practice and also contributes to the rational management of resources and minimises the environmental impact of medical research. Additionally, computational modelling allows the prediction of drugs effects in advance, in order to filter some of them before the required clinical trials. This optimizes the process of drugs development, making it more efficient and less dependent on clinical trials or physical resources to prove the effectiveness of pharmacological treatments. For this reason, the present thesis partly promotes SDG 12 "Responsible consumption and production", in particular the target 12.5 "By 2030, substantially reduce waste generation through prevention, reduction, recycling and reuse".

CHAPTER 9. REFERENCES

Agencia Española de Medicamentos y Productos Sanitarios. (2019). Nota informativa: Información sobre el suministro de Epanutin 100 mg cápsulas duras (fenitoína sódica). CIMA. Retrieved May 22, 2024 from https://www.aemps.gob.es/informa/notasinformativas/medicamentosusohumano-3/problemasSuministro/la-aemps-desarrolla-una-interfaz-para-permitir-a-prescriptores-saber-que-presentaciones-tienen-problemas-de-suministro-2/

Agencia Española de Medicamentos y Productos Sanitarios. (2020). Ficha técnica de Adalat Oros 30 mg comprimidos de liberación prolongada. CIMA. Retrieved May 22, 2024 from https://cima.aemps.es/cima/dochtml/ft/59538/FT_59538.html

Agencia Española de Medicamentos y Productos Sanitarios. (2020). Ficha técnica de Nitrendipino STADA 20 mg comprimidos EFG. CIMA. Retrieved May 22, 2024 from https://cima.aemps.es/cima/dochtml/ft/58172/FT_58172.html

Agencia Española de Medicamentos y Productos Sanitarios. (2021 - a). Ficha técnica de Epanutin 100 mg cápsulas duras. CIMA. Retrieved May 22, 2024 from https://cima.aemps.es/cima/dochtml/ft/58172/FT_58172.html

Agencia Española de Medicamentos y Productos Sanitarios. (2021 - b). Ficha técnica de Piperacilina/Tazobactam Kabi 4 g/0,5 g polvo para solución para perfusión EFG. CIMA. Retrieved May 24, 2024 from https://cima.aemps.es/cima/dochtml/p/71601/Prospecto_71601.htmlhttps://cima.aemps.es/cima/dochtml/ft/58172/FT_58172.html

Agencia Española de Medicamentos y Productos Sanitarios. (2023). Ficha técnica de Diltiazem Sandoz 60 mg comprimidos EFG. CIMA. Retrieved May 22, 2024 from https://cima.aemps.es/cima/dochtml/p/62328/P_62328.html

Amanfu, R. K., & Saucerman, J. J. (2011). Cardiac models in drug discovery and development: a review. *Critical Reviews™ in Biomedical Engineering, 39*(5).

Anttila, K., & Farrell, A. P. (2022). Physiology of cardiac pumping.

Bascuñana Gea, C. (2023). Desarrollo de un software para el estudio del efecto cardioprotector de fármacos combinados (Doctoral dissertation, Universitat Politècnica de València).

Beledo, J. F., Simón, J. A. A., & Martínez, Á. M. (Eds.). (2013). Farmacología humana. *Elsevier Health Sciences*. (page 616)

Carpio, E. F., Gomez, J. F., Sebastian, R., Lopez-Perez, A., Castellanos, E., Almendral, J., ... & Trenor, B. (2019). Optimization of lead placement in the right ventricle during cardiac resynchronization therapy. A simulation study. *Frontiers in physiology, 10*, 429987.

Cohen, B. J., & Hull, K. L. (2020). Memmler's the human body in health and disease. Jones & Bartlett Learning.

Cohen, B. J., & Taylor, J. J. (2009). Memmler's The Human Body in Health and Disease, 11th Edition

Doke, S. K., & Dhawale, S. C. (2015). Alternatives to animal testing: A review. *Saudi Pharmaceutical Journal, 23*(3), 223-229.

Dudás, B. (2023). Human histology: a text and atlas for physicians and scientists. *Academic Press*.

Feldman, D. S., & Mohacsi, Paul. (Eds.). (2019). Heart Failure [electronic resource] (1st ed. 2019.). *Springer International Publishing*. https://doi.org/10.1007/978-3-319-98184-0

Feldman, D. S., & Mohacsi, Paul. (Eds.). (2019). Heart Failure [electronic resource] (1st ed. 2019.). *Springer International Publishing*. https://doi.org/10.1007/978-3-319-98184-0

Ferrero, J. M. (2022). Apuntes Grado en Ingeniería Biomédica, año académico 2021-2022.

Fogli Iseppe, A., Ni, H., Zhu, S., Zhang, X., Coppini, R., Yang, P. C., ... & Grandi, E. (2021). Sex-specific classification of drug-induced torsade de pointes susceptibility using cardiac simulations and machine learning. *Clinical Pharmacology & Therapeutics, 110*(2), 380-391.

Gomez, J. F., Cardona, K., Romero, L., Ferrero Jr, J. M., & Trenor, B. (2014). Electrophysiological and structural remodeling in heart failure modulate arrhythmogenesis. 1D simulation study. *PloS one, 9*(9), e106602.

Guérard, N., Jordaan, P., & Dumotier, B. (2014). Analysis of unipolar electrograms in rabbit heart demonstrated the key role of ventricular apicobasal dispersion in arrhythmogenicity. *Cardiovascular toxicology, 14*, 316-328.

Hall, J. E. (2011). Guyton y Hall. Tratado de fisiología médica. *Elsevier Health Sciences*.

Hodgkin, A. L., & Huxley, A. F. (1952). A quantitative description of membrane current and its application to conduction and excitation in nerve. *The Journal of physiology, 117*(4), 500.

Hutchison, S. J. (2009). Pericardial diseases: clinical diagnostic imaging atlas with DVD. *Elsevier Health Sciences*.

Iaizzo, P. A. (Ed.). (2010). Handbook of cardiac anatomy, physiology, and devices. *Springer Science & Business Media*.

Iaizzo, P. A. (Ed.). (2015). Handbook of cardiac anatomy, physiology, and devices. *Springer Science & Business Media*.

Jennings, M. L. (2018). Carriers, exchangers, and cotransporters in the first 100 years of the Journal of General Physiology. *Journal of General Physiology, 150*(8), 1063-1080.

Jing, L., Agarwal, A., Chourasia, S., & Patwardhan, A. (2012). Phase relationship between alternans of early and late phases of ventricular action potentials. *Frontiers in physiology, 3*, 24421.

Johnsen, L. Ø., Friis, K. A., & Damkier, H. H. (2023). Transport of ions across the choroid plexus epithelium. In Cerebrospinal Fluid and Subarachnoid Space (pp. 257-271). *Academic Press*.

Kim, J. J., Němec, J., Papp, R., Strongin, R., Abramson, J. J., & Salama, G. (2013). Bradycardia alters Ca2+ dynamics enhancing dispersion of repolarization and arrhythmia risk. *American Journal of Physiology-Heart and Circulatory Physiology, 304*(6), H848-H860.

Kulkarni, K., Merchant, F. M., Kassab, M. B., Sana, F., Moazzami, K., Sayadi, O., ... & Armoundas, A. A. (2019). Cardiac alternans: mechanisms and clinical utility in arrhythmia prevention. *Journal of the American Heart Association, 8*(21), e013750.

Lancaster, M. C., & Sobie, E. A. (2016). Improved Prediction of Drug-Induced Torsades de Pointes Through Simulations of Dynamics and Machine Learning Algorithms. *Clinical pharmacology and therapeutics, 100*(4), 371–379. https://doi.org/10.1002/cpt.367

Laske, T.G., Shrivastav, M., Iaizzo, P.A. (2015). The Cardiac Conduction System. In: Iaizzo, P. (eds) *Handbook of Cardiac Anatomy, Physiology, and Devices*. Springer, Cham. https://doi.org/10.1007/978-3-319-19464-6_13

Liu, J., Laksman, Z., & Backx, P. H. (2016). The electrophysiological development of cardiomyocytes. *Advanced drug delivery reviews, 96*, 253-273.

Molnar, C., & Gair, J. (2022). 21.3. Mammalian Heart and Blood Vessels. *NSCC Academic Biology* 1050.

Naidu, S. S. (Ed.). (2019). Hypertrophic Cardiomyopathy [electronic resource] (2nd ed. 2019.). *Springer International Publishing*. https://doi.org/10.1007/978-3-319-92423-6

National Center for Biotechnology Information (2024 - a). PubChem Compound Summary for CID 39186, Diltiazem. Retrieved May 28, 2024 from https://pubchem.ncbi.nlm.nih.gov/compound/Diltiazem.

National Center for Biotechnology Information (2024 - b). PubChem Compound Summary for CID 4485, Nifedipine. Retrieved May 28, 2024 from https://pubchem.ncbi.nlm.nih.gov/compound/Nifedipine.

National Center for Biotechnology Information (2024 - c). PubChem Compound Summary for CID 4507, Nitrendipine. Retrieved May 27, 2024 from https://pubchem.ncbi.nlm.nih.gov/compound/Nitrendipine.

Nerbonne, J. M., & Kass, R. S. (2005). Molecular physiology of cardiac repolarization. *Physiological reviews, 85*(4), 1205-1253.

O'Hara, T., Virág, L., Varró, A., & Rudy, Y. (2011). Simulation of the undiseased human cardiac ventricular action potential: model formulation and experimental validation. *PLoS computational biology, 7*(5), e1002061

Pandit, S. V., & Jalife, J. (2013). Rotors and the dynamics of cardiac fibrillation. *Circulation research, 112*(5), 849-862.

Passini, E., Mincholé, A., Coppini, R., Cerbai, E., Rodriguez, B., Severi, S., & Bueno-Orovio, A. (2016). Mechanisms of pro-arrhythmic abnormalities in ventricular repolarisation and anti-arrhythmic therapies in human hypertrophic cardiomyopathy. *Journal of molecular and cellular cardiology, 96*, 72-81.

Pastore, J. M., & Rosenbaum, D. S. (2000). Role of structural barriers in the mechanism of alternans-induced reentry. *Circulation research, 87*(12), 1157-1163.

Pepine, C. J., Faich, G., & Makuch, R. (1998). Verapamil use in patients with cardiovascular disease: an overview of randomized trials. *Clinical cardiology, 21*(9), 633-641.

Petkov, G. V. (2009). Ion channels. In Pharmacology (pp. 387-427). *Academic Press*.

Plonsey, R., & Barr, R. C. (2007). Bioelectricity: a quantitative approach (3rd ed.). *Springer*.

Prajapati, C., Koivumäki, J., Pekkanen-Mattila, M., & Aalto-Setälä, K. (2022). Sex differences in heart: from basics to clinics. *European Journal of Medical Research, 27*(1), 241.

Rayner-Hartley, E., & Sedlak, T. (2016). Ranolazine: a contemporary review. Journal of the *American Heart Association, 5*(3), e003196.

Real Decreto 1098/2001, de 12 de octubre, por el que se aprueba el Reglamento general de la Ley de Contratos de las Administraciones Públicas (2001, October 26). Retrieved May 17, 2024, from https://www.boe.es/eli/es/rd/2001/10/12/1098

Rosen, M. R., & Pham, T. (2004). Impact of gender on the response to cardioactive drugs. *Principles of gender-specific medicine, 1*(24), 241-254.

Sarazan, R. D. (2014). The QT Interval of the Electrocardiogram.

Sigg, D. C., Iaizzo, P. A., Xiao, Y. F., & He, B. (Eds.). (2010). Cardiac electrophysiology methods and models. *Springer Science & Business Media*.

Stapleton, P. A., Knuckles, T. L., Minarchick, V. C., Gautam, G., & Nurkiewicz, T. R. (2014). Cardiovascular System. In *Encyclopedia of Toxicology: Third Edition* (pp. 730-747). Elsevier. https://doi.org/10.1016/B978-0-12-386454-3.00985-4

Tse, G. (2016). Mechanisms of cardiac arrhythmias. *Journal of arrhythmia, 32*(2), 75-81.

Vornanen, M., Badr, A., & Haverinen, J. (2023). Electrical excitation, action potential and impulse conduction.

Weiss, J. N., Garfinkel, A., Karagueuzian, H. S., Chen, P. S., & Qu, Z. (2010). Early afterdepolarizations and cardiac arrhythmias. *Heart rhythm, 7*(12), 1891-1899.

Zaza, A., Ronchi, C., & Malfatto, G. (2018). Arrhythmias and heart rate: Mechanisms and significance of a relationship. *Arrhythmia & Electrophysiology Review, 7*(4), 232.

II. BUDGET

CHAPTER 10. BUDGET

10.1. INTRODUCTION

With the purpose of valuing this engineering project economically, the corresponding budget has been calculated by an economical study in which labour, hardware and software costs have been taken into account.

Specifically, hardware and software costs have been calculated considering the amortization of each constituent, which is calculated following the equation 28.

$$Attributable\ cost\ without\ VAT = \frac{Project\ duration\ time}{Useful\ life} \cdot Cost\ without\ VAT \qquad (28)$$

The duration of this project was about eight months, and therefore this has been the time-frame in which all the budget calculations have been made. In the following sections budget will be described in detail.

10.2. DETAILED BUDGET

10.2.1. Labour costs

Labour costs are the ones that allude to the appropriate salary that the personnel that has been part of the project should receive. These costs are calculated according to the average hourly cost and the total of hours worked for each of those involved.

The hourly cost for each worker has been calculated according to the basic salary based on their profile, to which are added two extra economic benefits over the period of time devoted to this project, and the cost of social security contribution for each one.

Regarding social security cost, according to the data published by the Ministry of Labour and Social Economy in August 2023, 28.3% corresponds to common contingencies, such as common illness, non-occupational accidents, maternity or paternity leave or retirement, among others; 7.05% to unemployment insurance; 0.2% to the wage guarantee fund or FOGASA; and 0.7% to professional training.

Specifically, the involved members have been the following, a student of biomedical engineering who has been in charge of the execution of this project and her counsellor, a doctor in industrial engineering, which has been the responsible for the supervision and the mentoring of this thesis. Considering that there are 225 working days per year and a full working day of 8 hours, in the course of a year a full-time job implies 1800 hours worked.

In this way, on the basis of a base salary of 23,832 and 52,614 €/year for a junior engineer and a doctor engineer respectively, the hourly cost for each of them is 13.24 €/hour for the first profile and 29.23 €/hour for the second one. Thus, labour costs for this project are detailed in Table 10.1.

Table 10.1. Labour costs for each person who works in this project.

Nº	Description of the resource	Unit cost (€/hour)	Amount (h)	Chargable cost excluding employer's contribution	Employer's contribution (36.25%)	Attributable cost
1	Junior biomedical engineer (student)	13.24	330	4,369.20 €	1,583.84 €	5,953.04 €
2	Doctor industrial engineer (counselor)	29.23	50	1,461.50 €	529.79 €	1,991.29 €
TOTAL						7,944.33 €

10.2.2. Software costs

Software costs include the cost of computer programmes that have been used to conduct this project. These are specified in Table 10.2.

*Table 10.2. Attributable cost without VAT of software used for this thesis considering the usage period and the licence duration to calculate the amortization factor. * The OEM Windows 10 Key came pre-installed on the computers used, for that reason the attributable cost is zero.*

Nº	Software	Cost without VAT	Amount	Amortization factor	Attributable cost without VAT
1	Windows 10	119.99 €	1	8/60	*0.00 €
2	Microsoft Office 365	99.00 €	1	8/12	66.00 €
3	MATLAB R2020b	860.00 €	1	8/12	573.33 €
TOTAL					639.33 €

Specifically, on the one hand, Windows 10 is the operating system used in both, the student's laptop and tutor's desktop computer; on the other hand, Microsoft Office 365 is a subscription-based service that offers a suite of productivity applications and cloud-based services, this includes office software such as Word and Excel which have been used in the present thesis to write it and analyse the results, respectively. Moreover, regarding to MATLAB® (short of MATrix LABoratory), it is a programming and numerical calculation platform developed by MathWorks, which is used for data analysis, algorithm development, and visualization. In this project, MATLAB® has been used for both developing and modifying the code of computational models and executing and plotting the simulations.

10.2.3. Hardware costs

Hardware costs include the attributable cost of the different physical electronic devices used throughout the development of this project. As Table 10.3 shows, two computers were needed. The first one, a laptop, was employed in order to programme the code, analyse results and write this document. The second one is a desktop computer which has been employed to run the code and to carry out the simulations. Moreover, an external hard disk has been needed for saving all simulation files.

Table 10.3. Attributable cost without VAT of hardware used during the development of this project taking into account the usage time and the lifespan of each device to calculate the amortization factor.

Nº	Hardware	Cost without VAT	Amount	Amortization factor	Attributable cost without VAT
1	Laptop HP Pavilion - 15-bc415ns (i7-8750H 8GB RAM)	631.99 €	1	8/60	84.27 €
2	Desktop PC (i7-8700K - 32GB RAM)	1,700.00 €	1	4/60	113.33 €
3	Toshiba Canvio Basics HDD 2.5 4TB	99.68 €	1	4/60	6.65 €
TOTAL					204.24 €

10.3. TOTAL BUDGET

10.3.1. Material execution budget

Considering all previous calculations, the sum of labour, software and hardware costs amounts to eight thousand seven hundred eighty-seven euros and ninety-one cents (8,787.91 €).

10.3.2. Contracted operation budget

According to the Royal Decree 1098/2001 of 12th of October, approving the General Regulations of the Law on Public Administration Contracts, whose reference is BOE-A-2001-19995 (Ministerio de Hacienda, 2001), extra costs associated with general costs and industrial benefit have to be added in order to calculate the total budget. The document indicates that general costs have to be calculated taking from 13% to 17%, and for industrial benefit taking a 6% of the material execution budget. Considering these values, general costs and industrial benefit are going to be calculated by taking a 15% and a 6% of the material execution budget, respectively. Moreover, an additional 21% has to be added too with reference to Value Added Tax (VAT).

Therefore, the contracted operation budged is calculated in Table 10.4, ascending to twelve thousand eight hundred sixty-six euros and thirty-seven cents (12,866.37 €).

Table 10.4. Contracted operation budget considering general costs, industrial benefit and total budget before and after VAT.

Denomination	Cost (€)
Labour costs	7,944.33 €
Software costs	639.33 €
Hardware costs	204.24 €
Material execution budget	8,787.91 €
General costs	1,318.19 €
Industrial benefit	527.27 €
Total without VAT	10,633.37 €
VAT	2,233.01 €
Contracted operation budget	12,866.37 €